The Dissertation Committee for Hieu Trung Nguyen Certifies that this is the approved version of the following dissertation:

Controlling neural cell behavior with electric field stimulation across a conductive substrate

Committee:

Christine Schmidt, Supervisor

Richard Aldrich

Aaron Baker

Henry G. Rylander

Laura Suggs

Controlling neural cell behavior with electric field stimulation across a conductive substrate

by

Hieu Trung Nguyen, B.S.; M.S.E.

Dissertation

Presented to the Faculty of the Graduate School of

The University of Texas at Austin

in Partial Fulfillment

of the Requirements

for the Degree of

Doctor of Philosophy

The University of Texas at Austin

December 2012

Acknowledgements

The work presented in this dissertation would not be possible without major contribution from fantastic individuals.

I would like to thank the Schmidt lab for improving my knowledge in science and assisting the development of my project. I am especially indebted to the Polypyrrole Team: Jon Nickels, Jae Young Lee, John Fonner, Leo Forciniti, Nathalie Guimard, Craig Milroy, and John Hardy for helping me question the Why and How, which are so necessary for pushing the edge of science. I must also thank all other lab members who are part of the biological and hydrogel team: Zin Khaing, Scott Zawko, Sydney Geissler, Shalu Suri, Ryan Nagao, Derek Hernandez, Stephanie Seidlits, Richelle Thomas, Sarah Mayes, Chase Cornelison, Vanessa Aguilar, and Diana Gutierrez. And of course, I am indebted to the staff for making my life much easier, Hyma Durgam, Tera Sherrard, and Michelle Miller.

Research and technical advice from outside the Schmidt lab was also instrumental in providing much needed guidance in my research. My committee including Richard Aldrich, Aaron Baker, Grady Rylander, and Laura Suggs each gave me inspiration for new ideas and showed me how much I did not know about my own research. Collaboration with Silvia Luebben and Shawn Sapp from TDA Inc. and Bob Ross from VTI Inc. have shown me how teamwork is essential for developing products for biomedical applications. Their suggestions and trust in my work emboldened me to work harder on my projects. Technical assistance from other labs at UT have been especially helpful for my work. For that, I thank Mary Nguyen, Julie Rytlewski, Jason Cook, Alex Hannah, Prinda Wanakule, Shouliang Zhang, Julie Hayes, and Dwight Romanovicz.

Friends and family here in Austin have made my time here and absolute joy and life without them would be unthinkable. I have much gratitude for Tri Dang, Yuna Khemapatapun, Nam Nguyen, Vy Nguyen, Mary Nguyen, Lisa Smith, Deirdre Dawson, Alvin Nguyen, Alex Pham, Thao Nguyen, Wendy Jang, Annie Zheng, Tony Le, Dung To, Thao Linh Phan, Thomas Mathews, Hang Yang, and countless others who have made me smile when research was doom and gloom. My family have always supported me innumerable ways: Homer, mom, Trungy, Ly, Van Lang, Tweetybird, and our many many cousins.

I would be nowhere without the undergraduate students I have mentored. Their ceaseless dedication to our work amazes me and I could not imagine being successful without their contribution. For that, I thank Claudia Wei, Jacque Chow, Lindsey Nguy, Hieu K Nguyen, Jeff Coursen, Alvin Nguyen, Jan Nguyen, Thomas Mathews, Dan Walk, and Sung Ji Ahn. You guys have kept me on my toes for the last 4 years, and I think your questions, discoveries, and mistakes have greatly improved my ability as a researcher and mentor. Again, I cannot thank you enough.

And lastly, I would like to give a BIG THANKS to my mentor and PI, Christine Schmidt. She gave me a chance to work with her group and spent some time developing ideas with me, even though her lab and schedule was completely full to the brim. She gave me space so I can develop ideas on my own and for me to mature as a scientist and as a person. I think one of the most important things I gained here was learning how to learn. Learning how to think. My brain has evolved, and for that, I am forever indebted to Christine.

Thank you all for molding me and my research. I am like a cell, taking cues from my environment to differentiate into another phenotype.

Controlling neural cell behavior with electric field stimulation across a conductive substrate

Hieu Trung Nguyen, PhD

The University of Texas at Austin, 2012

Supervisor: Christine Schmidt

Abstract:

Electrical stimulation of tissues induces cell alignment, directed migration, extended processes, differentiation, and proliferation, but the mechanisms involved remain largely unknown. To reveal effects of electric fields (EF) through the media on cell behavior, voltage (7.45 – 22 V), current density (36 – 106 mA/cm^2), duration (2 – 24 hrs), and alternating currents (AC, 2 – 1000 Hz) were varied independently when exposed to cell cultures. It was determined that current density and duration are the primary attribute Schwann cells respond to when an EF is applied through the media. This implies that the number of charges moving across the cell surface may play a key role in EF-induced changes in cell behavior. Identical conditions were used to stimulate cells grown on the surface of a conductive substrate to examine if a scaffold can provide structural and EF cues. The effects of an EF through the substrate were examined by placing a protein gel on the surface during stimulation and observing the morphology of subsequent cell cultures and the physical topology of the gel. EFs were shown to create

Ca^{2+} redistribution across gels and subtle changes in collagen I fibril banding. Stimulated gels were able to induce perpendicular Schwann cell alignment on newly seeded cultures days after initial EF exposure, and the cell response decreased when seeded at longer times, indicating the effects of EF on the matrix environment has a relaxation time. These findings were then integrated into a biodegradable, electrically conductive polypyrrole-poly-ε-caprolactone polymer developed by collaborators. Dorsal root ganglia placed in matrix gels on top of conducting polymer exhibited significantly longer axons when stimulated with DC and AC signals. The overall results demonstrate that EFs have a significant effect on the extracellular environment. The broad implication of this data grants researchers with the ability to physically and metabolically control cell behavior with EFs, including improved wound healing or reduced cancer metastasis.

Table of Contents

List of Tables

List of Figures

Chapter I:

Purpose and Significance

The goal of the dissertation project is to explore the conditions and mechanisms associated with cell response to electric fields (EF) and to create a device that harnesses this ability for enhanced nerve repair. There are numerous advances in nerve repair techniques that focus on improving nerve regeneration efficacy by engineering biological, chemical, topological, and mechanical cues (Hudson et al. 2000, Schmidt and Leach 2003, Pfister et al. 2011). One method that has garnered greater attention in the recent decades is the use of EF stimulation to control cell behavior including cell migration and protein expression (Patel and Poo 1984, McCaig 1990, Borgens et al. 1994). By using EF to control cell behavior, we hope to improve nerve regeneration in those who have lost mobility and sensation from nerve damage involved in vehicle accidents, work-related injuries, surgery, war trauma, and diseases.

Depending upon the age of the patient and severity of injury, the estimated lifetime cost of motor disability can range between $1 – 4 million dollars (NSCISC 2008). Not only does this produce a financial strain to patients, families, and the state, loss of function devastates the victim's quality of life. In the 1990s, there were 12,000 annual cases of spinal cord injury in the U.S., but there is no standard procedure to repair spinal cord injuries. There were 50,000 peripheral nerve repair surgeries recorded in 1995 (NCHS 1995) which is most likely a lower approximation than the total number of injured individuals because not all peripheral nerve injuries can undergo surgery. Due to the complexity of the nervous system, not all peripheral nerve surgeries are effective with

the current technology. New techniques and advances in reparative technology will help reduce the population suffering from motor and sensory loss.

Since the end of the 1970s, there have been numerous findings that show EF exposure can alter cell activity, including cell migration, orientation, differentiation, and proliferation (Patel and Poo 1984, Hronik-Tupaj and Kaplan 2012). Investigators have explored the use of EF on various cell types under various electrical conditions, however, there is no comprehensive work that studies these conditions independently, nor has the mechanism of EF-induced change in cell behavior been fully examined. Application of EF on the human biology is a growing field, yet understanding it is still in its infancy.

Electric forces influence charged molecule mobility and cell membrane potential, hence, electric fields (EF) may be harnessed to control cellular activity. The primary method of exposing EF to cell cultures mimics in vivo conditions, where the flowing current is conducted through the fluid surrounding the tissue (McCaig and Rajnicek 1991, Borgens et al. 1994, Song et al. 2007). The proposed research will explore the use of electrical cues to observe cell morphology, cell alignment, and axon growth in various neural cell types. Alternatively, being able to stimulate cells using a conductive material may be beneficial for physical and electrical guidance. An electrically conductive polypyrrole (PPy) substrate implementing these cues to promote nerve repair will also be characterized and optimized for biocompatibility, conductivity, and mechanical stability. In collaboration with industry partners, our final project is to create an implantable conduit capable of electrical conduction. This device will incorporate electrical cues (through conductive PPy), chemical cues (hydrogel), and physical cues (hydrogel stiffness and conduit topology).

The work presented in this dissertation details the use of EFs to control neural cell growth. More specifically, relevant EF properties that induce cell morphological changes were found in Chapter 3 by observing cell behavior when exposed to EFs with independently controlled electrical parameters. Then a closer look at the cellular environment will show that EFs have a profound impact on controlling the milieu surrounding a growing cell in Chapter 4. And in Chapter 5, we demonstrate that EF stimulation through a conductive substrate has a tangible effect on improving axon regeneration. The report will conclude with the significance of our findings and its future implications for biomedical applications.

Chapter II:

Background

2.1 THE NERVOUS SYSTEM

The human nervous system is divided into the central nervous system (CNS) and the peripheral nervous system (PNS). The CNS, composed of the brain, optic nerves, olfactory nerves, auditory nerves, and the spine, is dedicated for information processing of sensory input. The PNS, composed of cranial nerves, spinal nerves, and sensory nerves, receives sensory information from external stimuli and sends the information to the CNS. The CNS can respond by returning a signal to the PNS, producing an excitatory stimulus for muscle and gland control. Physical sensation and motor control of the limbs is dependent upon the uninterrupted communication within these systems.

The central and peripheral nervous systems are composed of two cell types: neurons and glial cells, as depicted in **Figure 1**. Although both cell types are different for each system, their overall functions are analogous to each other. Neuronal cells carry data signals for communication between cells whereas glia typically play a supportive role by preserving signal integrity and maintaining general neural cell health.

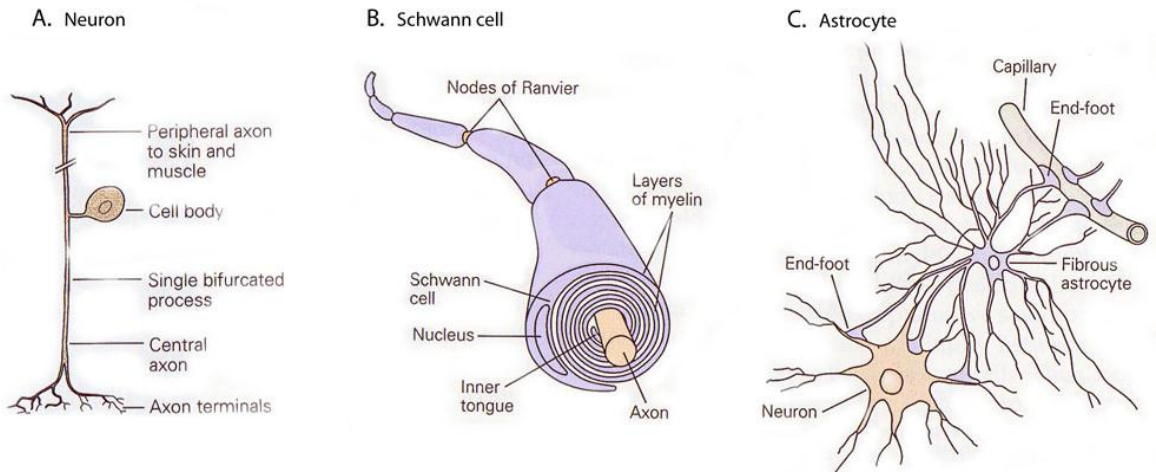

Figure 1. Neural cell types of the CNS and PNS can vary in morphology depending on its function. (A) A pseudo-unipolar dorsal root ganglion cell connecting the spine to peripheral tissue, (B) a Schwann cell myelinating an axon of the PNS, and (C) an astrocyte providing structural and nutritional support in the CNS. (Kandel et al. 2000)

The neuron is the basic functional unit for transmitting electric signals throughout the body and is structurally composed of a cell body (soma) and neuronal processes (neurites). The soma, containing the nucleus and organelles necessary for metabolism, typically produce two types of neurites: dendrites and axons. Dendrites are typically short, branched neurites which direct signals toward the soma. Axons are longer neurites which direct signals away from the soma. The longest axon in the human body can span over one meter in length, connecting the spine to the toe. Neurons can relay electrical information to other neurons or other cells by releasing chemical signals into small gaps between each other, called synapses. Neurons of the PNS may synapse with only several target cells, neurons of the CNS can have between 1,000 to 10,000 synapses and some have been estimated to have over 200,000 synapses (e.g. Purkinje cells).

There are 100 billion neurons in the brain and there are over 10 times as many glia to efficiently supply nutrients to neurons, remove harmful material from the cellular milieu, maintain structural support, assist in neuronal signal transmission, and provide growth cues for neural development. The CNS has many types of glial cells to help it function properly. Oligodendrocytes improve signal transmission efficiency by producing myelin to insulate axons, astrocytes act as structural support and regulate extracellular chemicals surrounding neurons, microglia are mobile phagocytic cells, radial glia are precursor cells that also provide developmental migration cues during neurogenesis, and ependymal cells secrete cerebrospinal fluid as the brain's circulation system.

Like the CNS, the glial cells of the PNS greatly outnumber the amount of neurons. The soma of each neuron of the PNS is located along the spine and projects axons to the extremities of the body. Therefore, a single axon that stretches from the spine to the end of a limb may have millions of glial cells along the structure. Schwann cells produce myelin along the entire length of the axon to increase signal transduction speed and surrounding satellite cells regulate the extracellular chemicals around the neuron.

The complexity of the nervous system limits its ability for self-repair. Neurons typically do not survive when the soma is damaged, but can regenerate neurites depending upon the conditions at the injury site. Glial cells retain their ability to divide and proliferate throughout their lifetime, but their role in nerve repair can be both promotional and inhibitory. Research in CNS repair continues to be more challenging than PNS repair because there is greater intricacy of cell interactions and less clinical accessibility. However, advances in PNS repair technology may provide greater insight to

the CNS. Because of greater ease in study and translation to practice, the remainder of this dissertation will focus on PNS repair.

2.1.1 Peripheral nerve physiology

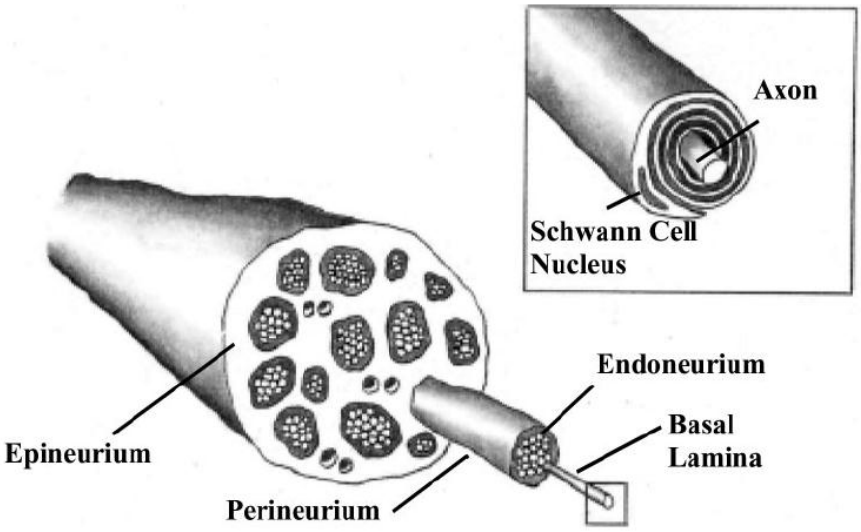

Figure 2. A cross-sectional drawing of a nerve of the PNS shows an axon enveloped by a myelinating Schwann cell (inset). The myelinated axon with a surrounding endoneurium is bundled together to form a fascicle within a perineurium. These fascicles are then grouped together by an epineurium to create a nerve cable. (Winter and Schmidt 2002)

A peripheral nerve connecting the spine to a target structure contains numerous bundles of axons surrounded by various cells and connective tissue. Efferent nerve fibers send stimulatory signals from the spine to muscles and glands, whereas afferent nerve fibers return information from sensory receptors in the skin and organs to the CNS. Schwann cells found along the length of each axon produce myelin to improve signal

transmission efficiency. This insulation allows neurons to transmit chemo-electrical signals at a speed of 80 m/s with no reduction in signal amplitude. The individual axon and associated Schwann cells are bathed in an endoneurial fluid contained within an endoneurium sheath made of organized collagen fibers, seen in **Figure 2**. Numerous individually sheathed nerve fibers are then bundled into fascicles within a perineurium sleeve consisting of perineurial cells and concentric layers of lamellar connective tissue. Finally, multiple fascicles are encompassed by connective tissue of the epineurium which integrates blood vessels to nourish cells.

A neuron of the PNS must properly innervate a target structure, such as the spinal cord, muscle fiber, skin, or an organ in order to survive. The formation of a physical-chemical connection between the axon terminal and the target cells is called a synapse. Neurotransmitter released from the axon and neurotrophic factors released from the target structure each provide signaling cues to direct a growing axon to terminate onto the target. The presence of these chemicals is necessary for the differentiation of both the axon terminal and target structure in the creation of a synaptic junction. The continued exposure to these chemicals is also required to maintain a mature synaptic connection. Without this chemical signaling positive feedback, the axon will degenerate and cease to exist.

Once a neuron establishes a synaptic connection, the neuron can send and receive signals between the brain and body. Each axon of the PNS is ensheathed with myelin produced from Schwann cells adjacent to the axon. Small gaps are left between each bundle of myelin, called nodes of Ranvier, which expose the axon to the surrounding endoneurial fluid. The axons are polarized, meaning that the intracellular concentration of

charged ions is different from the endoneurial fluid. The internal fluid of an unstimulated axon has more negatively charged molecules with a typical resting potential of approximately -70 mV compared to the outer fluid. An action potential is generated when neurotransmitters at a synapse initiate an increase in positive charge on the membrane. This membrane depolarization causes a sudden influx of positively charged ions (Na^+) through voltage gated ion channels and an equally sudden re-polarization of the membrane (K^+ efflux). The spike in ion flux at the nodes propagates the action potential from one end of the neuron towards an axon innervating a target structure (**Figure 3**).

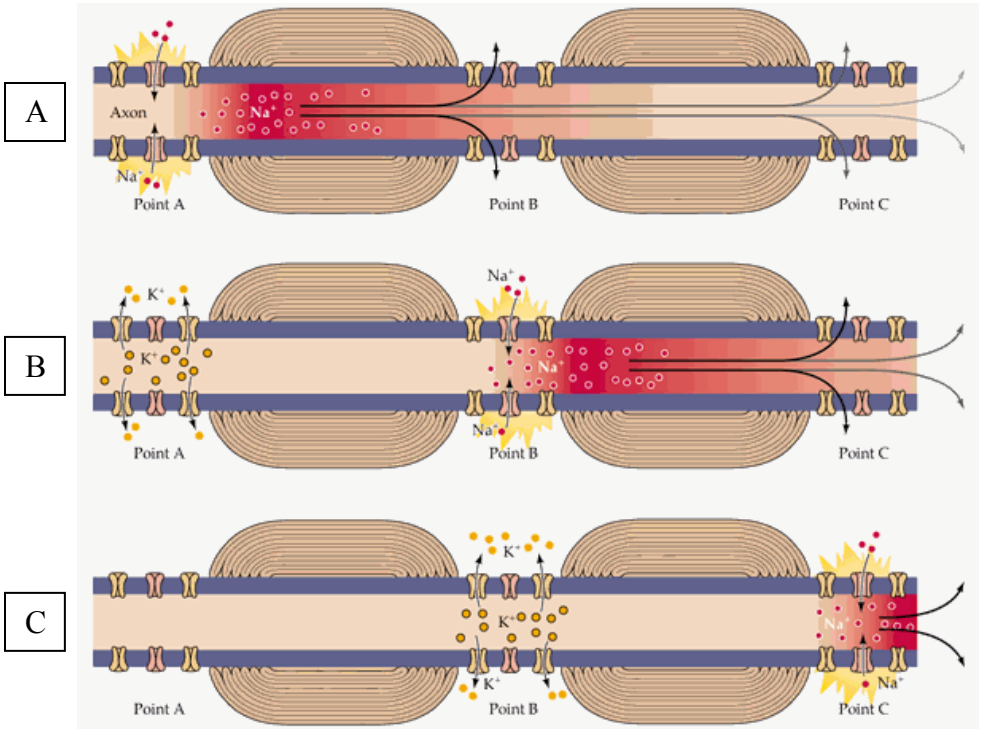

Figure 3. This diagram illustrates the events occurring during an action potential through a longitudinal section of a myelinated axon. The progression of action potential moves from A to B to C, creating a wave of Na^+ influx and sequential release of K^+ before resetting the voltage gated ion channels. (Lodish et al. 2007)

It should be noted that this balance of ionic concentrations inside and outside the neuron is essential for cell function, not only for action potential propagation but also for general cell interaction with its environment. Changes in the electric potential can result in changes in cell behavior.

2.1.2 Axon growth

Growing axons along a pathway towards its target structure can extend over great distances without innervating an incorrect target. The pathway provides diverse growth cues for the cell to follow and the axon has a complementary set of receptors to recognize and interpret the cues. The intricate interplay of the axon and its environment allows it to bypass infinite potential inappropriate connections before finally reaching its destination.

The growth of an axon develops from a series of cytoskeletal polymerizations in response to the presence of growth cues in its surrounding. The skeletal structure of a neuron is framed with larger microtubules that extend the length of the neuron and are key to developing the shape of the soma and neural processes. Intermediate-sized neurofilaments are more numerous than microtubules and form a strong scaffold for axon structure. Actin microfilaments are the smallest of the three and are found in various stages of polymerized and depolymerized states at the periphery of the neuron. Actin is highly concentrated in the extending edges and sharp protrusions from the cell's body, called the lamellipodia and filopodia, respectively. Actin is prominent at the tip of a growing axon known as the growth cone. The cytoskeletal structures have polar regions, so naturally complex with each other and various cellular proteins, creating a stable

polymerized state. The location and organization of these proteins in a neuron are depicted in **Figure 4**.

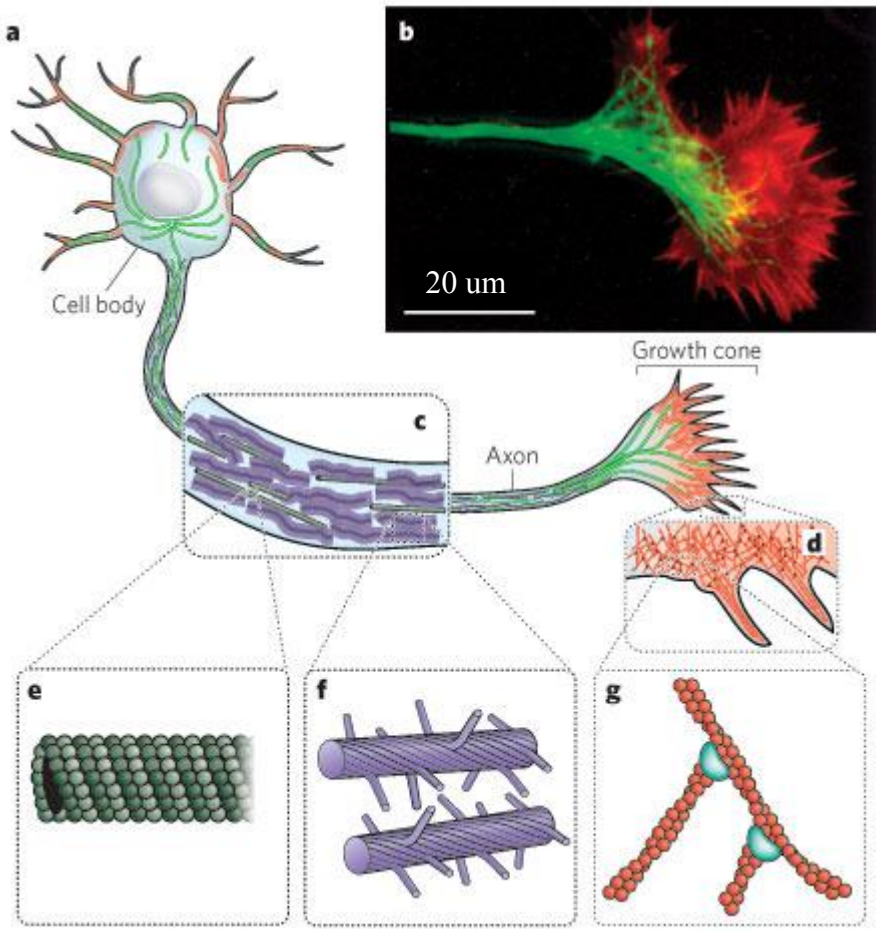

Figure 4. The cytoskeletal structures of a neuron are highly organized because of their specific functions in cell growth. (A,B) The three main components of the cytoskeleton consist of microtubules (green), intermediate neurofilaments (purple), and actin microfilaments (red). (C,D) The axon consists of microtubules and a higher concentration of neurofilaments whereas the edges of the growth cone mainly consists of actin. (E,F,G) Each of the three structures has a unique microstructure which dictates their thickness and stability as a role in axon growth (Fletcher and Mullins 2010)

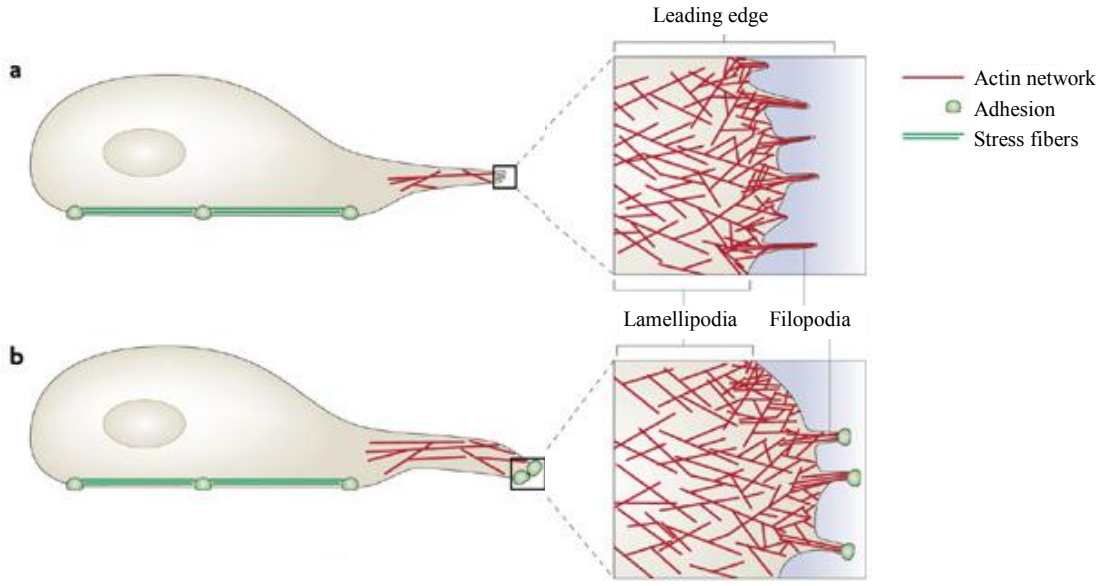

Figure 5. A cell typically extends lamellipodia and filopodia to adhere to its surrounding. (A) The actin microfilament network at the growth cone project filopodia outwards to sample the environment. (B) Once a receptor binds to an adhesion marker, the actin polymerizes and creates a cascade in the cell to designate the next step. Depending on the chemical, the cell projection may extend further or the entire cell may migrate. (Mattila and Lappalainen 2008)

Axon growth is determined by the selective response of the growth cone to cues found in its immediate environment. Physical cues presents the cell with a topological map in which the axon can easily attach and continue to creep along a pathway. Chemical cues provide a push-pull mechanism to direct growth cone orientation with the presence of chemoattractive and chemorepulsive molecules. Cells respond to these cues through activation of highly selective receptors that respond to specific stimuli, such that axons from a nerve fiber do not innervate the incorrect structure. Integrin receptors in the growth cone adhere to the extracellular matrix (ECM) proteins and the actin network then

polymerize to permit axon elongation, as in **Figure 5**. As the tip elongates, more cytoskeleton from the soma is extended into the axon, pushing growth forward. It is this harmony of cues surrounding the growth cone that directs the axon towards a specific destination.

2.1.3 Nerve regeneration

Because axons are typically much longer than the neuron body, damage to the nervous system usually involves injury of the axon and surrounding glial tissue. This is particularly true for the PNS because the neuron body is located at the spine and the axon extends out into the extremities of the body where injuries commonly occur. Nerve injuries can be classified by the amount of physical damage sustained, nerve function remaining, and the nerve's ability to naturally heal. A pinched nerve that will cause a leg to "fall asleep" may be considered as a low grade injury whereas a fully transected nerve would be labeled a high grade injury. For these extreme cases where the axons, Schwann cells, and connective tissue are damaged, the consequences are numerous.

In a full transection, the axon is separated into a proximal segment remaining intact to the soma and a distal end isolated from the soma. The proximal stump may survive the injury because the soma continues to supply metabolic energy to the axon, however, cell death will occur in some cases because of the sudden change in metabolic requirements, reorganization of organelles, and loss of target-derived trophic factors. Without an energy source, the distal stump will ultimately undergo Wallerian degeneration – the detached axon and surrounding myelin will degrade and become

phagocytized. The target structure, without input from a neuron, may atrophy and die as well. The damaged neuron will undergo a series of reactions, changing its morphology and metabolic processes. This response is reversible, but if regeneration of the axon to its target is not successful, the neuron will eventually die. Finally, a damaged neuron may retract all of its synaptic connections and infiltrating glia isolate the cell, leading to cell death.

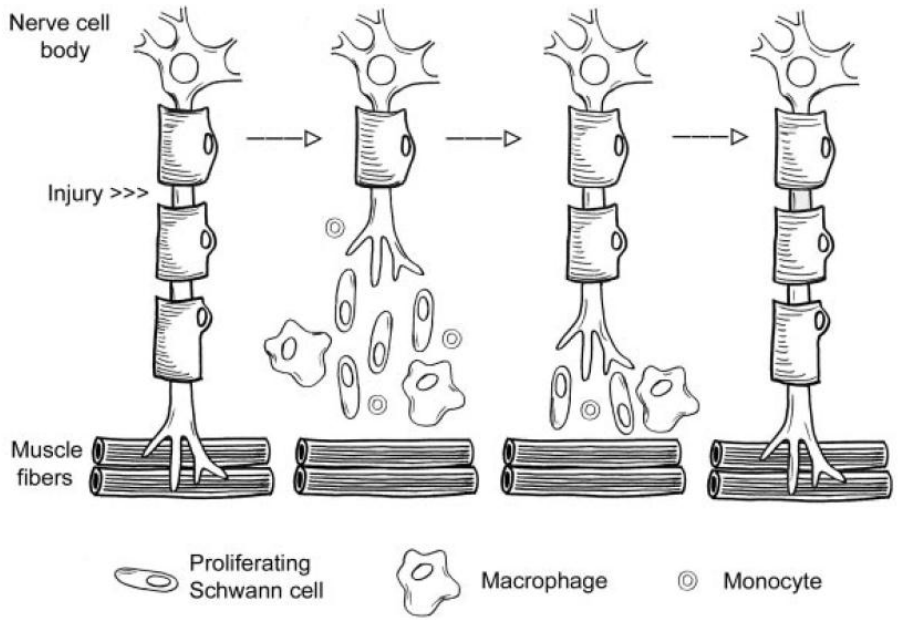

Figure 6. A myelinated peripheral neuron innervating a muscle follows several stages of regeneration after injury before complete reconnection with the target muscle fiber. After an injury to the axon, macrophages and monocytes clear up cellular debris from the degenerated distal end. Schwann cells remain in the vicinity of the nerve pathway, releasing chemical signals to attract the axon to regrow through the same pathway. (Bahr and Bonhoeffer 1994)

If the site of injury is large, glia and cells of the immune system may infiltrate the injured site in attempt to clear cellular debris and protect the body from further damage,

as shown in **Figure 6**. However, heavy infiltration leads to formation of a glial scar between the proximal and distal ends, preventing the axon from returning through the endothelial path. If the injury site and distal segment are properly cleared without glial scarring, axonal sprouts from the proximal stump will be able to cross the injury site. On the distal end, macrophages clear leftover cell debris, usually leaving the ECM intact. The ECM promotes axon growth and the remaining glial cells secrete chemotropic factors, further attracting axons through the distal tract. Axons can grow at a rate of 5 mm/day until they reach their destination where they form new nerve endings to reinnervate the target tissue. The axon will be remyelinated and metabolic activity supporting signal transmission returns, allowing the neuron to revert back to its original functional state.

2.2 NERVE REPAIR

2.2.1 Current clinical practice for nerve repair

The goal of current nerve regenerative therapies is not to guide axons all the way to their target, but to promote axon growth across an injury during the crucial healing period. Natural nerve regeneration occurs under ideal conditions where the gap is small between the proximal and distal ends of a damaged nerve. If there are no foreign bodies or glial scarring at the site, an axon has a chance to bridge the gap between the severed ends. The regrowing axon can follow native cues through the endoneurial tube of the distal segment towards its target without further intervention.

When a nerve is severed and the gap separating the proximal and distal sections is sufficiently small, end-to-end anastomosis may be performed if the nerve ends are adjacent and can be sutured together without causing tension, as in **Figure 7**. Axonal sprouts from the proximal end may grow directly into the distal end with minimal interference. If the gap is too large, suturing will place tension on the nerves, inhibiting nerve regeneration.

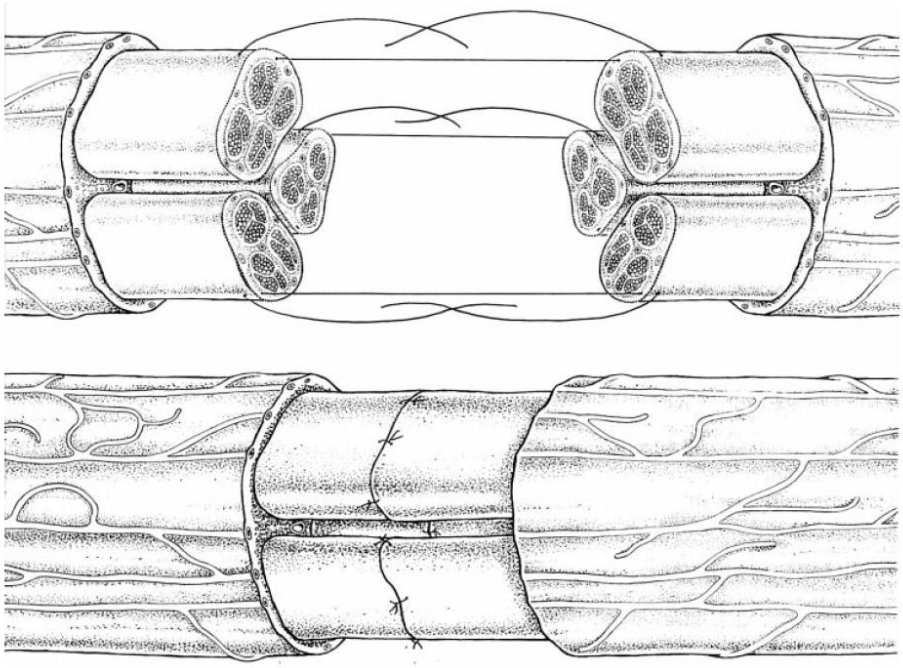

Figure 7. If the proximal and distal ends of a severed nerve are close enough and fasciculi are aligned appropriately, successful nerve regeneration can result from anastomosis of the nerve fiber through suturing of the perineurium and epineurium. (Lundborg 2000)

Another option for larger gaps is to perform autologous nerve grafting where a nerve is harvested elsewhere in the body and used to fill in the gap between the severed

ends of the injury site. Successful axonal regeneration across the graft has been attributed to the presence of Schwann cells found in healthy nerves which help guide axon growth. Aligned nerve bundles and cellular topography provide physical cues while ECM proteins and growth factors provide chemical cues for neural development. Moreover, replacement of the injured nerve with a healthy autograft promotes unhindered axon growth because of decreased immunological response at the damaged site and reduced scar tissue formation.

Although the use of an autologous graft to replace a nerve defect is the current clinical gold standard for damaged nerve repair, the necessity for multiple surgeries and loss of function at the donor site limits the procedure's overall efficacy. Furthermore, lack of success is attributed to poor axon development through the guide: thin axon cross-section, low axon density, misaligned axon steering, infections, and poor reconnection to structures beyond the guide can lead to poor functional reinnervation. The pitfalls linked with autologous nerve grafts have spurred the exploration for new approaches in nerve regeneration.

2.2.2 Alternative strategies for nerve repair

Because nerve regeneration is complex, various strategies have been approached to combat the issue. Researchers have developed therapies that mimic axogenic environments using chemical, cellular, physical, and electrical cues to guide axon growth across the nerve injury (Schmidt and Leach 2003, Yu et al. 2008). Although each strategy shows promise as an alternative solution to autologous nerve grafts, the current

studies presented will focus on electrical stimulation using a synthetic cell substrate. Thus, a brief review of chemical and cellular cues will precede a more detailed examination of physical and electrical cues.

2.2.2.1 Chemical guidance

During axogenesis, a host of biochemical cues are required for proper growth, guidance, and survival of the developing axon. Neurons respond to two groups of growth cues: neurotrophic and chemotropic factors. Trophic factors such as nerve growth factor (NGF), brain-derived neurotrophic factor (BDNF), neurotrophin-3 (NT-3), and neurotrophin-4/5 (NT-4/5) are proteins critical for cell maintenance and continued survival. Tropic factors that include netrins (chemoattractant), semaphorins (chemorepellant), and ephrins (combinatory) work together in steering axon cone growth through a "push and pull" (attraction and repulsion) mechanism. Neurons, glia, and target cells that make up the environment produce these guidance cues and direct axon growth by extracellular secretion of molecules or through direct cell surface contact with the axon.

Since its discovery in the 1950s, NGF has been intensively characterized because of the crucial role it plays in neuronal cell proliferation and neurite outgrowth (Lewin and Barde 1996). Primary explants of neuronal tissue such as dorsal root ganglia require NGF in order to survive in tissue culture while other cells such as rat adrenal pheochromocytoma PC12 cells can only differentiate and extend neurites when exposed

to NGF, as shown in **Figure 8**. Researchers have taken advantage of this dramatic cell response to neurotrophins by integrating them into implantable nerve repair devices.

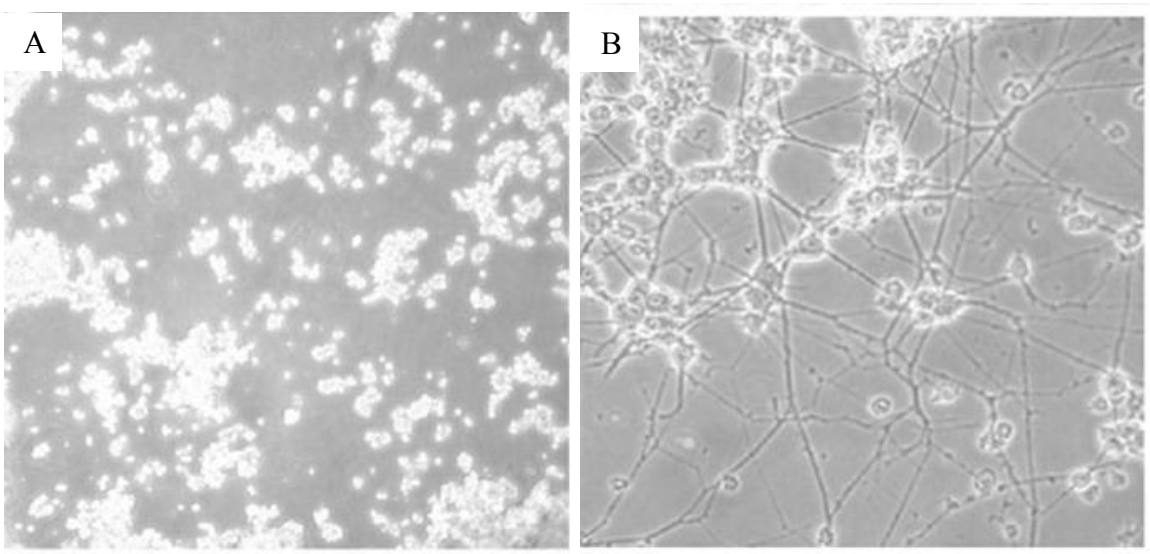

Figure 8. Nerve growth factor (NGF) has a dramatic genotypic and phenotypic effect on PC12 cells. (A) PC12 cells without NGF are circular in shape and clumped together. (B) With NGF exposure, PC12 cells differentiate into a neuronal phenotype, extending a network of neurites. Magnification 200x. (Zhang et al. 2007)

Pfister et al. (2008) created a nerve conduit that would slowly release NGF into the lumen by slow degradation of the inner layer. When placing PC12 cells in the conduit, they were able to control cell differentiation in vitro by manipulating the release rate of the device. Gomez and Schmidt (2006) found that immobilized NGF on electrically conductive polypyrrole substrates significantly increased the ratio of cells with neurites compared to negative controls without NGF, although the immobilization was not as effective as solubilized NGF. Detailed studies of other neurotrophins and their vital role in nerve regeneration can be found in Calabrese's (2008) recent review

and **Table 1** lists more recognized neurotrophic factors and their effects on neural cell behavior (Schmidt and Leach 2003). Although cell response to neurotrophic factors has been dramatically positive, drawbacks including extensive neurite branching of uninjured axons and improper innervation present additional problems for researchers to consider.

Table 1. Brief overview of neural response to neurotrophic factors

Neural response promoted	Neurotrophic factors
Motor neuron survival	BDNF, NT-3, NT-4/5, CNTF, GDNF
Motor neuron outgrowth	BDNF, NT-3, NT-4/5, CNTF, GDNF
Sensory neuron survival	NGF, NT-4/5, GDNF
Sensory neuron outgrowth	NGF, BDNF, NT-3
Spinal cord regeneration	NGF, NT-3, CNTF, FGFs
Peripheral nerve regeneration	NGF, NT-3, NT-4/5, CNTF, GDNF, FGFs
Sensory nerve growth across the PNS-CNS transition zone	NGF, NT-3, GDNF, FGFs

Neurotrophic factors play multiple roles in guiding neural behavior, often having synergistic effects on cells. (Schmidt and Leach 2003)
BDNF - Brain-derived neurotrophic factor
CNTF - ciliary neurotrophic factor
FGF - fibroblast growth factors
GDNF - glial cell line-derived growth factor
NGF - nerve growth factor
NT-3 - neurotrophin-3
NT-4/5 - neurotrophin-4/5

Applying chemotropic factors to in vitro cultures have also been effective to promote axon growth. Tropic factors are not involved in survival cues like NGF, rather,

they provide attractive cues to guide axon growth towards them or repulsive cues to veer axon growth away, as depicted in **Figure 9**.

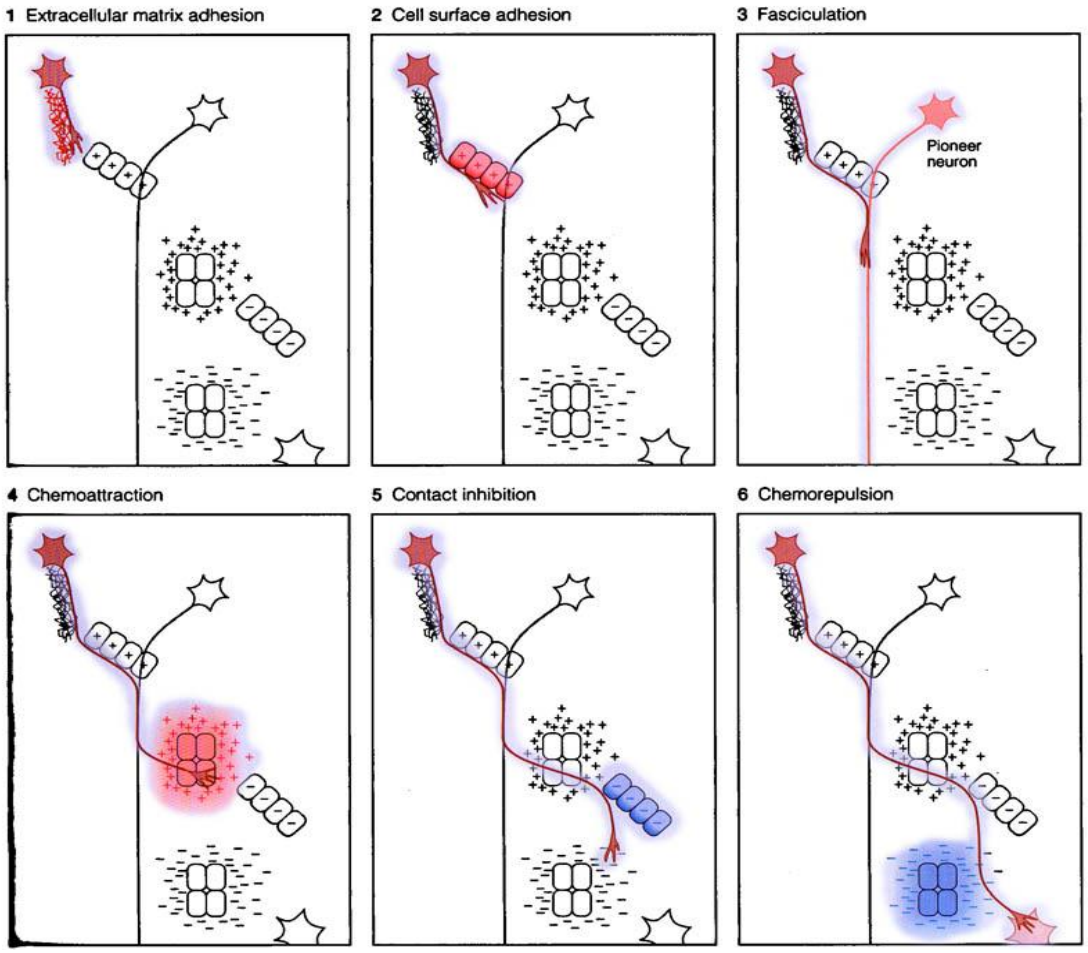

Figure 9. Guidance cues exhibit various roles that direct developing axons towards a target. Molecular cues in the interstitial fluid and contact cues on surfaces of tissues can attract or repel the axon growth cone. The diagram features six common chemical growth cues that axons face while exploring its environment. (adapted from Kandel et al. 2000)

An interesting example of this complex interplay of chemotropic factors occur during the corticospinal tract innervation of the spinal cord which fully matures

postnatally (Canty and Murphy 2008). Because axons originating from the cortex must span through the mid and lower brain before coming in contact with the spine, each cell type and layer of tissue must guide the axon in the correct direction. It is amazing that axons can traverse across multiple layers of tissue and correctly innervate the spine since the spatio-temporal cues must be orchestrated perfectly when there are many choices and paths the axons can take during its development.

Kuffler (1996) discusses that use of tropic cues for cell engineering is possible but will be difficult to topographically map in vivo. Additional information about chemotropic factors and their role in CNS development is presented in Curinga and Smith's (2008) recent review. Consideration of cue expression patterns and altered biochemical environment of the injured nerve is necessary to avoid disruption of endogenous attempts to heal, which make this task even more daunting. However, current studies demonstrate that spatial patterning and controlled release of neurotrophic factors are able to direct axon growth.

2.2.2.2 Cellular guidance

Successful axogenesis is a process requiring the correct spatio-temporal presentation of ECM, growth cues, and axon guidance cues. Under natural conditions, cells surrounding an axon's growth cone provide growth cues by secreting soluble extracellular molecules and by presenting cell surface contact cues. It would be logical that nerve repair therapies integrate these types of supportive cells as part of the solution.

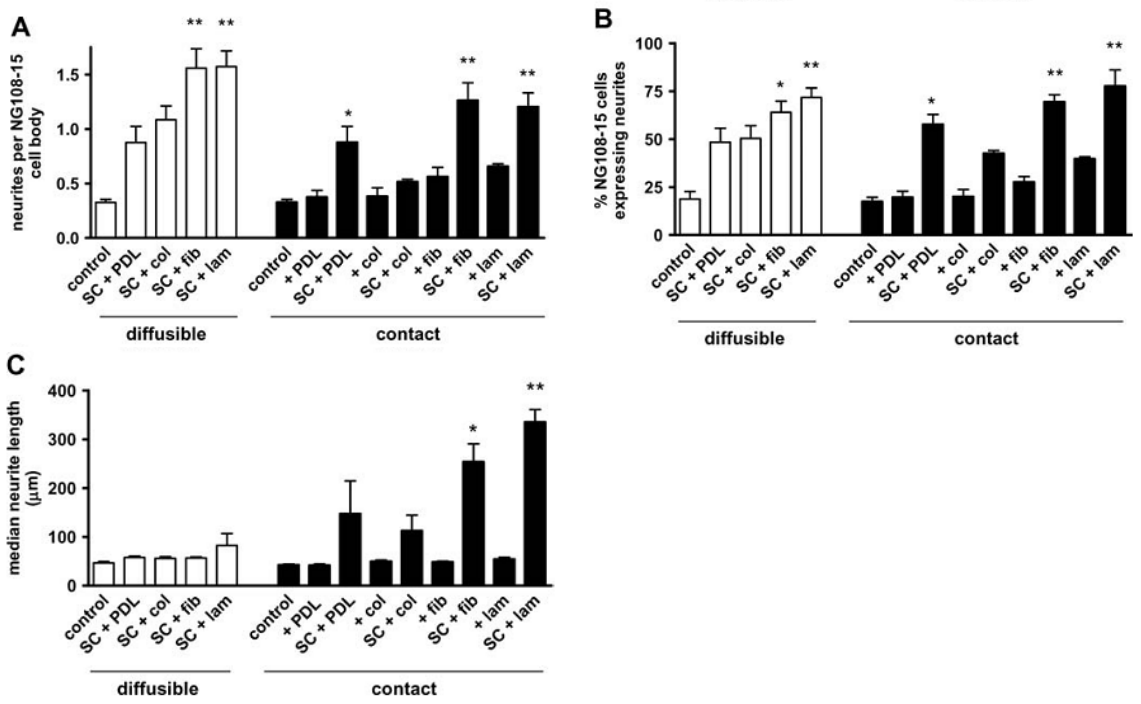

Figure 10. Neurite outgrowth from NG108-15 cells when cultured with Schwann cells seeded on various ECM molecules show a change in number depending upon glial contact. Leftmost white bars represent neurite growth with diffusible secretions from Schwann cell co-cultures. Rightmost black bars represent neurite growth when in physical contact with Schwann cells. Neurites per cell (A), percent of cells expressing neurites (B), and median neurite length (C) are depicted. SC = Schwann cells, PDL = poly-D-lysine, col = collagen, fib = fibronectin, lam = laminin (Armstrong et al. 2007)

A study performed by Armstrong et al. (2007) demonstrated that Schwann cells co-cultured with mouse neuroblastoma – rat glioma NG108-15 cells resulted in different cell behavior when cultured with or without cell contact. When Schwann cells were physically isolated such that NG108-15 were only exposed to secreted soluble factors, the percent of neuronal cells extending neurites significantly increased by over 70%. Moreover, when Schwann cells were co-cultured in direct contact with NG108-15 cells, the percent of cells extending neurites was again over 70% plus neurite length increased

from 40 um in control cultures versus 334 um in co-cultures, shown in **Figure 10**. This two-level improvement compared to control values indicates that presence of supporting glia provides soluble and physical guidance cues favoring axon regeneration.

Use of astrocytes, stem cells, and olfactory sheathing cells (Alexander et al. 2006, Schmidt and Leach 2003) has also been successfully incorporated into nerve repair strategies, suggesting that axon pathfinding is not completely dependent upon neighboring cell type but may respond to a variety of recognizable cues.

2.2.2.3 Physical guidance

In addition to chemical or biological cues, growth cones extending from an axon can be shaped and influenced by the physical constraints surrounding it. By manipulating the surface profile surrounding a cell, scientists can present topological cues for the cell to explore.

Mimicking microscale structures (e.g. glial cell morphology) and micropatterning of the substrate have been shown to induce preferential alignment of neural cells (Miller et al. 2002, Li and Folch 2005). Hoffman-Kim's group created synthetic polymers templated with Schwann cell topology by aligning Schwann cells using laminin micropatterns, then fixing the culture with paraformaldehyde and pouring poly(dimethyl siloxane) (PDMS) on the solidified cells, shown in **Figure 11** (Bruder et al. 2007, Richardson et al. 2011). When removed, the PDMS molds accurately outlined the microscale features of the aligned Schwann cells. When dorsal root ganglia (DRG)

neurons were placed on the polymer template, growing axons extended in an aligned pattern guided by the substrate topology.

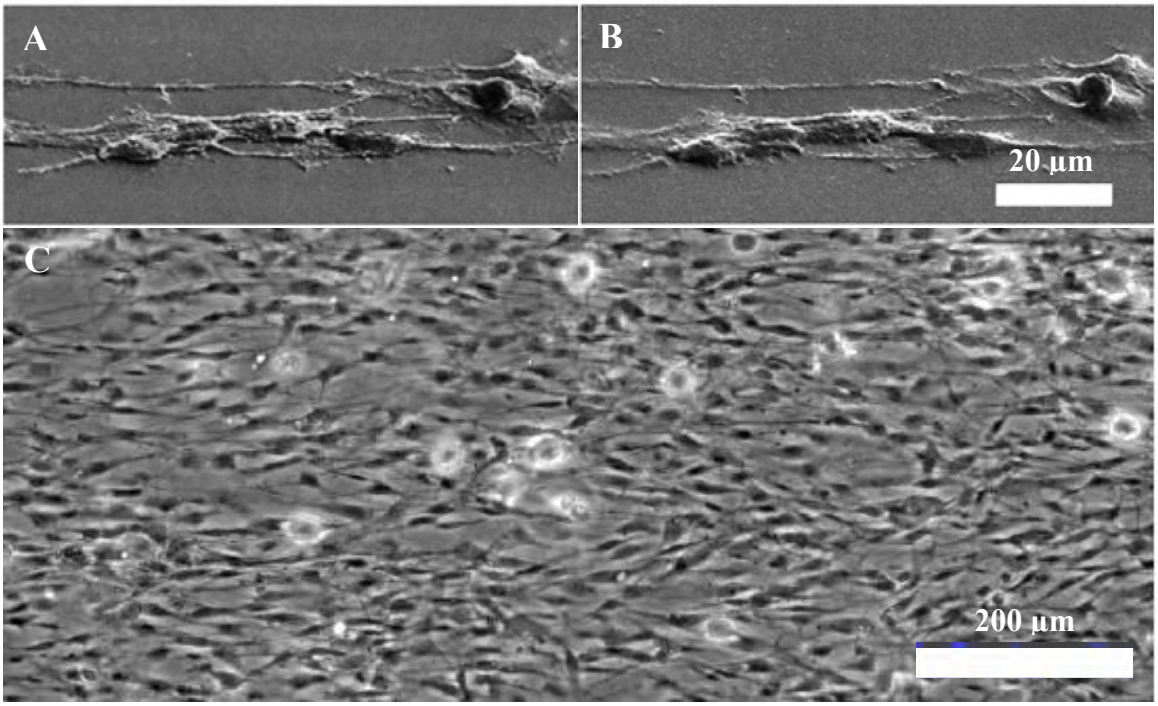

Figure 11. Exposing neurons to polymer templates of patterned glial cell cultures is effective for aligning neurite growth. (A) An SEM image of Schwann cells growing on a laminin-patterned surface shows alignment of cultures. (B) SEM image of a PDMS mold from the cell culture from image A shows that small topological features can be accurately templated into the polymer. (C) When adding DRG neurons on top of the templated polymer, the neurites exhibit alignment mirroring the underlying substrate. (Bruder et al. 2007)

Using photolithography, Mahoney, et al. (2005), etched microchannel wells of various wall heights and widths on polymers to mimic two-dimensional space of an endoneurium, as shown in **Figure 12**. In vitro experiments using neuron-like PC12 cells demonstrated that micropatterned wells of 10-30 µm in width enhanced orientation and

speed of axonal extension inside the wells (Rutkowski et al. 2004). It was hypothesized that fibers in the filipodia are not elastic enough to bend orthogonal to their projection, so when they hit a wall, their extensions can only continue along the well, and not traverse up the wall. This manner of restriction confirms that cells can be controlled by small features in its physical environment.

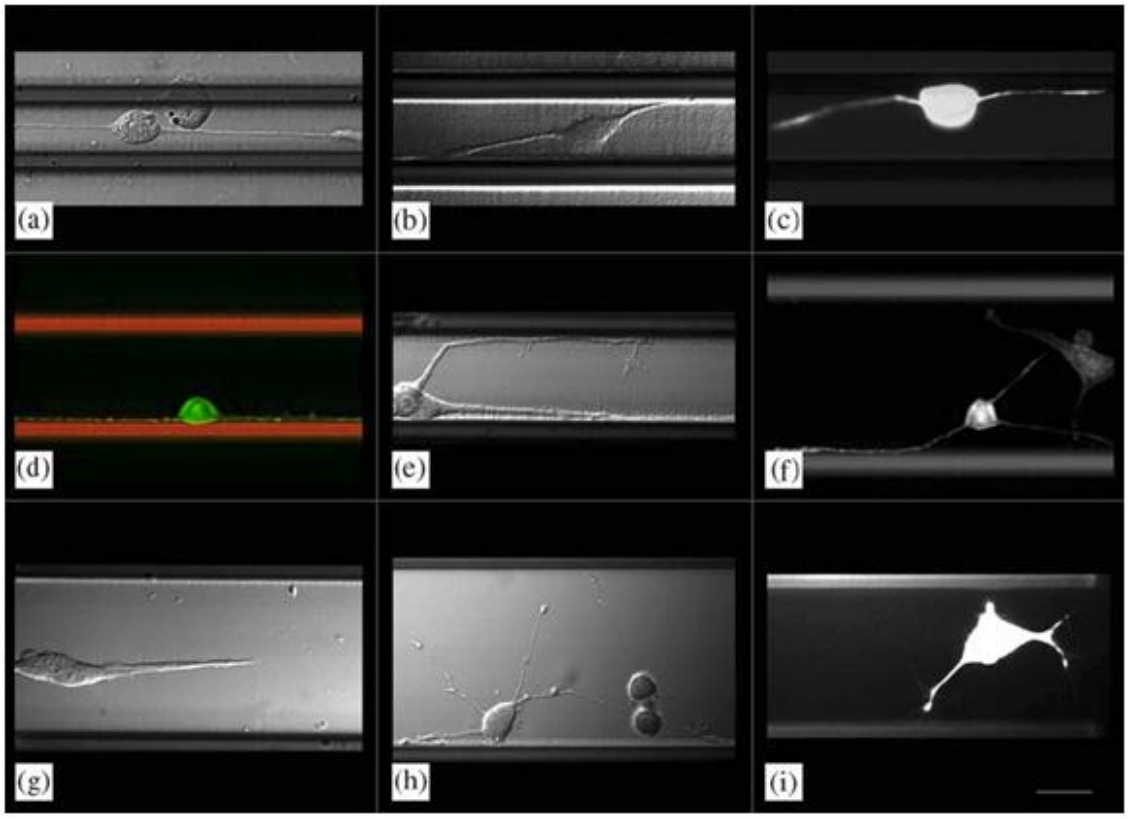

Figure 12. PC12 cells cultured for 3 days on polyimide microchannels of various widths demonstrate neurite extension along the edges of the channels. (a) 20µm, (b,c) 30µm, (d,e) 40µm, (f,g,i) 50µm, and (h) 60µm. (Mahoney et al. 2005)

In damaged nerves of the PNS, axons are physically guided back to the sites it once innervated by retracing the endoneurial tube through the distal stump. Similarly, conduits that bridge the two ends of an axotomized nerve constrain axon growth in an axial direction and prevent axons from wandering astray. An enclosed cylinder can guide chemotropic molecules secreted from the distal axon stump towards the proximal stump and can also prevent cell infiltration, preventing glial scarring at the injury site.

To assess cellular restrictions in a three-dimensional environment, neurons were cultured on the surface of cylindrical rods and within the lumens of hollow tubes (Duchet et al. 1998, Hadlock et al. 2000, Yu and Shoichet 2005). Parallel rods provide a high surface area for cell attachment and space for cells and nutrients to penetrate into the scaffold between rods. Scaffolds with aligned hollow tubules direct cell growth axially within the lumen, similar to microchannel wells discussed previously. Individual tubules can be synthesized and banded together like a nerve bundle, or pores can be bored through blocks of polymer as shown in **Figure 13**. Hadlock, et al., performed an in vivo comparison of axon fiber widths of DRG growing through porous block polymers versus growing through autologous nerve grafts. The group found that DRG axons had larger diameters when traversing through the synthetic conduits compared to using an autograft (3.73 mm compared to 2.54 mm in diameter).

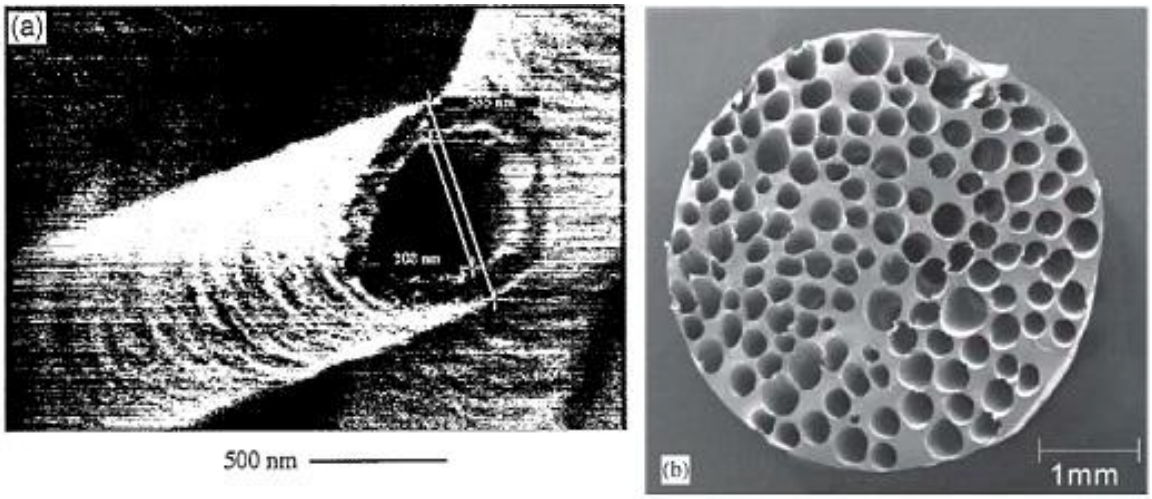

Figure 13. A pair of SEM images of synthetic conduits shows the ability to vary the pore size for nerve repair. (A) Hollow tubules of several hundred nanometers in diameter and (B) a porous block polymer with channels several hundred micrometers in diameter both mimic the native endoneurium. (Duchet et al. 1998)

The most natural conduit for axons to grow through would be through the distal end of a severed nerve. When this is not possible another nerve from one's own body is the next best alternative, however, harvesting autologous tissue necessitates donor site morbidity (loss of function at the donor site) and there is a limited supply for graft retrieval. To avoid this issue, use of allogenic and xenogenic tissue have gained attention. In order for nonautologous tissue to be used, grafts must be rendered sterile and nonimmunogenic to prevent disease transmission. This process of decellularization typically involves use of detergents to remove all traces of cells and nucleic acids. Additionally, the processing must be gentle enough to retain structural integrity and preserve ECM components within the nerve graft.

Work done by Hudson et al. (2004) demonstrated that detergent treatment of allogenic nerves can selectively remove immunogenic components with low ECM

disturbance (**Figure 14**). The author's "optimized acellular grafts" were sutured between a transected sciatic nerve of a Harland Sprague Dawley rat and given 28 days or 84 days for axonal regeneration before harvesting for histological comparisons. In comparing axon density in cross sections of the grafts, it was shown that acellular graft performed as well or better than fresh isografts. The authors also showed that their optimized nerve processing effectively removed immunogenic components while retaining the native matrix structure.

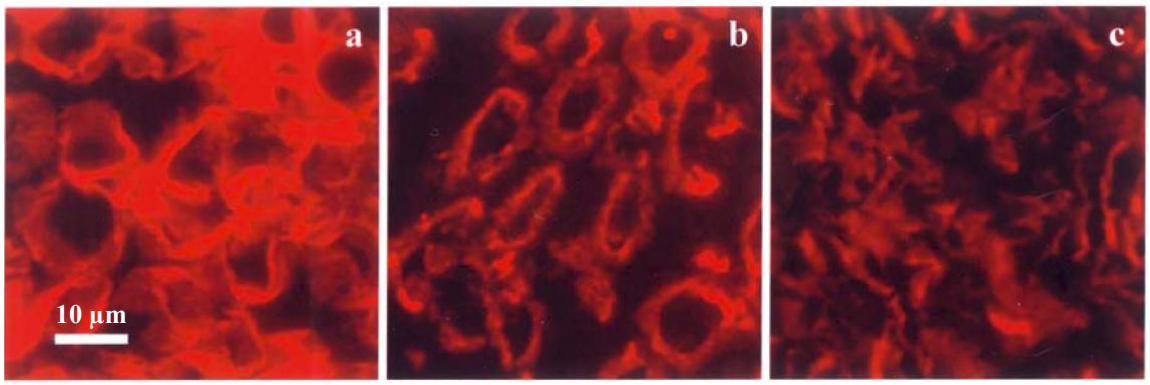

Figure 14. Laminin protein stains in a cross section of nerve tissue show the basal lamina integrity of (A) fresh nerve tissue, (B) the author's optimized decellularization method, and (C) older Sondell protocol for tissue decellularization. The figure demonstrates that the process of removing cells is detrimental but can be optimized for minimal damage to native architecture and protein content. (Hudson et al. 2004)

Physical guidance cues mimic the nerve's endoneurial structure, providing a simulated environment conducive to axon regeneration. Additionally, conduits can funnel biochemical cues across nerve injuries between the distal and proximal ends, while preventing infiltration of growth-inhibiting cells. Alternative nerve guides such as synthetic conduits and acellular nerve grafts are able to circumvent some of the

limitations found in autologous nerve grafts. Incorporating physical guidance as part of neural regenerative therapy may be a crucial aspect to improve the efficacy of nerve repair.

2.2.2.4 Electrical guidance

An electric field (EF) is defined as a space surrounding an electrically charged object or time-varying magnetic field. The EF describes the force exerted on another charged particle when placed within this space. For example, the EF surrounding a positively charged particle can be described as a field of radial vectors pointing away from the source charge. When another electrically charged particle is placed in this EF, the second particle can be attracted or repelled from the source charge at a force described by the EF, shown in **Figure 15**. This can also be exemplified with charged molecules within the body. A region with a higher concentration of Na^+ and K^+ produces an EF such that cations like Ca^{2+} would be pushed away while anions like Cl^- would be pulled into the region. Simply put, an endogenous EF is created when there is an unbalance of electrical charge in the body.

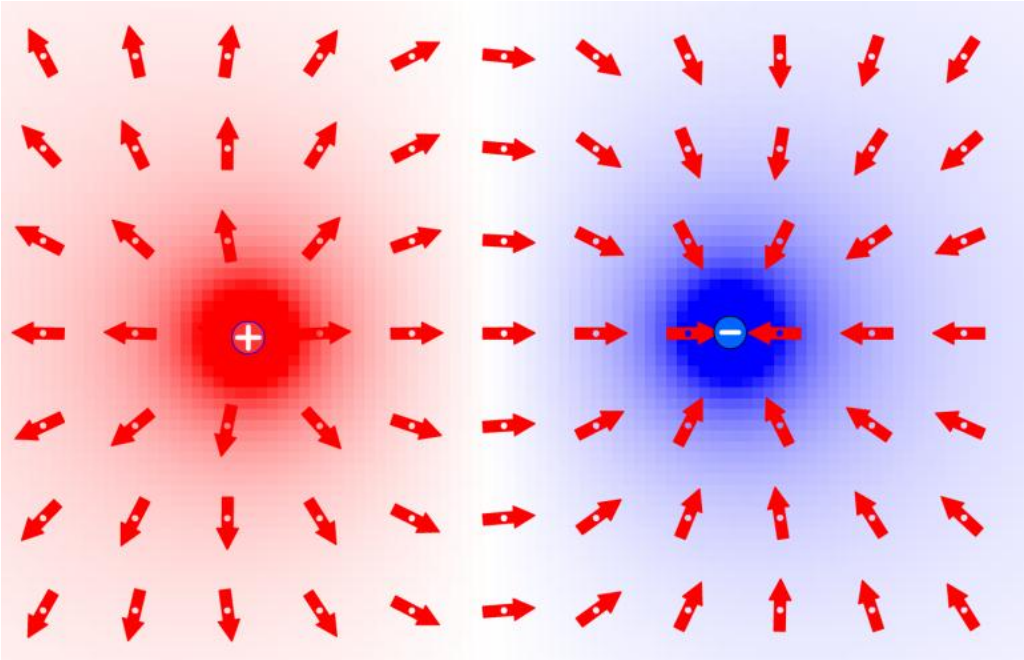

Figure 15. The EF vectors surrounding a positive and negative point charge is represented with red arrows. If another positive charge is placed in this EF, the force applied to the particle is described by the red arrows drawn. (modeled with an EF simulator by Dubson 2011)

Separation and movement of charged molecules within a cell's local environment create a natural EF in the fluid. This is evident during embryological development, where surges in cell activity create extreme differences in biochemical concentrations throughout the body. EF strengths up to 1600 mV/mm have been found along the neural tube of developing posterior end of amphibian and avian embryos (Hotary and Robinson 1994, Shi and Borgens 1995). It is theorized that endogenous EF provides a spatio-temporal electrical cue that is essential to neural migration and axon extension. McCaig et al. (2002) depicted the voltages measured across various structures along the neural tube of a Xenopus embryo, **Figure 16**, indicating the dynamic range of the EF. Because cells define their function by continuously interacting with their environment, disruption

of the EF during the embryonic stage led to developmental abnormalities (Hotary and Robinson 1994, Metcalf and Borgens 1994).

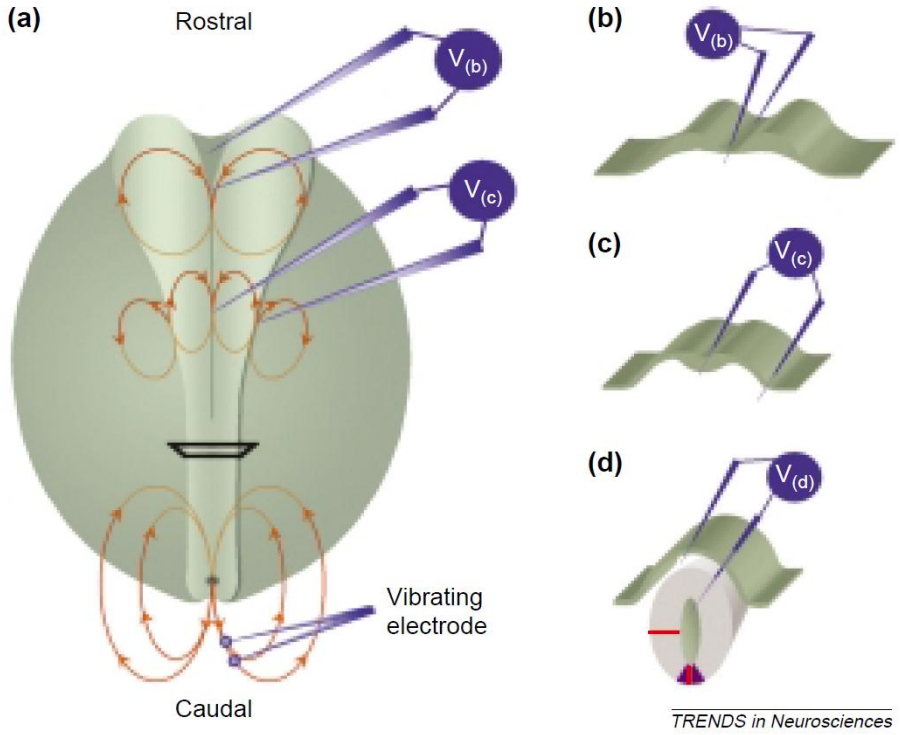

Figure 16. (A) Schematic diagram showing the extracellular electric fields (EF) found during embryonic development of an amphibian neural tube. Electrodes were placed at various tissue folds (B,C,D) to measure EF ranging 18 - 1600 mV/mm depending upon amphibian species and location on the neural tube. (McCaig et al. 2002)

Skin epithelium creates an electrical potential by separating ions on opposing sides of the tissue, however, tissue injury disrupts the epithelium barrier, creating an ionic current flowing between the two sides. The presence of the EF surrounding the wound and between the two layers provides a continuous ionic current until the epithelium layer closes the gap (**Figure 17**) to restore the native electric potential. Since the EF plays a

significant role in tissue development and wound-healing, control of the electrical gradient may allow us to control tissue regeneration.

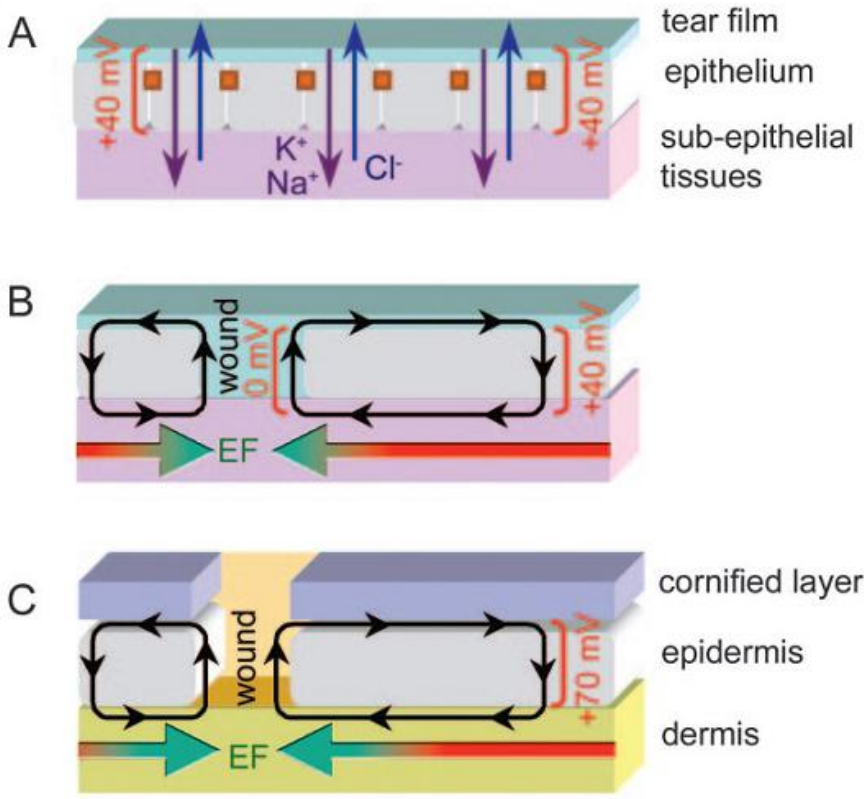

Figure 17. Epithelial cells create an electric potential on opposite sides of the tissue using an ion pump when functioning normally (A). An ionic current is generated in a wounded mammalian corneal epithelium (B) and mammalian skin (C). Electrodes placed at various areas surrounding the wounded tissue measured EFs parallel and perpendicular to the wound. (McCaig et al. 2005)

In early studies, Borgens (1999) partially incised the spinal cord of adult female guinea pigs and implanted a silicone rubber tube guidance channel between the gap so that neural tissue covered both ends of the tube. A battery-powered electrode producing 2.5mV/mm across the tube was inserted subcutaneously to maintain an electric field over

the period of 1-2 months. It was found that there was an increase in neural regeneration and axonal growth axially into the tube compared to controls where there was no electric field applied across the silicone tube.

Cells respond differently to various EF parameters including current direction, current strength, voltage, frequency, orientation, pulse load, early/late stimulation (after injury), and total duration, however thorough characterization of cell response to variations in EF has not been performed. Geremia, et al. (2007) applied a continuous 20 Hz electric field with a 3 V, 100 us pulse, for 1 hour to 14 days around transected femoral nerve enveloped in a silastic nerve cuff (**Figure 18**). The femoral nerves of young adult female Sprague Dawley rats showed improved axon density and realignment under short stimulation times compared to transected femoral nerves without EF stimulation. The reasons for choosing this method of stimulation and these exact parameters for the EF have not been explained, however the work does show that more work is needed to optimize electrical signals for improved nerve repair.

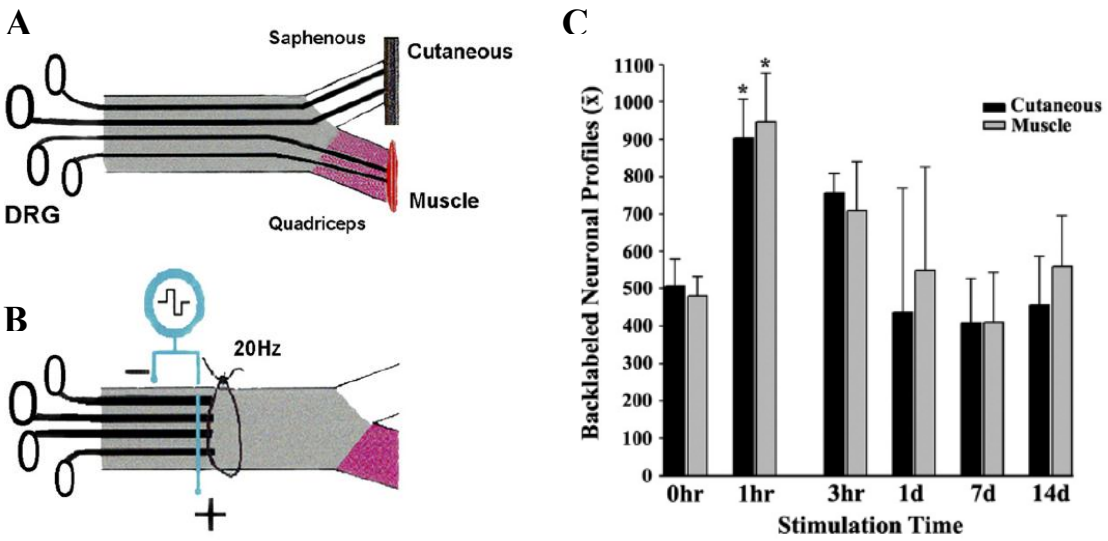

Figure 18. (A,B) An insulated wire was wrapped around a transected femoral nerve enveloped inside a silastic nerve cuff. (C) The wire was then stimulated with a 20 Hz signal for 1 hour or up to 14 days. Backlabeled neurons showed that the mean number of axons growing through the distal end increased with 1-3 hours of EF stimulation, whereas longer stimulation times resulted in no significant gains. (Geremia et al. 2007)

If cell behavior changes when exposed to an EF, there is a likelihood that intracellular processes also change. Zhao et al. (2003) observed when a physiologic 150 mV/mm EF was applied across corneal epithelial cell cultures in vitro, activation of ERK (mitogen-activated protein kinase, necessary for intracellular response to bound growth factor) and accumulation of F-actin (cytoskeleton) are found preferentially on the cathodal side of the cell (**Figure 19**). In chemotaxis, asymmetry of membrane receptors is normally found in migrating growth cones, where a gradient is found to increase towards the leading edge. But the irregular high concentration of receptors found at the cathodal edge of a cell in an EF suggests that another unknown mechanism may be involved. Similar experiments from Rajnicek et al. (2006) demonstrated that growth cones of

amphibian spinal neurons align towards the cathode during when exposed to an EF 150 mV/mm for 5 hours, as shown in **Figure 20**. Another study from the same group (Yao et al. 2009) found that neonatal rat hippocampal neurons exposed to an EF reorganized their organelles such that Golgi apparatus and centrosomes were located towards the cathodal side and cell division occurred on an axis perpendicular to the EF. These findings suggest that the EF has an effect on charged components inside the cell and on the membrane, possibly forcing the charges to separate asymmetrically, leading to cathodal steering of the growth cone and asymmetric organelle reorganization.

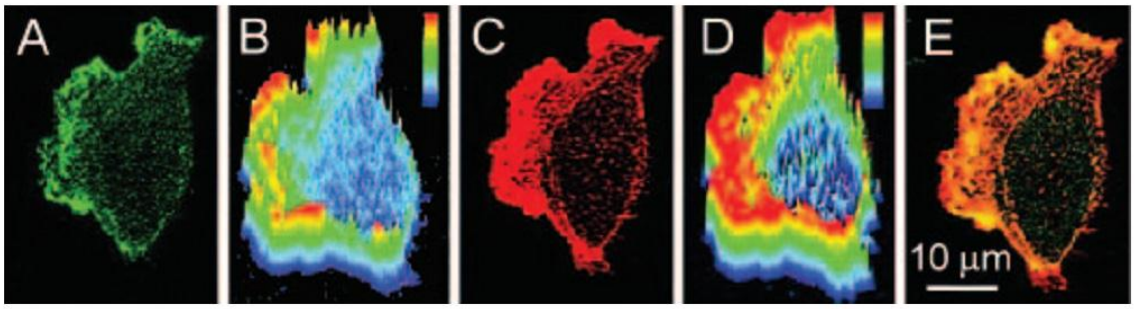

Figure 19. Asymmetry of ERK (A) and F-actin (C) staining shows preferential activation on the cathodal side of corneal epithelial cells exposed to 150 mV/mm. (B, D) shows the fluorescence intensity of the stains and (E) is the co-localization of the stains. (Zhao et al. 2003)

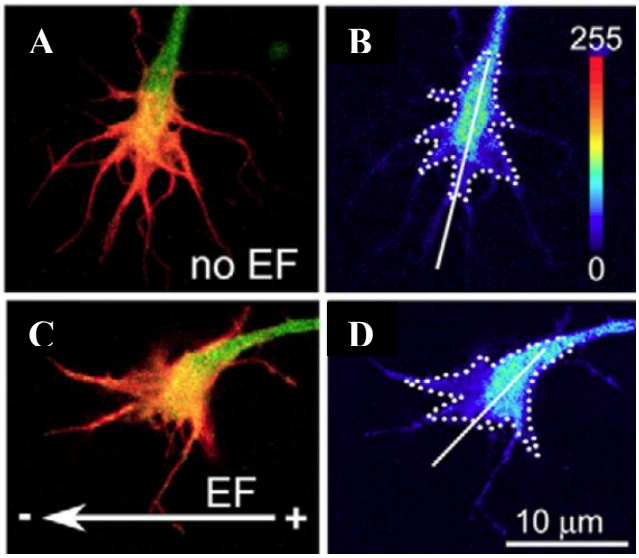

Figure 20. An electric field along the direction of the arrow of 150mV/mm caused Xenopus spinal neurons to orient after 5 hour exposure. (A,C) Neurons extend axons without EF and with EF show changes in radial projections from the growth cone (red = actin, green = RhoA stained stress fibers). (B,D) Fluorescence intensity images of A,C allow authors to calculate mean angles of the growth cone. Data indicate that cells exposed to a direct current electric field were able to reorient their filopodia and soma in the direction towards the cathode. (Rajnicek et al. 2006)

Using the same method for cell stimulation, Zhao et al. (1996) was able to control corneal epithelial cell migration in the direction of the EF. After several hours of migration in one direction, the author reversed the EF to lead the cells in the opposite direction, shown in **Figure 21**. Unlike chemotaxis where a constant release or gradient of cues need to be exposed to the cells and remain in the media, or physical guidance where the topology is permanent, controlling cell behavior with EF has greater spatio-temporal flexibility. EF can be applied in any direction and can easily be activated or inactivated like a switch.

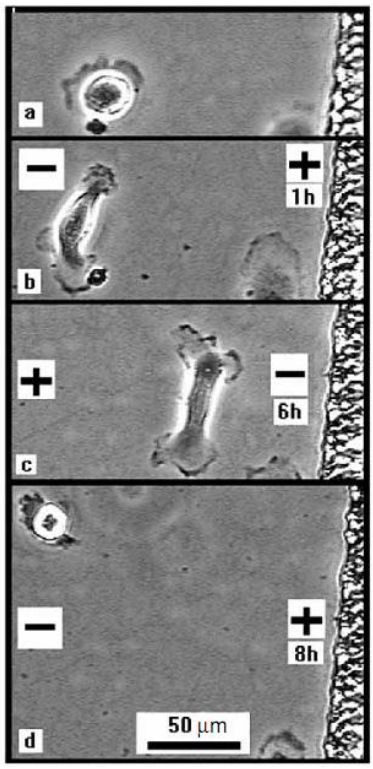

Figure 21. Cathodal steering of corneal epithelial cells in a DC EF of 150 mV/mm. (A) no EF, (B) cathode placed on the left for 1hr, (C) polarity reversed for 6hrs, and (D) polarity adjusted once more for 8hrs. The cell migrates toward the cathode each time the polarity has changed. (Zhao et al. 1996)

Almost all previous work exploring EF effect on cells follow a similar protocol by placing electrodes in the liquid to create an ionic current through the media above the cells. This may mimic the endogenous EF found in the body, but use of electrical stimulation is also interesting for bio-electrical interfaces where the substrate itself acts as a conductive medium. Schmidt et al. (1997) has shown that exposing PC12 cells to an EF perpendicular to the growing substrate enhances neurite extension after several hours of exposure (**Figure 22**). PC12 cells were supplemented with NGF to extend neurites for one week before seeding into polycarbonate wells attached onto conductive

biocompatible polypyrrole films. A 100 mV potential was applied perpendicular to the cells for 2 hours where the film served as the anode and a gold wire electrode inserted into the media served as the cathode. There were noticeably more neurites in the cultures under the short stimulation conditions. Further work by the group suggests that electrical stimulation of the substrate induced greater protein adsorption to the surface, possibly inducing greater neurite extension and attachment (Kotwal and Schmidt 2001).

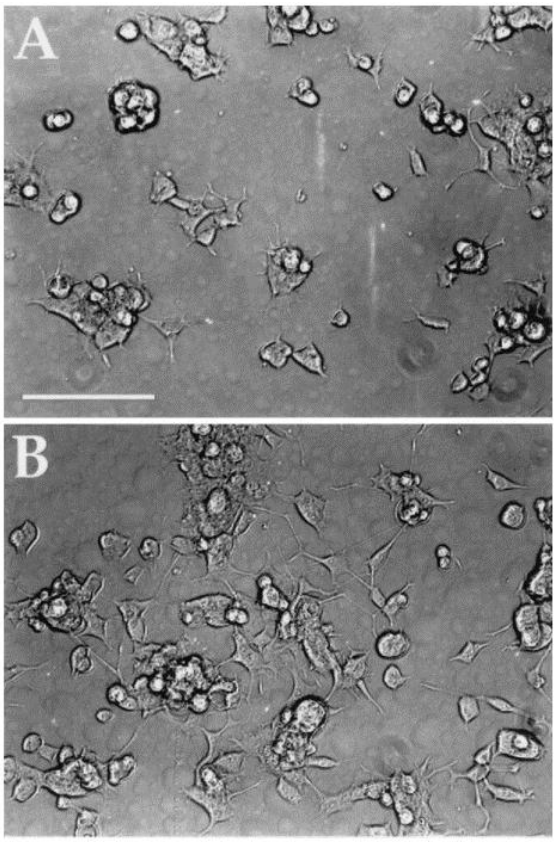

Figure 22. Phase contrast images of cell cultures on biocompatible conductive substrates show changes in cell morphology when exposed to EF. (A) PC12 cells stimulated with NGF grown on a polypyrrole film and (B) the same cells showing greater neurite density after 100mV stimulation for 2hr and imaged 24hr afterwards. (Schmidt et al. 1997)

Cell polarization and growth cones are directed by gradients of ions, proteins, and growth factors. This natural bioelectric field found in the extracellular substrate may provide a key to understanding the cues for successful nerve regeneration. The studies presented demonstrate that cells respond to synthetic EF application to in vitro cultures, however further exploration of various EF parameters are needed to discover which extracellular cues are relevant to cell development.

Although the mechanism is not completely understood, application of EF on in vitro cell cultures indicate that cell growth can be manipulated in a variety of ways, whether in the media above the cells or through the substrate below the cells. This dissertation explores a possible mechanism of how the EF affect cell behavior, what EF parameters have the greatest impact on cell stimulation, and how EF stimulation can be translated into a clinical product.

Chapter III:

Schwann cell alignment in response to electric field stimulation through the media and substrate

3.1 INTRODUCTION

Endogenous electric fields (EF) have been found to be essential in directing cell growth during tissue development and wound healing where disruption of the natural EF can lead to developmental deformities (Altizer et al. 2001, McCaig et al. 2002, Nuccitelli 2003, McCaig et al. 2005, Levin 2009). During embryogenesis, the developing neural tubes of amphibian and avian animals have significant spatial and temporal organization of EFs ranging from 10 – 1600 mV/mm that can change over days or minutes (McCaig et al. 2002). In wounded rat cornea models, ionic flow is permitted through broken tissue creating EFs directed towards the site of injury (Reid et al. 2005). In both cases, the presence of EFs has an effect on cell growth rate, direction of growth, and cell orientation.

Any time there is a separation of charge, an electric potential is created. Cell membranes and epithelial tissue provide natural semi-permeable barriers to ions and other charged species, resulting in a potential across the layer. When the barrier is damaged, ions from either side will attempt to reduce the electric potential by flowing down its gradient. This creates an ionic current that directs cell growth to the site of injury until the barrier is repaired and the electric potential is restored. A simulated EF can be reproduced in vitro by applying an electric potential across two electrodes

submerged in ionic conductive fluids such as buffer solution or cell culture media. Because there is little information about which electrical parameters may be most effective for controlling cell behavior, a thorough study of cell reaction to EF signals is necessary.

Electrical stimulation through the media is effectively an electrolytic cell where electrical energy is applied to the system, often decomposing compounds in the solution. An issue to address with this manner of stimulation is the gradual accumulation of cytotoxic species when reduction-oxidation reactions occur at the anode and cathode. In vitro studies performed by numerous groups (Borgens et al. 1994, Alexander et al. 2006, Song et al. 2007, Ariza et al. 2010, Koppes et al. 2011) use agar salt bridges to separate the electrodes and reactive byproducts from the central cellular component of their stimulation setup. However, electrode isolation may not be feasible for in situ nerve stimulating applications. In fact, insulated surgical wire with bared ends have been directly sutured around the proximal nerve stump and target structure to create an EF for the regrowing nerve (Al-Majed et al. 2000, Brushart et al. 2002, Geremia et al. 2007). These experiments show varying amount of success, and a majority of the investigators apply alternating current (AC) signals to prevent corrosion of lead tips whereas endogenous EF are direct current (DC).

An alternative method to expose tissue to endogenous EFs may be to stimulate a conductive material adjacent to the tissue. Current passing through a conductive surface will induce a current through an adjacent conductive medium. By passing DC current through a conductor instead of directly through the media, the electrode interface is removed limiting the production of red-ox byproducts. Furthermore, conductive

substrates can be modified to be cell scaffolds, bioelectrical interfaces, or biosensors (Ravichandran et al 2010, Seil and Webster 2010) to create a multifunctioning biomedical device.

The ability to electrically stimulate tissue through the cell media and through a conductive substrate will be compared by observing change in cell behavior within these two systems. Schwann cells were chosen for these studies because of their essential role in peripheral nerve repair. In healthy nerves of the peripheral nervous system (PNS), myelinating Schwann cells provide neural functional support and secrete biochemicals necessary for neuron survival. When a nerve is damaged, Schwann cells infiltrate the injury preceding axon growth to remove cellular debris from the site, lay an extracellular matrix (ECM) substrate for axon adhesion, provide contact guidance for axon extension, and excrete chemical cues to guide axon regrowth across the lesion (Fawcett and Keynes 1990, Schmidt and Leach 2003). Schwann cells typically arrange into Bands of Bungner when not innervated, providing an aligned topology important for guiding regrowing axons. Using EFs to control Schwann cell growth and alignment may increase the chances for successful nerve regeneration.

The work presented will highlight the difference in cell morphology when cultures are electrically stimulated through the media versus through the substrate. Voltage, current density, duration, and alternating frequency of the EF signal was assessed individually to determine which parameters best generate a cell response in the two EF stimulating models. Being able to deliver endogenous EF growth cues by directing current through the substrate will be an innovative technique to implement in nerve guidance conduits.

3.2 MATERIALS AND METHODS

3.2.1 Schwann cell culture

Neonate rat Schwann cells isolated from sciatic nerves were purchased from ScienCell (Carlsbad, CA). Cells cultures were grown on tissue culture plastic and maintained in high glucose DMEM medium supplemented with 10% fetal bovine serum, 3 μg/ml bovine pituitary extract (Invitrogen, Carlsbad, CA), and 2 μM forskolin (Sigma-Aldrich, St. Louis, MO). To maintain proper phenotype, only cultures between passages 4-8 were used for experiments. Cultures were passaged prior to reaching 80% confluency, detaching cells with 0.25% Trypsin-EDTA for 2 minutes, centrifuged at 800 rpm for 4 minutes, resuspended in fresh medium, then seeded onto new plates. Medium was changed every third day and kept at 37^{o}C with 5% CO_2 in a humid incubator. For EF experiments, Schwann cells were seeded onto the experimental substrates at 5000 cells/cm^2 for 30 minutes before stimulation. Cultures were maintained in 500 μl of medium for the duration of the experiment before fixing and imaging.

3.2.2 Setup for EF through media

The electrical stimulation channel for placing EF through the media was modified from a protocol developed by Song et al. (2007). Cell cultures were confined between glass coverslips arranged on top of tissue culture plastic. Two agar salt bridges placed in contact with media supporting the cells were connected to saline reservoirs, one being the

cathode and the other the anode. The bridges are necessary to isolate electrode red-ox byproducts from the cell culture. The two-electrode setup connected to the reservoirs was stimulated with a multipotentiostat (1000C Multipotentiostat, CH Instruments, Austin, TX). A function waveform generator (33220A, Agilent Technologies, Santa Clara, CA) was used for experiments requiring alternating current (AC). Schwann cells grown in channels without electrical stimulation served as controls. The protocol for creating and applying an EF across a media channel (MC) is described in greater detail below, refer to **Figure 23**:

1) Two No.2 thickness microscope cover slips measuring 22 x 22 mm^2 were adhered onto 100 mm diameter tissue culture plastic using high vacuum silicone grease (Dow Corning, Midland, MI). The two base cover slips were normally placed 0.5 cm apart from each other, and up to 3 cm depending upon experimental conditions. A third cover slip measuring 22 x 35mm^2 was adhered on top of the two base cover slips with grease, creating a cell culture channel 0.2 x 5 x 22 mm^3 (H x W x L).

2) Polydimethylsiloxane (PDMS) (Sylgard 184 Silicone elastomer, Dow Corning, Midland, MI) was cured in a rectangular dish several days prior to experimentation. Two strips of PDMS were cut 8 x 4 x 100 mm^3 (H x W x L) and secured above the edges of the glass channel with grease to separate the anodic and cathodic sides.

3) Cells injected into the glass channel at 5000 cells/cm^2 were allowed to adhere for 1 – 2 hours in a humid 37^oC incubator with 5% CO_2 before 6 ml of cell culture media

with supplements was added to each side of the channel.

4) Agar salt bridges were made by boiling 4% agar diluted in phosphate buffer saline (PBS) and pouring into curved glass tubes of 6 mm inner diameter and 8 cm in length. A separate 60mm diameter dish containing 10 ml PBS is prepared with a slotted cover so a 20 x 30 mm^2 sheet of stainless steel metal connected to an electrode can extend into the PBS. Openings cut into the lids allow the agar salt bridges to be placed in contact with the PBS and cell culture media.

5) The multipotentiostat connected to the stainless steel plates stimulated samples using various signal parameters. The complete length between electrodes was 22 cm. Channel resistance was controlled by varying the widths of the channels between 0.5 and 3 cm. Schwann cell morphology exposed to changing current density (30, 60, 90 mA/cm^2), voltage (7.45, 10, 22 V), duration (2, 8, 20 hours), and AC (2, 60, 1000 Hz) signals were observed and dominant cell angle was measured in relation to the EF direction. Cells seeded into channels receiving no electric stimulation served as controls.

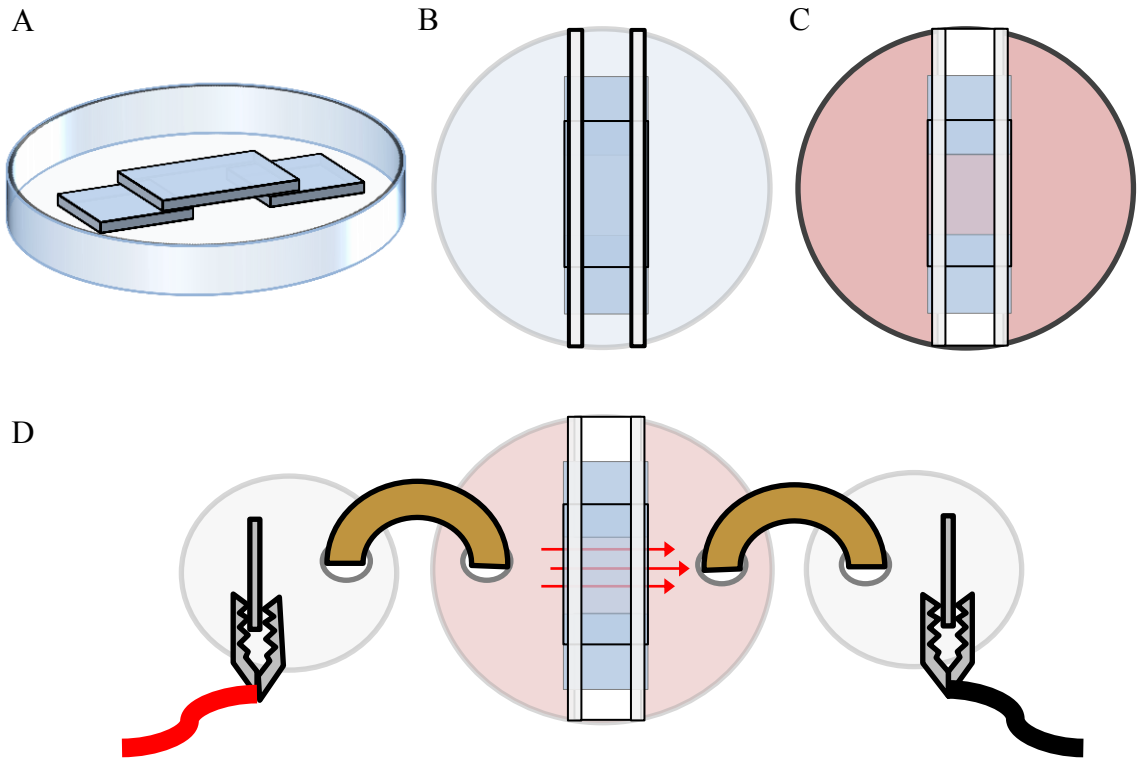

Figure 23. Assembly of MC units begins with (A) stacking glass cover slips to create a 0.2 mm high channel in a tissue culture plate. (B) Two long strips of PDMS are placed above the channel away from the center to allow viewing of cells. (C) The PDMS blockades isolate media on either side so ionic flow is confined within the channel. (D) Agar salt bridges are fitted into lid openings to create an electrical circuit between the cell media and separate PBS reservoirs.

3.2.3 Setup for EF through substrate

The electrical stimulation channel for directing EF through the substrate has a similar setup as the MC, however, no agar salt bridge was required. Cell cultures were

confined between glass coverslips arranged on top of electrically conductive indium tin oxide (ITO) coated glass slides (25 x 75 mm^2, sheet resistance 30-60 Ω, Delta Technologies, Loveland, CO). A working electrode was attached to one end of the ITO glass and the counter/reference electrode was placed on the opposite end. A multipotentiostat supplied electricity between the electrodes, stimulating the cell culture in the center. Schwann cells grown in channels without electrical stimulation served as controls. The protocol for creating and applying an EF through the substrate channel (SC) is described in greater detail below, refer to **Figure 24**:

1) The surface of an ITO coated glass slide was etched with a diamond tip rotary tool to create a center lane across the long axis of the glass with a specified width (0.5 – 3 cm). Two parallel lines etched on the ITO surface removes conductivity, constraining electrical current within the center lane. To change the resistance of the material, the entire ITO glass slide was dipped in 12 M HCl acid for approximately 40 – 70 seconds to chemically etch the surface. Once the target surface resistance was reached, the acid etched glass was neutralized in 1% Na_2HPO_4 solution, washed with PBS and water, then dried.

2) Two No.2 glass cover slips were cut into 5 x 22 mm^2 strips and adhered onto the ITO glass with grease bordering the center lane to serve as base walls. Another glass cover slip 22 x 22 mm^2 was adhered on top of the base cover slips to create a cell culture channel 0.2 x 5 x 22 mm^3 (H x W x L). The width, determined by the distance between the two base cover slips, was dependent upon the width of the etched

conductive center lane.

3) The unit was sterilized under UV light for 20 minutes before coating the inner channel with Matrigel (BD Biosciences, Franklin Lakes, NJ) diluted to 0.2 mg/ml with PBS. Protein was adsorbed onto the surface for 30 minutes, aspirated, and air dried at room temperature. Coated glass were stored at 4^{o}C until use.

4) Cells were injected into the channel at 5000 cells/cm^2 and small 200 µl reservoirs of media were corralled on each open side of the channel with a hydrophobic pen, to increase nutrient availability and prevent excessive evaporation from the unit. Cultures were allowed to adhere for 1 – 2 hours in a humid incubator at 37^{o}C with 5% CO_2.

5) Electrodes were clasped to opposite sides of the ITO glass center lane so the applied EF was directed beneath the cell culture. Prior to channel assembly, channel resistance was controlled by vapor etching the surface of the ITO with gaseous hydrochloric acid. Schwann cell morphology exposed to changing current (0.6, 1.4, 4 mA), voltage (7.45, 10, 22 V), duration (2, 8, 20 hours), and AC (2, 60, 1000 Hz) were measured for dominant cell angle in relation to the EF direction. Cells seeded into channels receiving no electric stimulation served as controls.

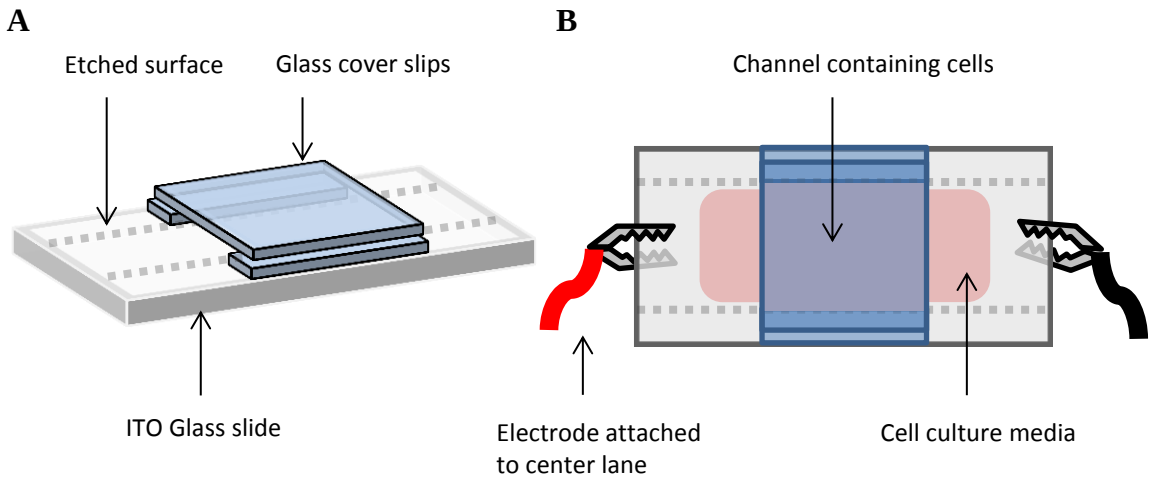

Figure 24. An isometric view (A) depicts how base cover slips were placed on the outer edge of the etched center lane (etches ITO shown in gray dotted line). A glass cover slip was stacked on top of the base to create a channel. (B) Cells and media were injected into the channel, with extra media around the edges to prevent dehydration of the culture. Electrodes were clasped on opposite ends of the ITO glass to conduct electricity through the center lane.

3.2.4 EF Modeling

COMSOL Multiphysics software (Burlington, MA) was used to create finite element models of EF stimulation through ITO. The Electric Current module was applied to models drawn in nanoscale dimensions. ITO was represented as a thin metal with a conductivity of 10^5 S/m and media was represented as saline with a conductivity of 1.5 S/m. The models do not take into account of electrokinetic properties, such as the interfacial double layer, nor the electrical properties of cells, which would be necessary

for greater accuracy. Rather, the ITO and media are modeled as simple conductive elements in electrical contact.

3.2.5 Imaging and data analysis

Immediately after electric stimulation, media was aspirated from each unit and quickly disassembled to expose cell cultures. The samples were fixed with a 4% paraformaldehyde solution for 15 minutes at room temperature then replaced with PBS for imaging. An inverted light microscope (IX-70, Olympus, Center Valley, PA) with an attached CCD camera (Optronics MagnaFire S608000, Goleta, CA) was used to take 100x magnification phase contrast images of fixed Schwann cells. Samples were oriented so the EF direction is aligned horizontally when imaged.

Cell alignment relative to the EF was analyzed with NIH ImageJ open source software (version 1.46, available at http://rsbweb.nih.gov/ij/). Cell angle was measured as the angle between the horizontal EF (0^o in polar coordinates) and a line drawn through the long axis of the cell, adapted from cell analysis methods in previous works (Erickson and Nuccitelli 1984, Sun et al. 2006). The long axis was defined as the major axis of an ellipse drawn around the cell that was at least 50% greater than the minor axis. Spread cells with a major axis less than the criteria were calculated as having no overall orientation. All cells were measured with angle values between 0^o and 180^o (quadrants I and II of a cartesian coordinate system) because the effect of the EF (directed along 0^o) is mirrored on both sides of the x-axis, as in **Figure 25**. If θ is the cell angle relative to the EF, then $-\cos 2\theta$ will give a convenient description of cell alignment (Erickson and

Nuccitelli 1980, Sun et al. 2006). All cells having an alignment closer to 0^o parallel to the EF will have values near -1, all cells having an alignment closer to 90^o perpendicular to the EF will have values near +1, and cells having a randomly distributed alignment close to 45^o will have values near 0.

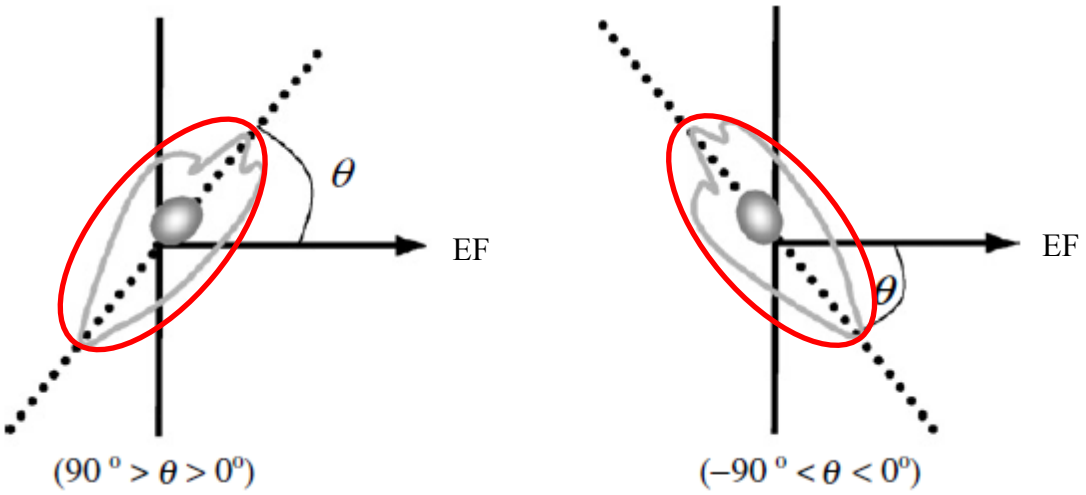

Figure 25. A line is drawn through the long axis of the cell, determined by an ellipse with a major axis 50% greater than the minor axis. Cell angles in the fourth quadrant provide the same orientation information as cell angles in first quadrant. Therefore, cell angles were measured between 0^o and 180^o (Adapted from Sun et al. 2006)

All experiments were repeated three times. At least three fields of view chosen at random were imaged for each repetition, yielding approximately 400 cells for each experiment. Cells with indiscernible orientation were given cosine alignment values of 0. Statistical significance was determined with Student's t-test, comparing the average cell angle of an experimental variable against the average cell angle of control samples. Statistical significance was defined as $p<0.01$.

3.3 RESULTS

Ohm's law states that an electrical current through a conductive element is proportional to the applied voltage and material's resistance. The relationship is described by the mathematical equation,

$$I = \frac{V}{R} \tag{1}$$

where I is current (in amperes, A), V is voltage (in volts, V), and R is the resistance of the material (in ohms, Ω). In order to independently change voltage while keeping current constant, resistance will need to change in proportion to voltage. Resistance of the MC was altered by changing the width of the culture channels. As the cross sectional area increases, resistance decreases.

It is important to note that cells attached to a substrate can only detect molecules within its environment that are sufficiently near its surface. The height of the media is inconsequential as long as transport of nutrients, waste, and gases is adequate. When an ionic current flows above a cell culture, however, an increase in the cross sectional area of the MC will result in a decrease in current density (J, in A/m^2) described as,

$$J = \frac{I}{A} \tag{2}$$

where A is the cross sectional area of current flux (in m^2). This equation describes the number of electrical charges in an instance of time passing through a two dimensional cross section of the conductor. Combining Equations 1 and 2, J is commonly expressed,

$$J = \sigma E \tag{3}$$

where E is the electric field (in volts per unit length, V/m). Electrical conductivity, σ, has units of siemens per unit length (S/m). Alternatively, electrical conductivity is the reciprocal of resistivity, ρ (in units of $\Omega \cdot m$) defined as,

$$\rho = \frac{1}{\sigma} = R\,\frac{A}{l} \tag{4}$$

l being the length of the conductor (in meters, m). From Equations 3 and 4, it is evident that J is dependent upon the volume and resistance of the conductor. Increase in either of these parameters will be perceived by cells as a decrease in the number of ions flowing across the cell surface. This change in charge movement near the cell may have an impact on cell behavior.

The lengths of the channels are identical for all samples, so resistance and cross sectional area are the only parameters available to change, and as with many conductors, they have a proportional relationship. By keeping the height constant using a 0.2 mm thick cover slip, resistance of the channel was decreased by increasing channel width from 0.5 cm to 3 cm. Resistance of the channel was calculated from measuring the voltage directly across the cover slip and recording the current collected from the

potentiostat, and was found to have an inverse relation to the channel width shown in **Figure 26**.

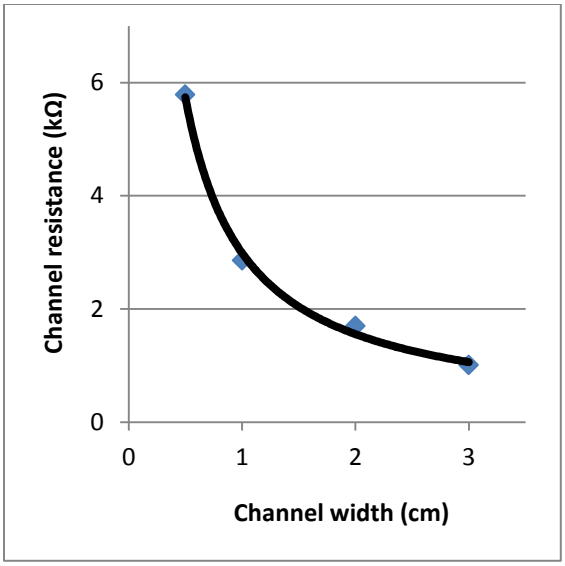

Figure 26. The resistance of the PBS, agar bridge, and media across the channel was calculated from known voltages and currents. The graph indicates that there is an inverse relation between resistance and cross sectional area when the width was changed from 0.5 to 3.0 cm wide.

The average resistance of 0.5 cm channels was 5.8 kΩ, 2.9 kΩ for 1 cm, 1.7 kΩ for 2 cm, and 1.0 kΩ for 3 cm (n=3 for each width). Channel resistance quickly plateaus to a minimum when increasing the width beyond 3 cm and resistance dramatically increases when the width is reduced less than 0.5 cm. These resistance-width values were used to calculate the required currents or voltages for the following experiments.

3.3.1 Cell response to EF through media

Gradients of ionic species across interstitial fluid create endogenous EFs within the body, similarly, creating an ionic gradient in media surrounding cell cultures can mimic endogenous EFs in vitro. An ionic gradient was created by placing a potential across two electrodes in electrical contact with the cell culture. The voltage, current density, duration, and alternating frequency of the electric signal were independently varied to determine which properties have an effect on cell morphology.

3.3.1.1 Schwann cell alignment is proportional to current density and EF

Current density through the MC was changed by varying channel widths between 0.5, 1, and 3 cm and applying a constant potential of 10 V between electrodes. As the channel width increases, the cross sectional area above the cell culture also increase. By measuring the current and voltage directly across the channels, cell response to current density (mA/cm^2) and EF (mV/mm) can be compared.

Schwann cells seeded into MC channels were allowed to adhere for 1 – 2 hours, stimulated for 6 hours, fixed in paraformaldehyde, imaged with a phase contrast light microscope, then analyzed for cell orientation relative to the EF direction. Experiments were repeated three times and cell angle measurements were compiled to calculate a single average angle for each channel width. Sample images of cells stimulated on 0.5 and 3 cm width channels are shown in **Figure 27**, displaying greater cell alignment perpendicular to the EF.

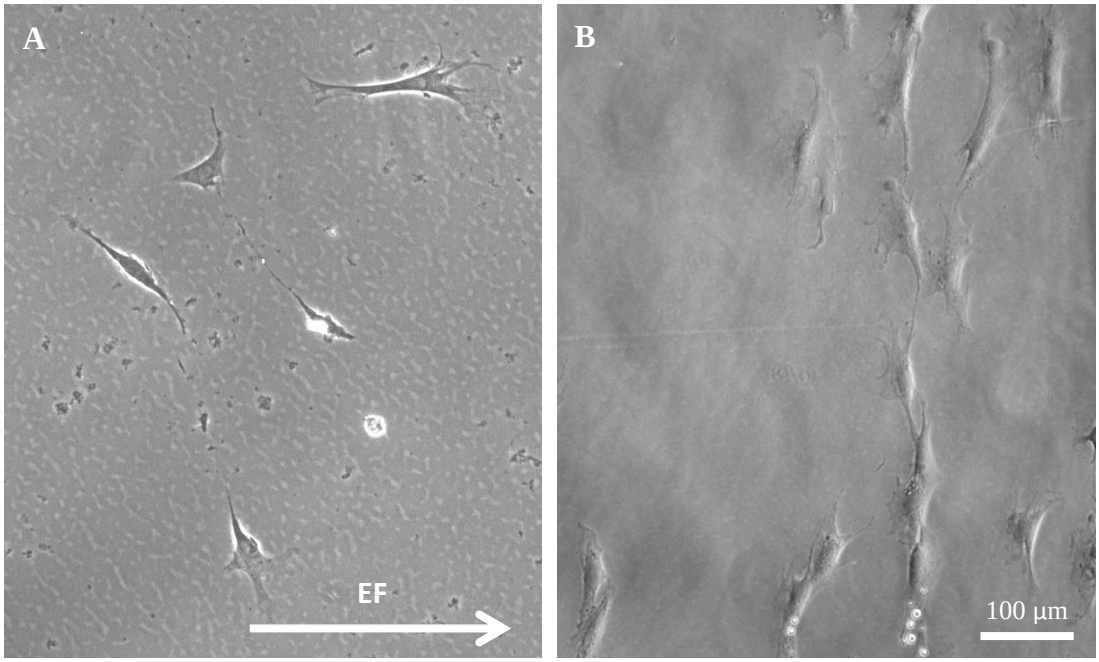

Figure 27. Phase contrast images of EF stimulated Schwann cells display the degree of perpendicular alignment when cultured on (A) 3 cm channels with 36 mA/cm^2 and (B) 0.5 cm channels with 106 mA/cm^2. All images were analyzed with the EF directed from left to right. Scale bar is 100 µm.

Figure 28 depicts a plot graph of Schwann cell angle and length (radius) measurement in polar coordinates. The origin represents one end of the cell and the green triangle represents the location of the opposite end of the cell, where the angle is the cell orientation and the radius is the cell length (µm). There are four graphs, one for each channel width 0.5, 1, and 3 cm, and a graph of cell angle under control conditions.

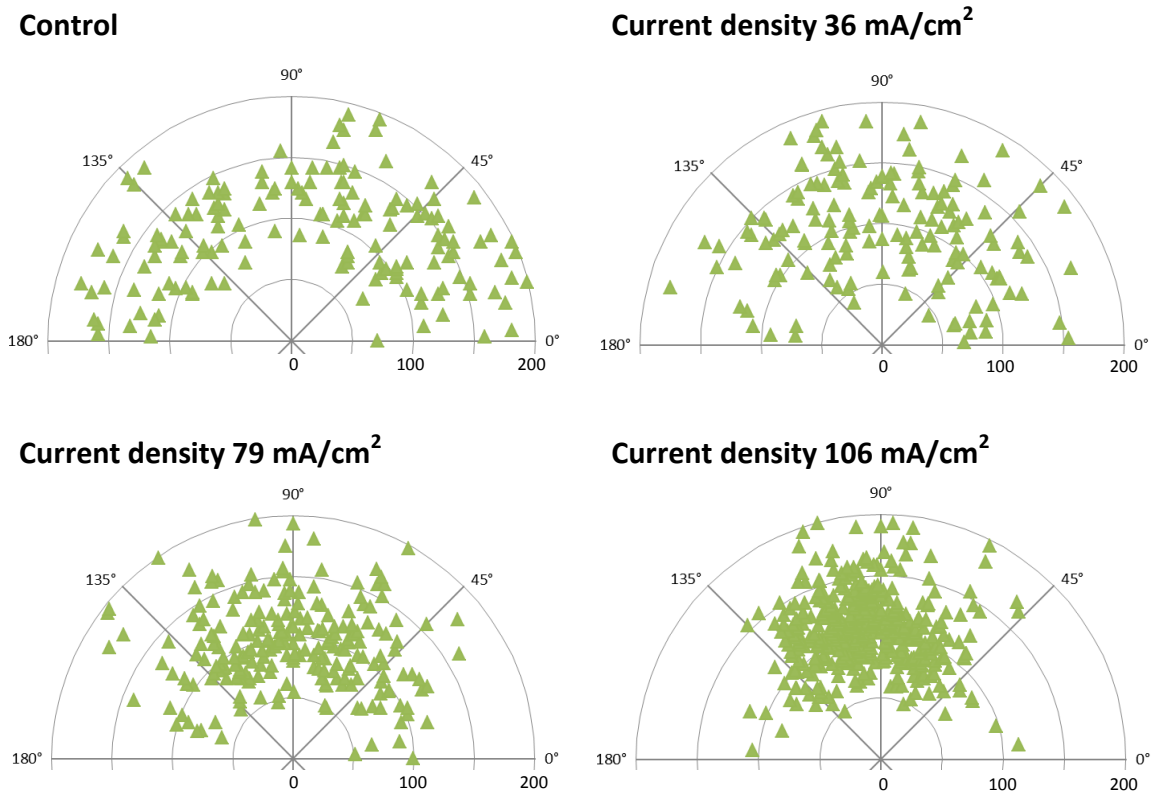

Figure 28. Polar graphs depict the length (radius, in μm) and angle of Schwann cells (represented as triangles) exposed to a constant potential across various channel widths. Control samples were not stimulated with an EF. MCs with smaller widths had greater cell alignment perpendicular to the EF.

The average cosine cell angle of cultures without electrical stimulation was -0.01, which is near the theorized 0 for randomly oriented cells. Cell cultures receiving electrical stimulation had average cosine angles of varying degrees depending upon channel width, and thus the current density. The average cell angle for 0.5 cm width channels was 0.71, 1 cm was 0.44, and 3 cm was 0.29. The current density across 0.5 cm width channels was 106 mA/cm^2, 1 cm was 79 mA/cm^2, and 3 cm was 36 mA/cm^2. The

EFs calculated were 245, 175, and 90 mV/mm for 0.5, 1, and 3 cm wide channels, respectively. The electrical properties and cell angle values measured for this experiment have been summarized in **Table 2**.

Table 2. Electrical parameters and cell measurements of experiments with changing current density through the media

Width (cm)	Current (mA)	Current density (mA/cm^2)	EF (mV/mm)	Cell angle	Standard deviation	n	p-value
control	-	-	-	0.01	0.66	169	
0.5	1.06	106	245	0.71	0.36	434	10^{-29}
1	1.59	79	175	0.44	0.55	228	10^{-11}
3	2.18	36	90	0.29	0.64	158	10^{-5}

The current density is a calculation based on the measured current and the corresponding cross sectional area of the channel. The EF is a calculation based on measurement of the voltage using a multimeter placed directly across the 22 mm channel. Column "n" is the number of cells measured to calculate the average cell angle, column "p-value" is the probability that the distribution is random using Student's t-test comparing the variable and the control values. Using these collected values, line graphs were created to visually assess the relationships between the channel width, cell orientation angle, EF, current strength, and current density (**Figure 29**).

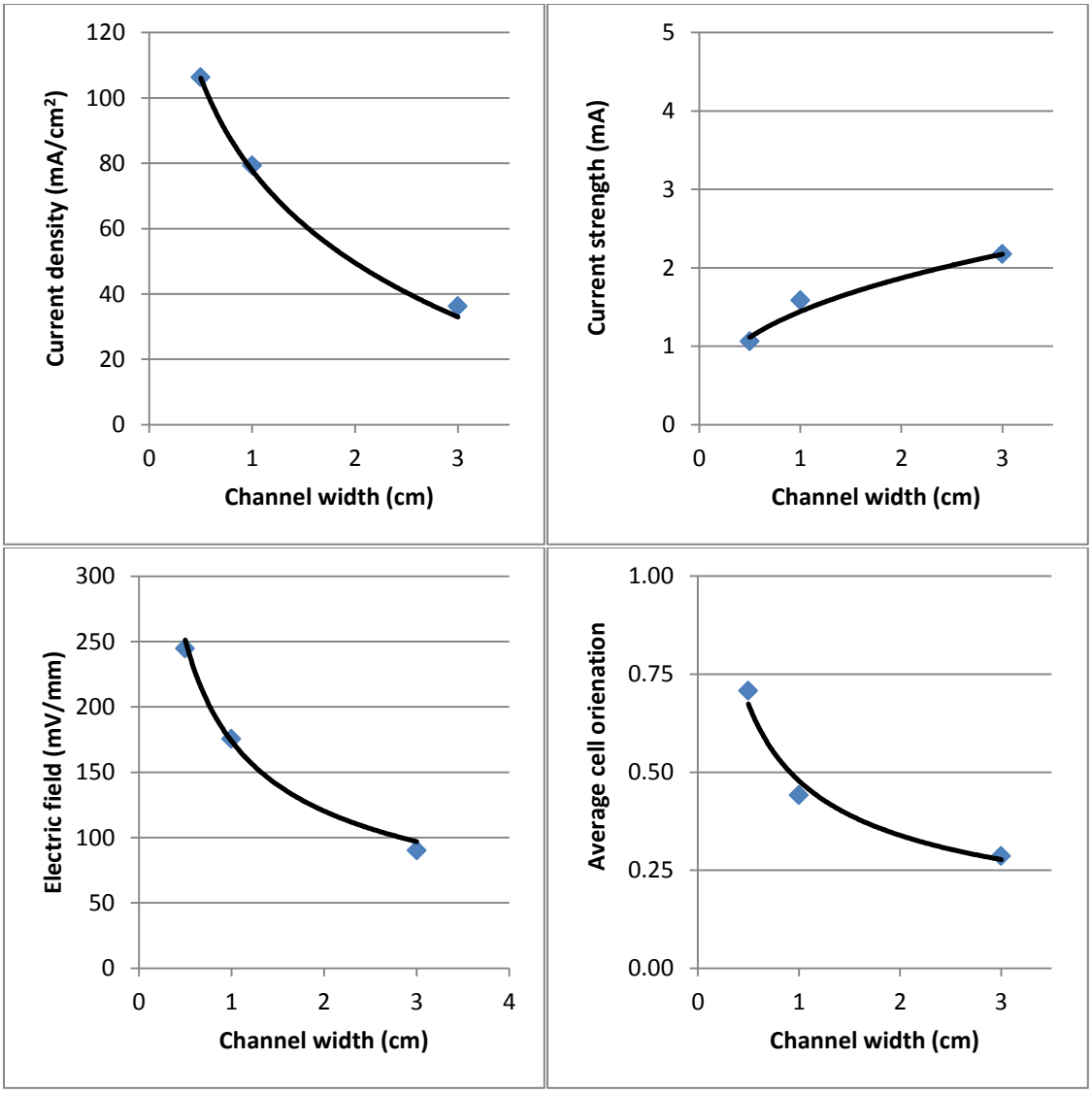

Figure 29. Current density, current strength, EF, and average cell angle are plotted against channel width for experiments with a constant 1-2 mA stimulation. Average cell angle shows a linear relationship between the current density and EF, indicating greater perpendicular cell alignment with a stronger current density or EF.

Larger channel width leads to lower resistance because the larger cross sectional area allows more available ions to flow through the volume. Although the current and voltage applied across the electrodes remain relatively constant, the current density and EF above the cells both decrease with larger channel widths. Average cell alignment also decreases with larger channel widths. This relationship indicates that absolute current is not an effective means to control cell alignment. It was observed that high current density or EF induce greater perpendicular Schwann cell alignment.

3.3.1.2 Schwann cells do not respond to changing current strength

By changing the widths of the MC to 0.5, 1, and 3 cm, and applying potentials of 7.45, 10, and 22 V between electrodes, respectively, the current density was calculated to maintain a constant 80 mA/cm^2 through the 0.2 mm tall channel. The current strength through the MC was increased from 0.5 to 4 mA.

Similar to the above experiment, Schwann cells were stimulated for 6 hours, imaged with a phase contrast light microscope, and analyzed for cell orientation relative to the EF direction. Experiments were repeated three times and cell angle measurements were compiled to calculate a single average angle for each channel width (i.e. each voltage group). Images of EF stimulated cells cultured in 0.5 cm channels and 3 cm channels are shown in **Figure 30**. These images represent the low and high values of voltage used in the experiment. Cells show a similar degree of perpendicular alignment in relation to the horizontal EF.

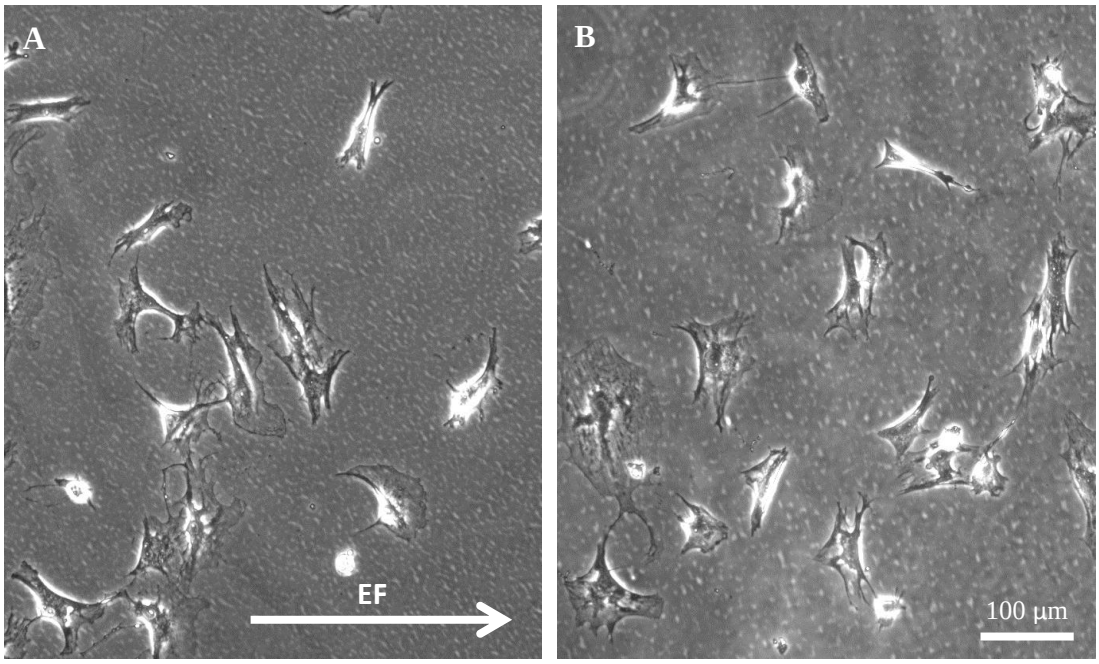

Figure 30. Phase contrast images of EF stimulated Schwann cells display the degree of perpendicular alignment when cultured on (A) 0.5 cm channels and (B) 3 cm channels. All images were analyzed with the EF directed from left to right. Scale bar is 100 µm.

Figure 31 displays two polar plots of Schwann cell angle measurements when stimulated in channels of 0.5 and 3 cm widths. Schwann cell length is represented as the radial distance (in µm) and cell angle was measured relative to the EF direction (0^o). Only two graphs representing the low and high voltages are shown in **Figure 31**.

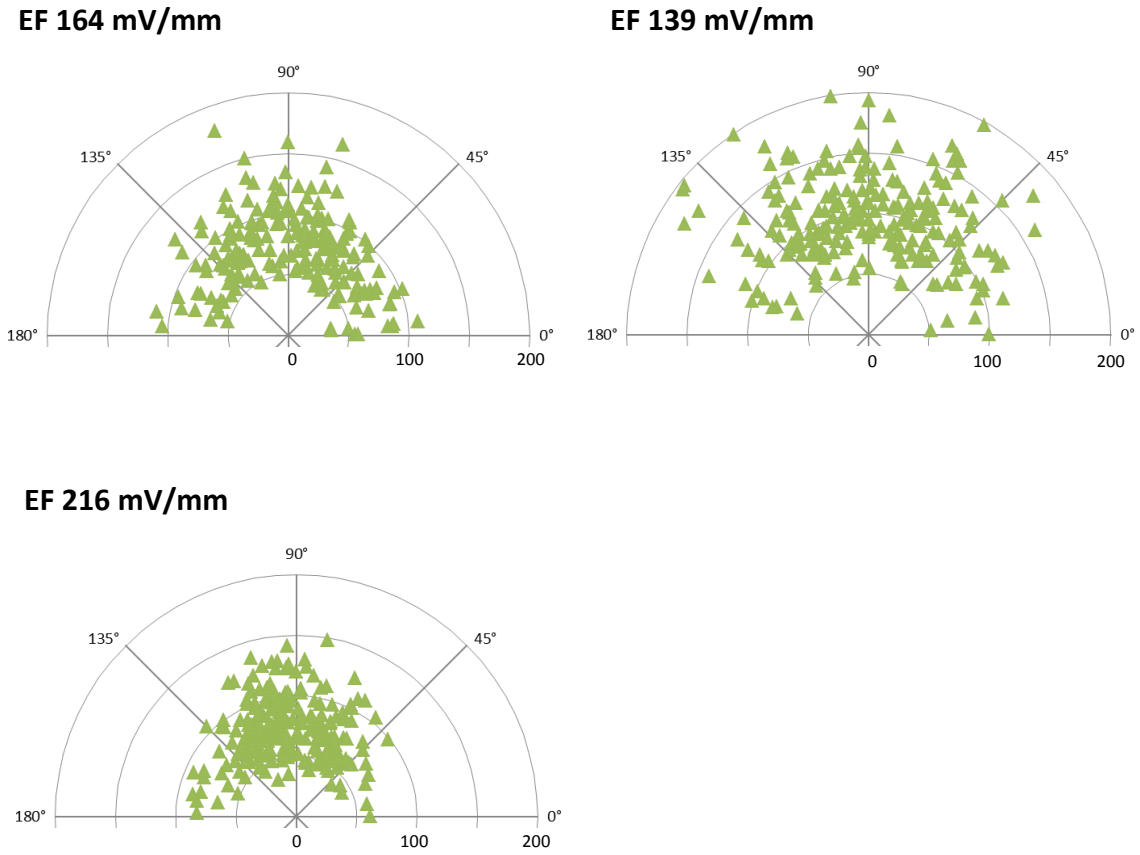

Figure 31. Polar graphs depict the length (radius, in µm) and angle of Schwann cells (represented as triangles) exposed to a constant current density of 80 mA/cm^2 across various channel widths.

The average cell angle of cultures without electrical stimulation was -0.01, found in the previous experiment. Cell cultures receiving electrical stimulation had average angles of similar degrees regardless of channel width. The average cell angle for 0.5 cm width channels was 0.33, 1 cm was 0.44, and 3 cm was 0.57. The EF measured directly across 0.5 cm width channels was 164 mV/mm, 1 cm was 139 mV/mm, and 3 cm was 216 mV/mm. The electrical properties and cell angle values measured for this experiment have been summarized in **Table 3**.

Table 3. Electrical parameters and cell measurements of experiments with constant current density

Width (cm)	Current (mA)	Current density (mA/cm^2)	EF (mV/mm)	Cell angle	Standard deviation	n	p-value
control	-	-	-	-0.01	0.66	169	
0.5	0.55	55.5	164	0.33	0.64	204	10^{-6}
1	1.38	69.0	139	0.44	0.55	228	10^{-11}
3	3.89	64.8	216	0.57	0.48	234	10^{-18}

Line graphs were created to visually assess the relationships between the voltage, current strength, channel width, and average cell angle (**Figure 29**). The current density calculated from the current measurements was below the target 80 mA/cm^2 at an average 63 mA/cm^2. The current increases linearly with wider channel widths, however, average current density and measured EF increased by a small amount. Schwann cell orientation appears to have a greater correlation with current density and EF compared to the current strength.

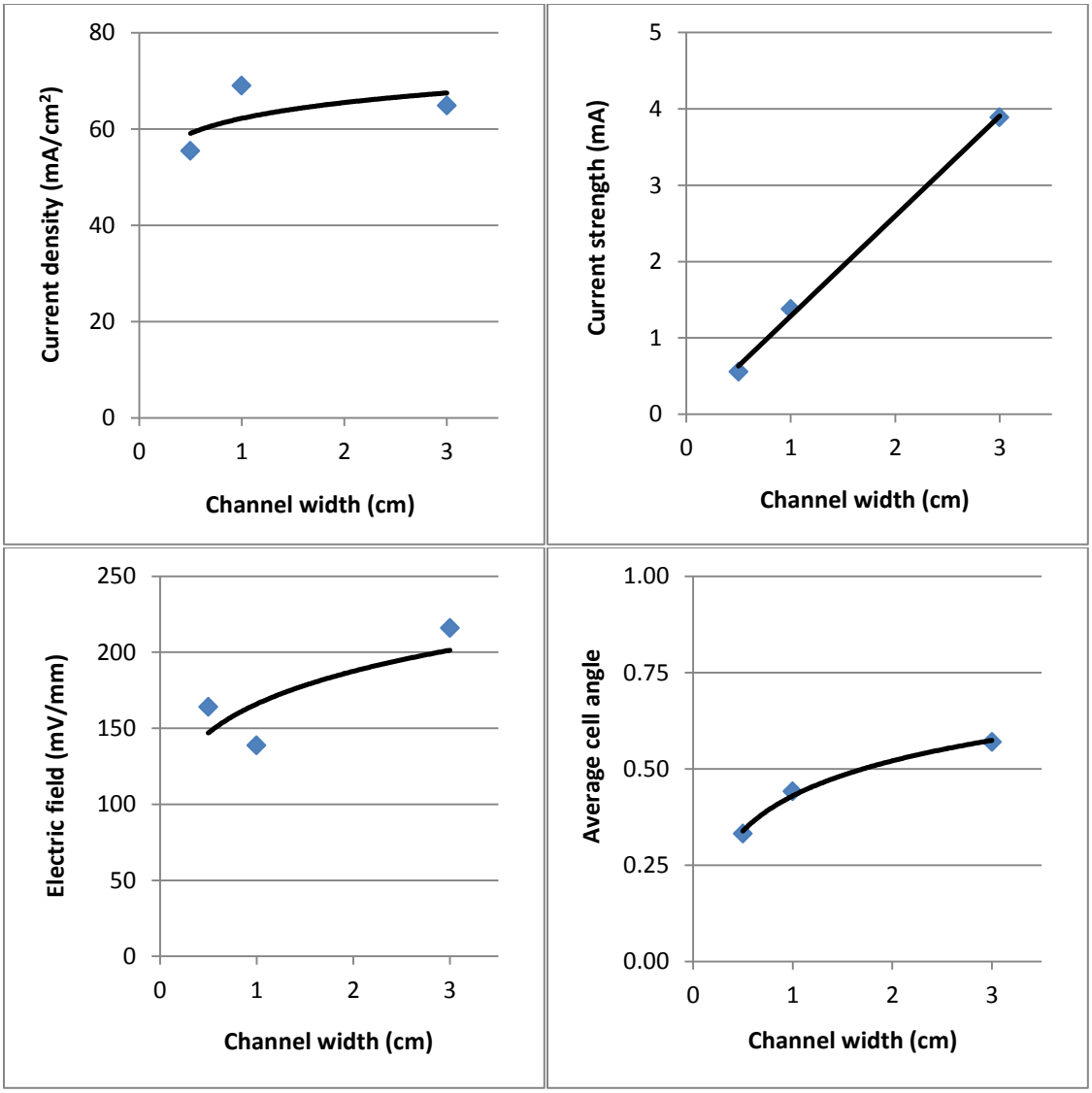

Figure 32. Current density, current strength, EF, and average cell angle are plotted against channel width for experiments with constant current density stimulation. External voltage applied across the electrodes and current strength both increase with larger channel widths, however average cell angle does not increase proportionally. Average cell angle appears to correlate with current density.

3.3.1.3 Changing duration with constant EF

MC units with 1 cm wide channels were stimulated with a constant 10 V across the system for 2, 8, and 24 hours to determine if duration of stimulation can affect cell orientation. Schwann cells stimulated in MC channels were fixed, imaged, and analyzed for cell orientation relative to the EF direction. Experiments were repeated three times and cell angle measurements were compiled to calculate a single average angle for each duration. Sample images of cells stimulated 2 and 24 hours are shown in **Figure 33**, displaying greater perpendicular alignment to EF when exposed for longer durations.

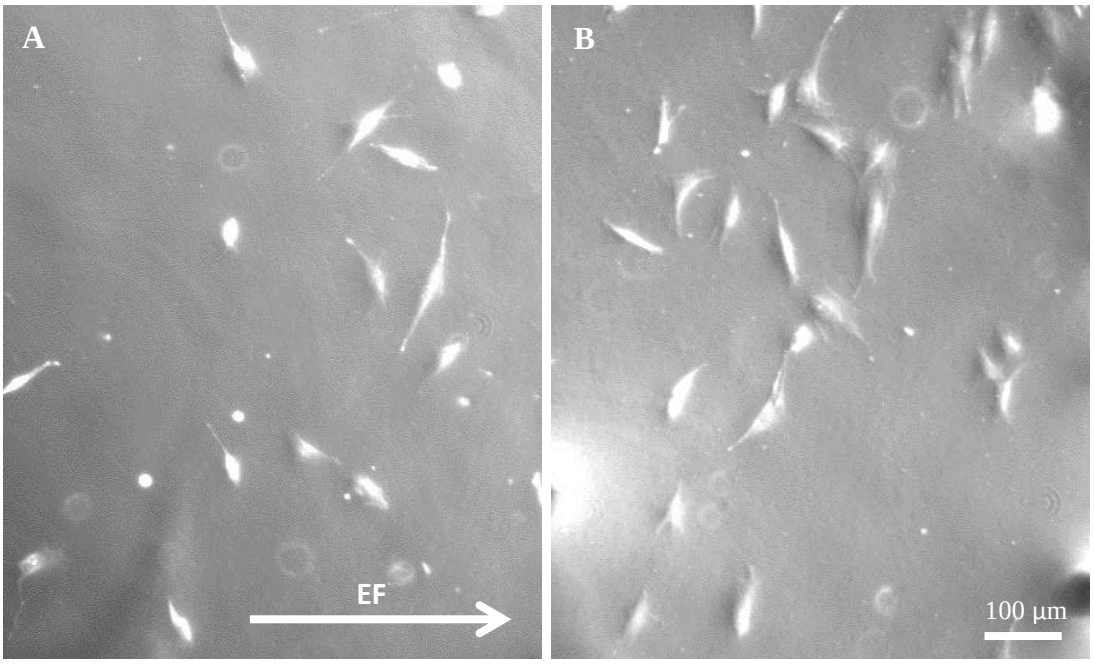

Figure 33. Phase contrast images of EF stimulated Schwann cells show cell alignment of (A) 2 hour stimulated samples is not as strong as (B) samples stimulated for 24 hours. Scale bar is 100 µm.

Figure 34 displays three polar plots of Schwann cell angle measurements when stimulated with 2, 8, and 24 hours in channels using identical physical and electrical parameters. Schwann cell length is represented as the radial distance (in μm) and cell angle was measured relative to the EF direction (0^o).

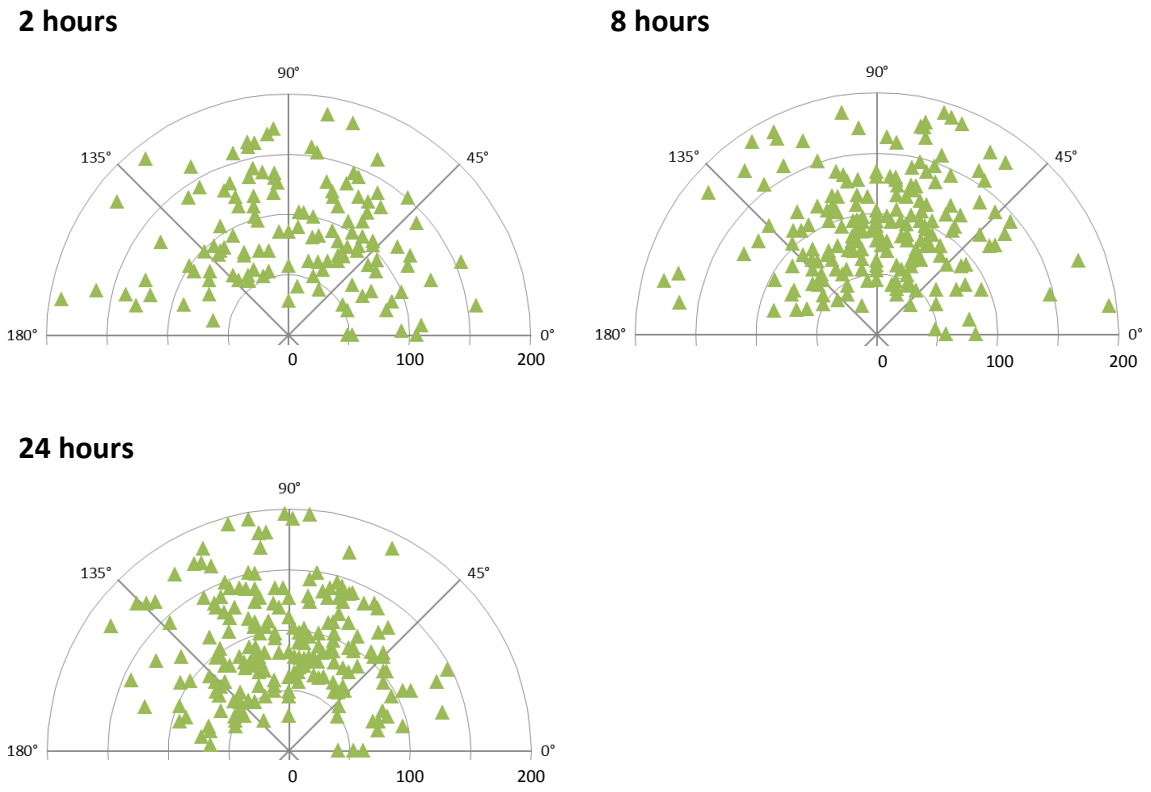

Figure 34. Polar graphs depict the length (radius, in μm) and angle of Schwann cells (represented as triangles) exposed to identical physical and electrical conditions, but for different durations. Samples stimulated for 8 and 24 hours show a similar amount of cell alignment, greater than stimulation for 2 hours.

The average cell angle for cell cultures stimulated for 2 hours was 0.27, 8 hours was 0.47, and 24 hours was 0.42. The voltage and channel width were identical for all experiments. The average voltage measured across channels from all samples was 3.05 V with an EF of 139 mV/mm. The average current from all samples was 1.38 mA with a calculated current density of 69 mA/cm^2. The electrical properties and cell angle values measured for this experiment have been summarized in **Table 4**.

Table 4. Electrical parameters and cell measurements of experiments with changing duration and identical EF stimulation

Duration (hours)	Current (mA)	EF (mV/mm)	Current density (mA/cm^2)	Cell angle	Standard deviation	n	p-value
control	-	-	-	-0.01	0.66	169	
2	1.38	139	69	0.27	0.63	139	10^{-3}
8	*	*	*	0.47	0.56	207	10^{-12}
24	*	*	*	0.42	0.59	215	10^{-9}

** The voltage, current, and current density are average values of all experiments with 1 cm channel width and stimulated with 10 V. The values are identical to the ones above it.*

There is an increase in cell alignment within 2 hours of stimulation. After 8 hours, cell alignment increases alignment perpendicular to the EF. Beyond 8 hours, the average cell angle does not appear to change any further. A line graph plotting the average cell angle versus the stimulation time shows the logarithmic increase in cell alignment over time (**Figure 35**).

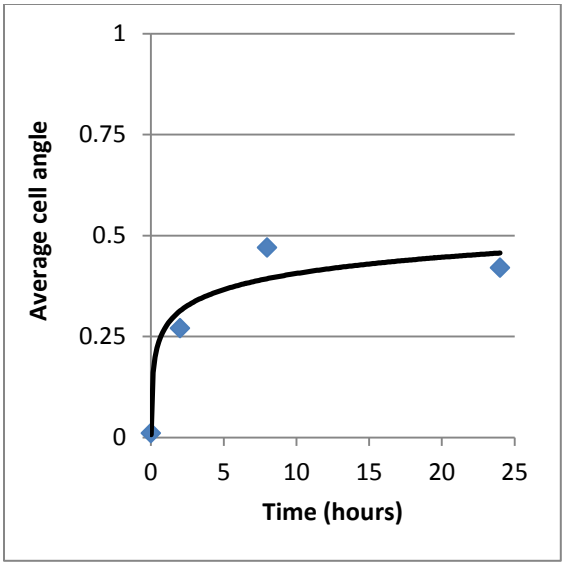

Figure 35. Voltage, channel width, and current strength are kept constant while the duration of the experiment changes increases from 2 hours up to 24 hours. The effect of EF stimulation reaches a maximum over several hours.

3.3.1.4 Changing AC frequency

A constant DC current was applied to the three preceding experiments to observe cell response with varying current density, voltage, and duration. Cell response to AC signals was evaluated by stimulating 2 cm wide channels with 10 V amplitude for 6 hours. The frequencies examined in this experiment were 2, 60, and 1000 Hz, cycling between +10 V and -10 V between electrodes. These frequencies were chosen because bioelectromagnetic studies from various authors have observed conflicting results with in vitro and in vivo experiments using AC electrical parameters between 1 Hz up to 7.5 GHz (Al-Majed et al. 2000, Aydin et al. 2006, Sontag and Kalka 2006, Zhang et al. 2006, Ahlborn et al. 2007, Deans et al. 2007, Walker et al. 2007, Lu et al. 2008, Sheikh et al.

2012). Studies using magnetic fields to induce electric fields within their subject have calculated the induced EF to be between 1-150 mV/mm and current densities near 10-100 mA/cm^2, values that are all within physiological range. Some studies have targeted the role of external electromagnetic fields emitted from daily technologies as a source for biological exposure. The idea of this study is to examine Schwann cell response to several electrical frequencies that have demonstrated to be beneficial to wound healing.

Values measured from the previous experiments indicate that the DC EF is approximately 130 mV/mm across the channel when 10 V is applied across the electrodes. This was the electrical condition for all experiments with different AC frequency stimulation. After stimulation, cells were fixed, imaged, and analyzed for cell orientation. Experiments were repeated three times and cell angle measurements were compiled to calculate a single average angle for each AC frequency. Sample images of cell cultures exposed to 60 and 1000 Hz are shown in **Figure 36**.

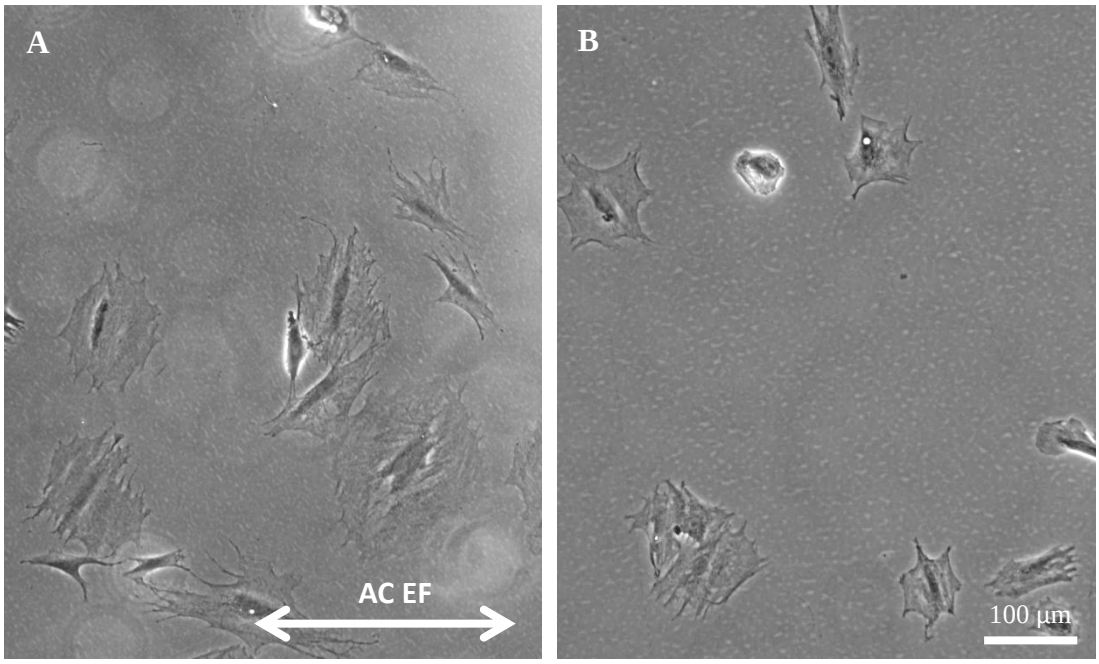

Figure 36. Phase contrast images of AC EF stimulated Schwann cells show cell orientation when exposed to 130 mV/mm cycled at (A) 60 Hz and (B) 1000 Hz. Cells have a flatter spread morphology compared to DC stimulated cultures. Scale bar is 100 µm.

The morphology of Schwann cells exposed to AC stimulation is noticeably different compared to controls or cells exposed to DC stimulation. Cells appear to have more lamellipodia and are spread wide, as opposed to their sickle-shaped morphology under normal culture conditions and during DC stimulation. Polar plots of measured cells show the cell angle alignment and the cell length (radius) (**Figure 37**).

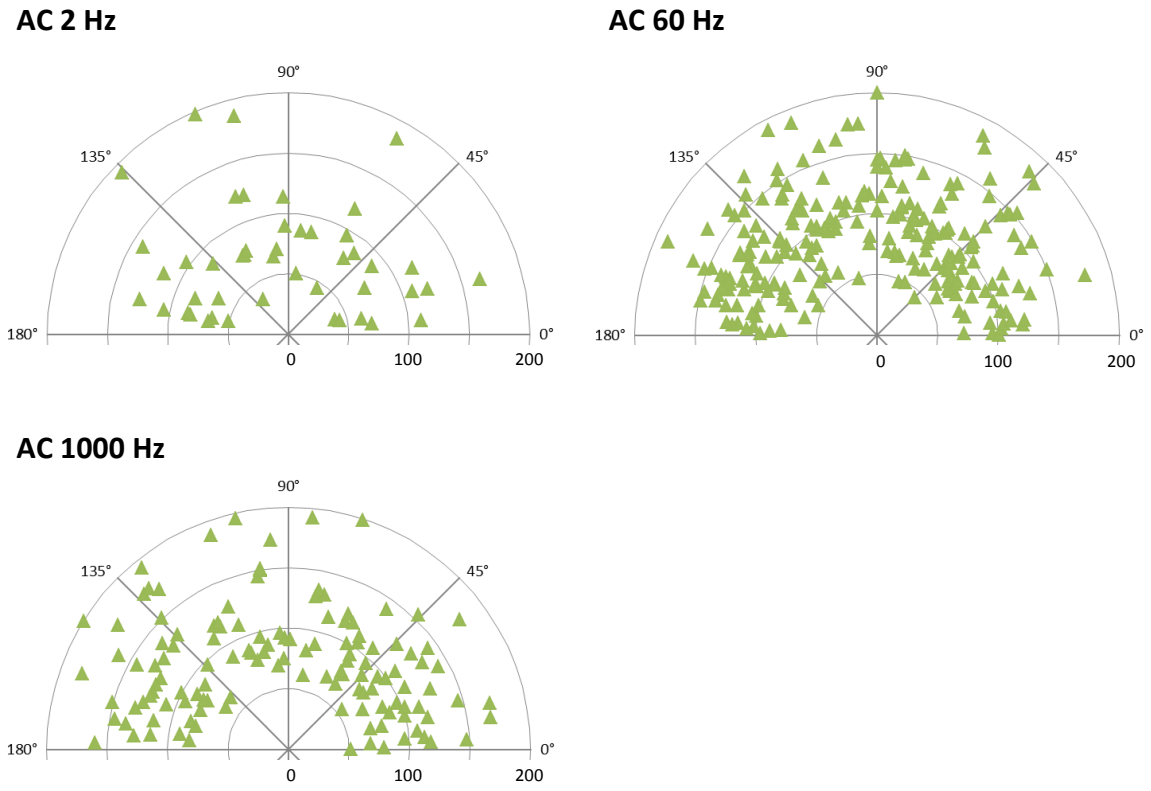

Figure 37. Polar graphs depict the length (radius, in µm) and angle of Schwann cells (represented as triangles) cultured in 2 cm wide channels, and exposed to 139 mV/mm AC EF with frequencies of 2, 60, and 1000 Hz for 6 hours.

Cell cultures receiving 139 mV/mm electrical stimulation at 2 Hz had an average cell angle of -0.06, 60 Hz was 0.01, and 1000 Hz was -0.09, all other parameters being the same. These values are all near 0, indicating that the cells are randomly oriented. The electrical properties and cell angle values measured for this experiment have been summarized in **Table 5**.

Table 5. Electrical parameters and cell measurements of experiments with changing AC frequency

AC Frequency (Hz)	Width (cm)	Voltage (V)	EF (mv/mm)	Cell angle	Standard deviation	n	p-value
control	-	-	-	-0.01	0.66	169	
2	2	10	139	-0.06	0.74	47	0.68
60	2	10	139	-0.01	0.68	234	0.81
1000	2	10	139	-0.09	0.69	129	0.30

The average cell angles of cultures exposed to 10 V AC of different frequencies were not statistically significant when compared to the control. A line graph is drawn to depict the trend in cell angle when plotted against frequency (**Figure 38**).

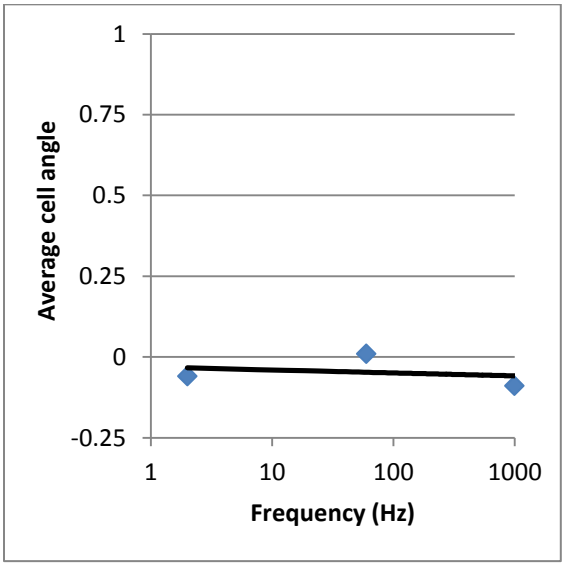

Figure 38. Voltage, channel width, current, and stimulation time were kept constant while the AC frequency was changed from 2 to 1000 Hz. The log scale shows that cell angle remains relatively near the 0 axis, indicating that cells may not reorient themselves when exposed to an AC EF.

A 10 V DC potential applied across electrodes creates a 3 V signal across a 2 cm channel and influences cells to align perpendicular to the EF, however, applying an AC signal between 2 – 1000 Hz under identical conditions does not affect cell alignment. Schwann cells do have a more round soma and a greater amount of filopodia spiking from the cell perimeter when exposed to AC stimulation.

3.3.2 Cell response to EF through substrate

An alternative method to expose cell cultures to EFs is to apply a potential across the growth substrate. This was achieved by culturing Schwann cells on conductive ITO glass coated with Matrigel and enclosed in a glass chamber 0.2 mm in height, 15 mm in width, and 22 mm in length (termed 'substrate channels', SC). In contrast with the MC setup, SC experiments all had identical dimensions but the resistance of the ITO was changed. When a potential is placed across the ITO, current primarily flows across the surface, but a small portion will also flow through the less conductive media adjacent to the surface. Furthermore, the EF across the ITO surface is replicated in the media in intimate contact with the conducting surface. This setup can be described as a current flowing through two resistors in parallel. **Figure 39** is a model created through COMSOL detailing the x-component of the EF (surface color gradient), the electric potential (contour lines), and the current density (red arrows) when a 10 mV/mm potential is placed across a 5 nm width ITO surface with a contacting block of saline.

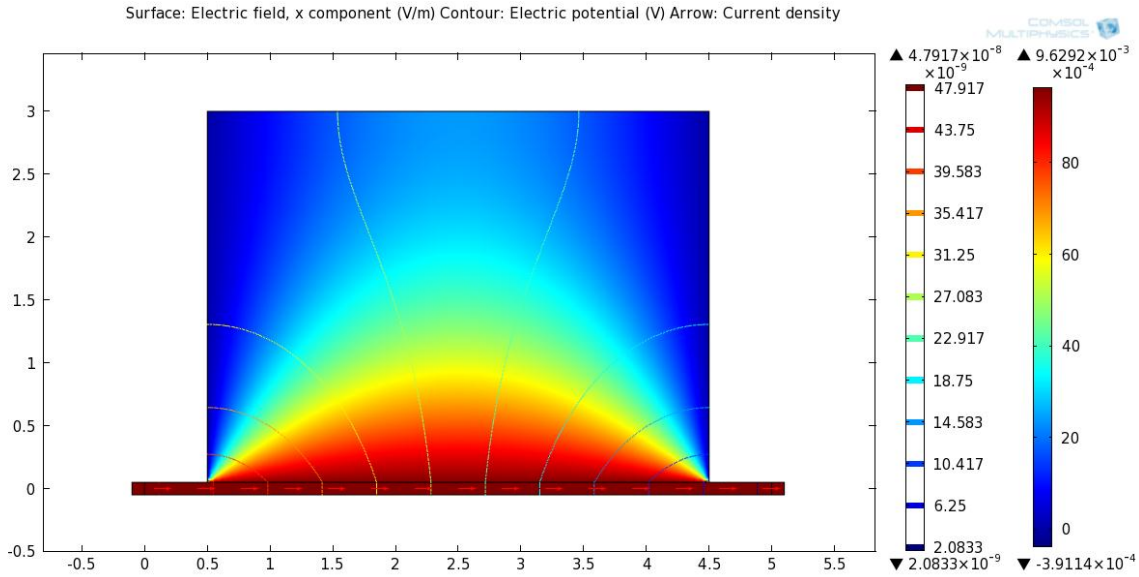

Figure 39. A cross sectional representation of the SC setup was modeled with COMSOL to determine the electrical components produced from applying a potential across the ITO. The bottom structure is a highly conductive thin sheet of ITO, where the left side is grounded and the right side has a potential of 50 nV, equating to 10 mV/mm. The x- and y-axes are measurements in nanometers. The surface color gradient represents the x-component of the EF with values described by the rightmost scale bar. The contour lines represent the voltage across the SC with values described by the left scale bar. The red arrows represent current density, which is mainly through the ITO structure.

The plot shows that the majority of the current density flows through the ITO substrate, but the EF still penetrates into the fluid, indicating that is possible for forces to be applied to mobile charges in the fluid to create an ionic current. However, the image is a model of two conductors in contact. To better represent the true behavior of electrical properties through this system, introduction of surface charges on the ITO, mobile charges in the conducting media, and double layer charges near the surface described by the Gouy-Chapman theory will need be needed to determine the EF in the media induced

by the EF through the ITO. Finding the zeta potential and Debye length will provide a more accurate model of what cells and proteins near the conducting surface will experience, however, that is beyond the scope of this project.

To compare EF through the media (from the previous section) with EF through the substrate, voltage, current, duration, and frequency parameters used to stimulate cells grown on ITO were chosen to be relevant to values used when stimulating through the media. Similar to the previous section, each parameter was changed independently to determine how cells behave.

3.3.2.1 Changing current density with constant voltage

To change the current density across cell cultures while maintaining a constant voltage, three resistances of the ITO glass was used – 300, 1500, and 8500 Ω. Placing a constant 1 V across the glass (equating to approximately 15 mV/mm), the currents measured an average 3.3, 0.67, and 0.12 mA. Because the physical dimensions of the SC were all identical, decrease in current results in a decrease in the current density.

Schwann cells seeded into SC channels were allowed 1 – 2 hours to adhere, stimulated for 6 hours, fixed in paraformaldehyde, imaged with a phase contrast light microscope, then analyzed for cell orientation relative to the EF direction. Experiments were repeated three times for each current value and cell angle measurements were compiled to calculate a single average angle for each current. Sample images of cells without stimulation and with 3.3 mA stimulation are shown in **Figure 40**.

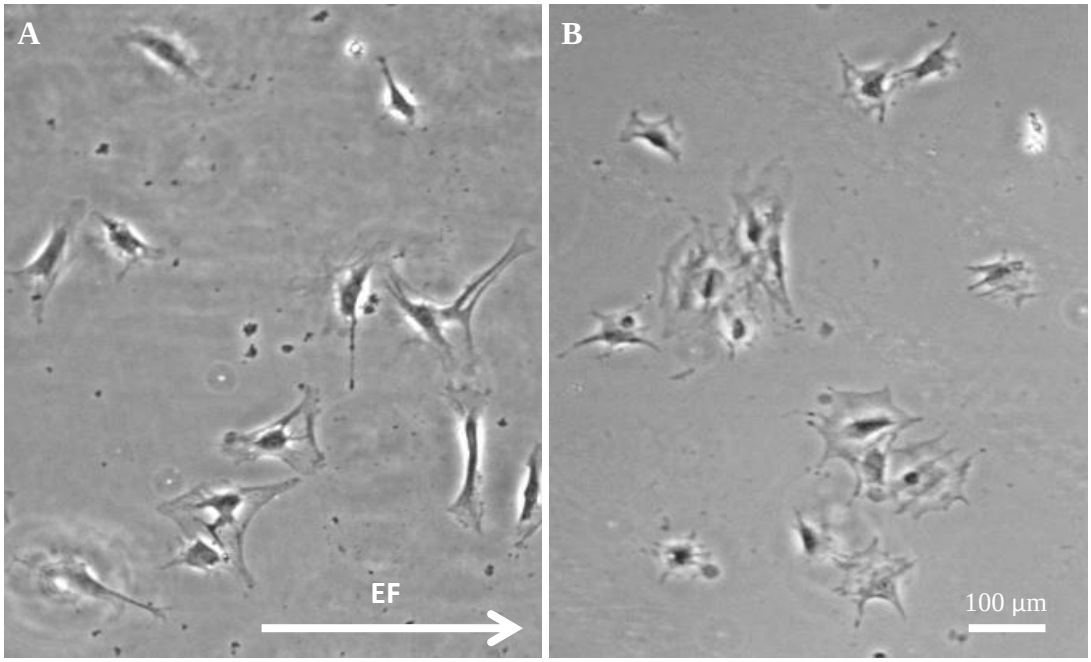

Figure 40. Phase contrast images of Schwann cells grown on (A) ITO glass without stimulation and (B) cells exposed to 15 mV/mm with a 3.3 mA current. The cultures look fairly similar, although cells without stimulation have a more bipolar phenotype compared to the spread morphology of stimulated samples. Scale bar is 100 μm.

Schwann cells typically have a bipolar shape when cultured without external stimulation, however, it was observed that cells exposed to stronger current densities had a more rounded morphology with a greater number of processes.

The next set of polar plots in **Figure 41** show the Schwann cell angle and length measurements for cells without stimulation (control), and cells exposed to 0.12, 0.67, and 3.3 mA currents with a constant 15 mV/mm EF. The plots show that cells did not change orientation in response to these conditions.

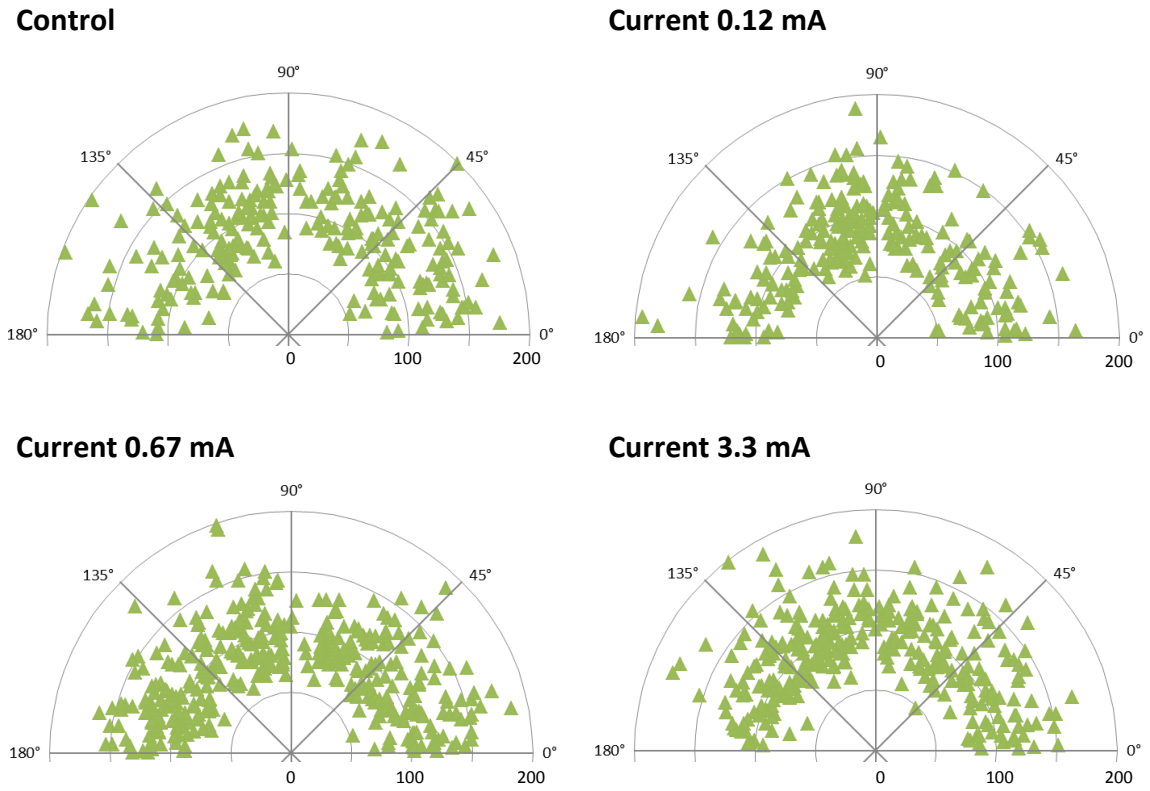

Figure 41. These polar graphs depict the cell length (radius, in μm) and angle of cultures exposed to a constant 15 mV/mm EF with varying currents. Control samples were not stimulated with an EF. There were no significant differences between the control and EF stimulated samples.

The average orientation of control samples on SC was 0.02, which is near the ideal 0 for randomly oriented cells. The average orientation angle of cell cultures receiving stimulation of 0.12 mA was 0.07, 0.67 mA was -0.05, and 3.3 mA was 0.05. However, none of these values were significantly different from the control samples. The electrical conditions and cell angle values measured in this experiment have been summarized in **Table 6**.

Table 6. Average electrical and cell measurements for experiments with changing current through the substrate

Current (mA)	Voltage (V)	Resistance (Ω)	EF (mV/mm)	Cell angle	Standard deviation	n	p-value
Control	-	-	-	0.02	0.59	348	
0.12	1	8500	15	0.07	0.56	453	0.23
0.67	1	1500	15	-0.05	0.58	590	0.08
3.3	1	300	15	0.05	0.50	563	0.59

3.3.2.2 Changing voltage with constant current density

By using the three different resistances of ITO (300, 1500, and 8500 Ω) the voltage, and resulting EF, could be changed independently to the current density. The current was kept at 1 mA across the entire ITO glass resulting in voltages of 0.3, 1.5, and 8.2 V across the 75mm glass. The EF across the cell cultures equate to 4, 20, and 110 mV/mm, respectively. Because the physical dimensions of the SC were all identical, the current density was the same for all samples.

Schwann cell culture and processing were identical to the previous section. Experiments were repeated three times for each EF value and cell angle measurements were compiled to calculate a single average angle for each EF. Sample images of cells stimulated with 4 and 110 mV/mm are shown in **Figure 42**.

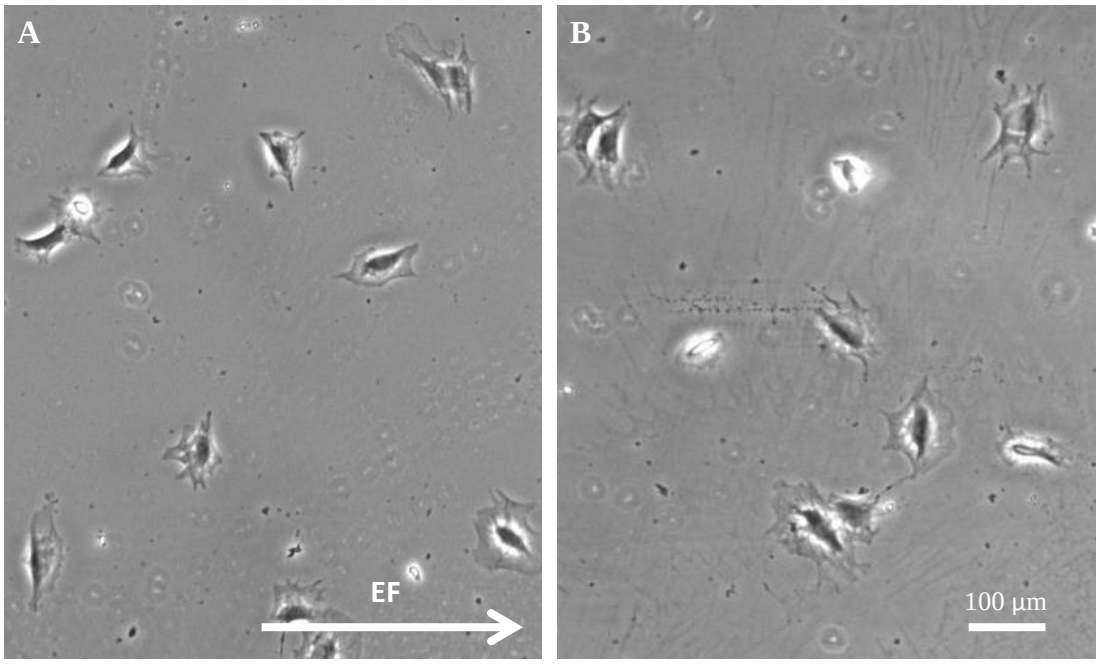

Figure 42. Phase contrast images of Schwann cells grown in SC with (A) 4 and (B) 110 mV/mm with a 1 mA current. The cell morphologies of both samples appear similar. One major difference is the change in Matrigel coating, which appears discontinuous and is often seen sloughed off the glass. Scale bar is 100 µm.

Schwann cell cultures exposed to a low or high EF had similar cell morphology, lacking a bipolar shape. At higher EF, the coated Matrigel on the ITO glass began to shed off of the surface. The shedding was observed over the entirety of the coated area and there did not appear to be any pattern to the Matrigel removal. An example of this is shown in **Figure 43**.

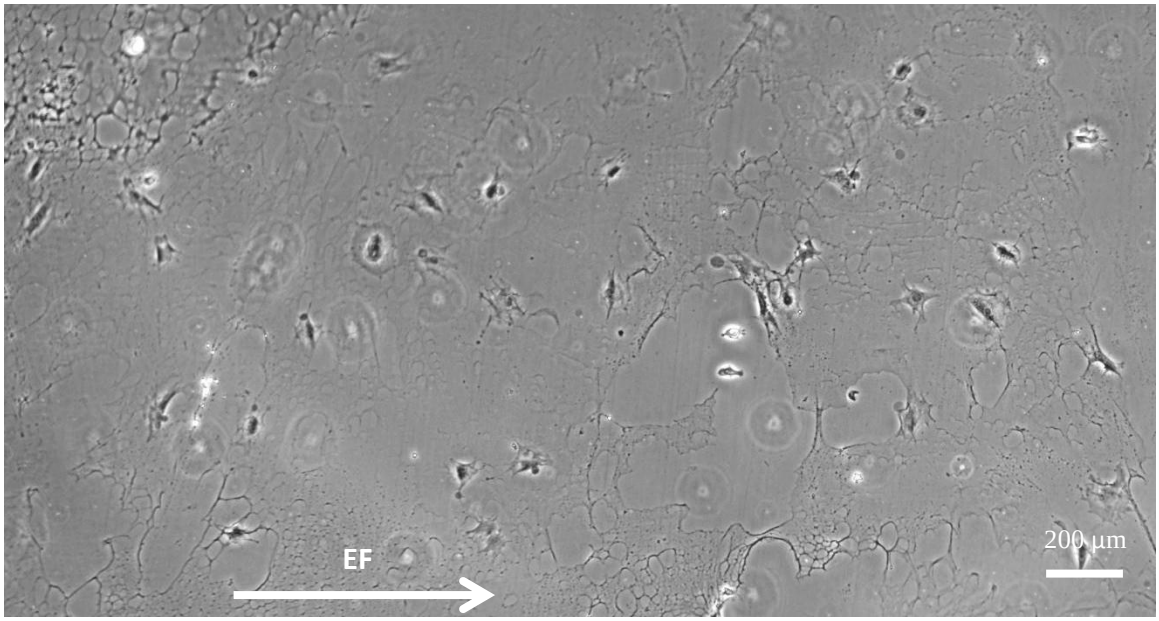

Figure 43. The Matrigel coating becomes heterogeneous when the cell culture was exposed to a stronger 110 mV/mm EF. The cells appear healthy and can be seen aligning along the edges of the peeling ECM. Scale bar is 200 µm.

The next set of polar plots in **Figure 44** show the Schwann cell angle and length measurements for cells exposed to 4, 20, and 110 mV/mm EF with a constant 1 mA current. The plots show that cells did not change orientation in response to these conditions.

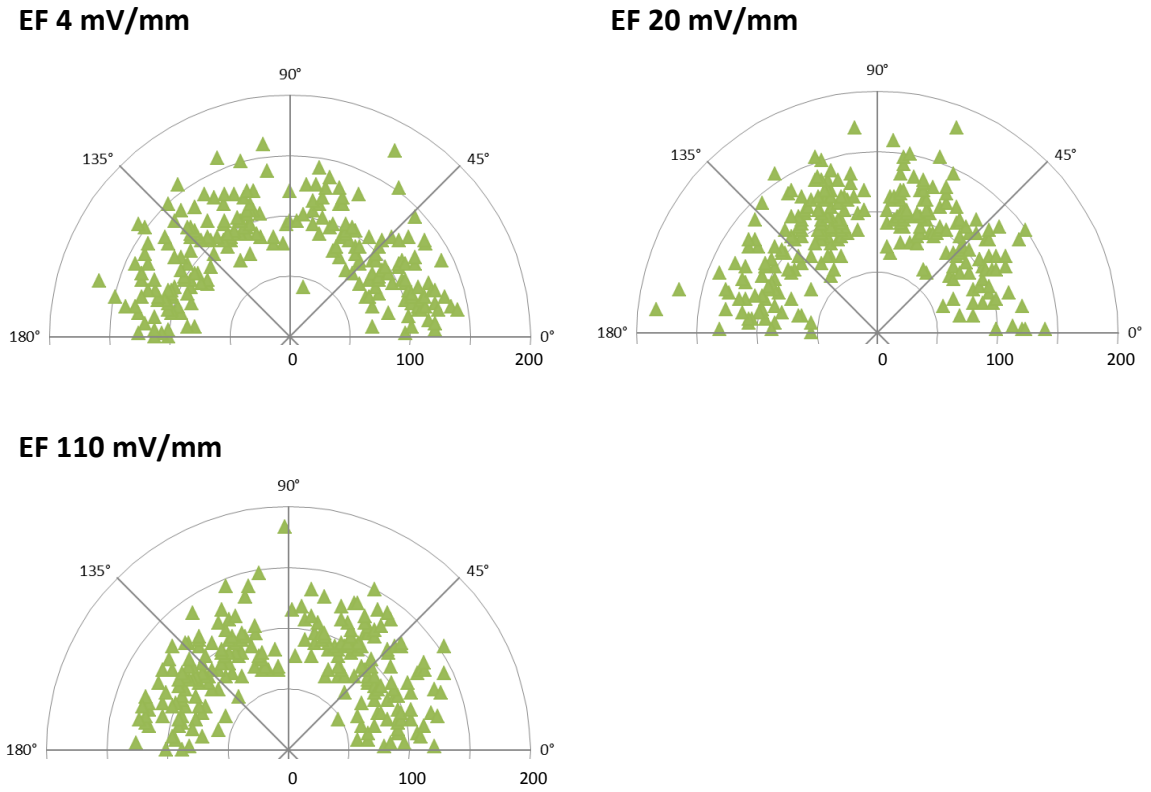

Figure 44. These polar graphs depict the cell length (radius, in μm) and angle of cultures exposed to a constant 1 mA current with varying EFs. There were no significant differences between the control and EF stimulated samples.

The average orientation angle of cell cultures receiving stimulation of 4 mV/mm was -0.04, 20 mV/mm was 0.08, and 110 mV/mm was -0.02. However, none of these values were significantly different from the control samples. The electrical conditions and cell angle values measured in this experiment have been summarized in **Table 7**.

Table 7. Average electrical and cell measurements for experiments with changing EF through the substrate

Current (mA)	Voltage (V)	Resistance (Ω)	EF (mV/mm)	Cell angle	Standard deviation	n	p-value
Control	-	-	-	0.02	0.59	348	
1	8.2	8500	110	-0.02	0.50	406	0.27
1	1.5	1500	20	0.08	0.52	473	0.16
1	0.3	300	4	-0.04	0.49	466	0.08

3.3.2.3 Changing duration with constant EF

A stimulating 15 mV/mm EF with 3.3 mA current was applied across 300 Ω ITO glass for 2, 8, and 24 hours to determine if the duration of stimulation affects cellular behavior. All samples had identical electrical parameters and culturing conditions, except for the duration of stimulation. Schwann cell culture and processing were identical to the previous section. Fixing of cultures was performed immediately after stimulation, so samples had different culture lifetimes. Experiments were repeated three times for each duration value and cell angle measurements were compiled to calculate a single average angle for each duration. Sample images of cells stimulated for 2 and 24 hours are shown in **Figure 45**.

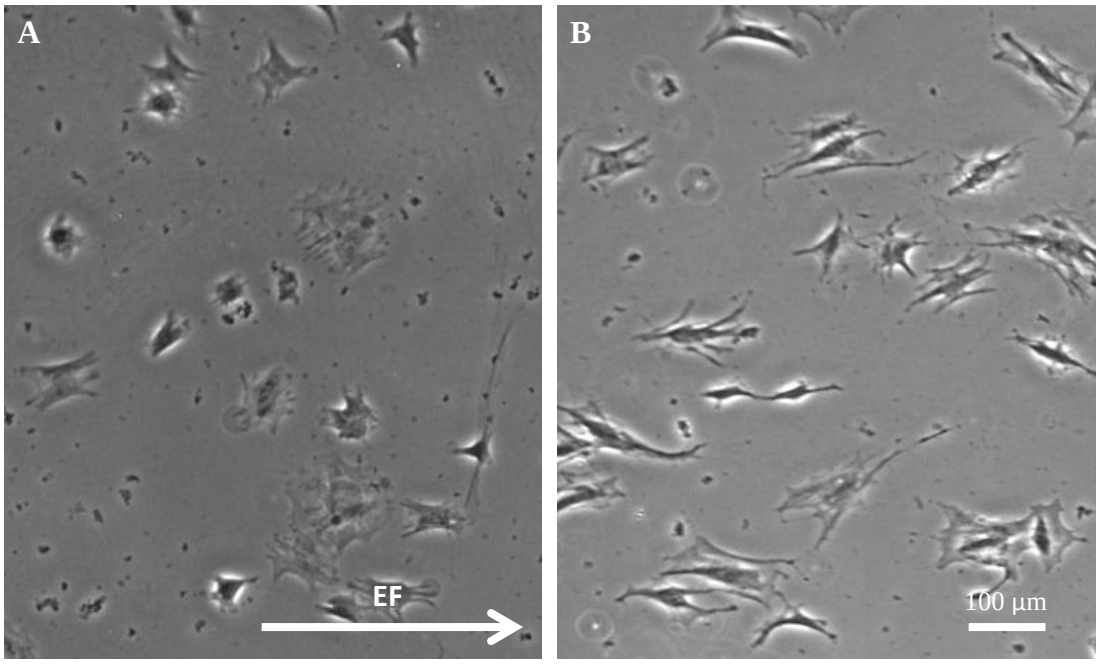

Figure 45. Phase contrast images of Schwann cells in SC stimulated with 15 mV/mm and 3.3 mA for (A) 2 and (B) 24 hours. Cells stimulated for 2 hours show a more rounded morphology, most likely due to a shorter stimulation time. Cells stimulated for 24 hours orient their body parallel to the EF. Scale bar is 100 μm.

The next set of polar plots in **Figure 46** show the Schwann cell angle and length measurements for cells exposed to 2, 8, and 24 hours with identical stimulation conditions. The plots show that cells did not change orientation in response to these conditions at shorter times, but appear to reorient after 24 hours of exposure.

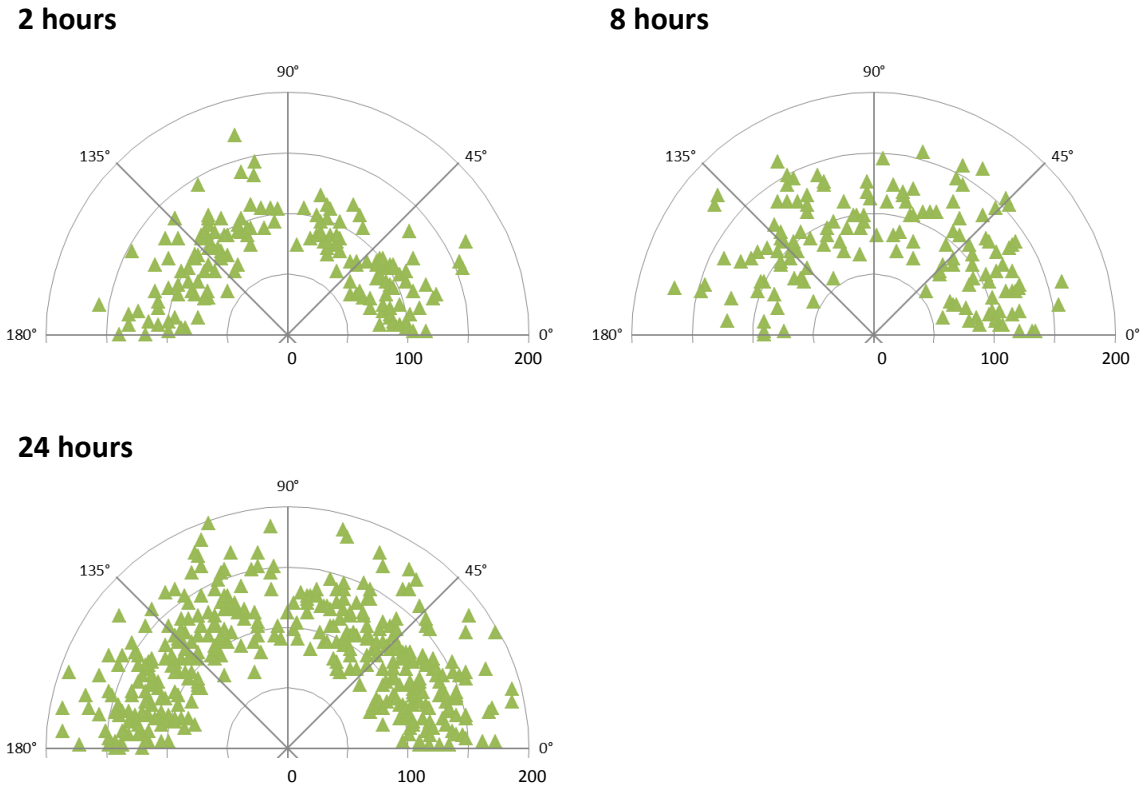

Figure 46. These polar graphs depict the cell length (radius, in μm) and angle of cultures exposed to a constant 15 mV/mm and 3.3 mA current with varying duration times. Cell cultures under 24 hour stimulation had orientation angles significantly different than control.

The average orientation angle of cell cultures receiving stimulation 2 hours was -0.04, 8 hours was -0.02, and 24 hours was -0.12. Values collected from cultures stimulated for 24 hours were significantly different from the control samples. The cells in these cultures had greater alignment parallel to the EF. The electrical conditions and cell angle values measured in this experiment have been summarized in **Table 8**.

Table 8. Average electrical and cell measurements for SC experiments with various durations under constant EF stimulation

Duration (hours)	Current (mA)	EF (mV/mm)	Resistance (Ω)	Cell angle	Standard deviation	n	p-value
Control	-	-	-	0.02	0.59	348	
2	3.3	15	300	-0.04	0.38	540	0.06
8	3.3	15	300	-0.02	0.50	290	0.30
24	3.3	15	300	-0.12	0.58	564	0.0003

3.3.2.4 Changing AC frequency

A stimulating AC signal was applied to cultures grown in SCs using an AC 15 mV/mm RMS (root mean square) EF across 300 Ω ITO glass for 6 hours to determine if changes in AC frequency affects cellular behavior. All samples had identical electrical parameters and culturing conditions, except for the 2, 60, or 1000 Hz AC signal. Schwann cell culture and processing were identical to the previous section. Experiments were repeated three times for each freqency value and cell angle measurements were compiled to calculate a single average angle for each frequency. Sample images of cells stimulated for 2 and 1000 Hz shown in **Figure 47**.

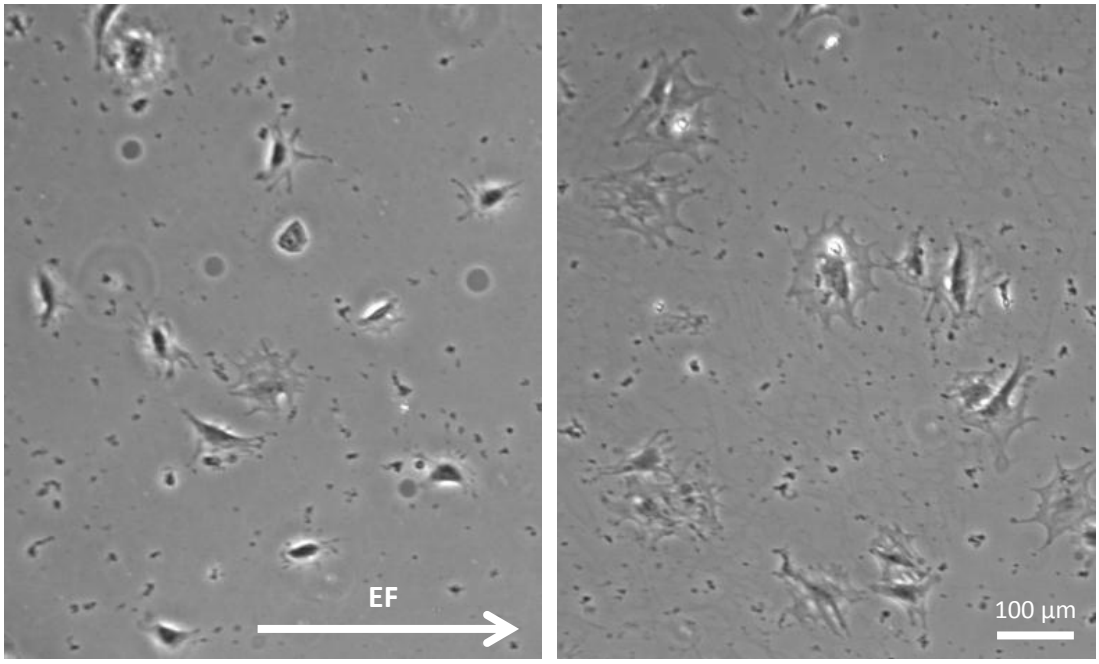

Figure 47. Phase contrast images of Schwann cells in SCs stimulated with 15 mV/mm RMS and 3.3 mA with (A) 2 and (B) 1000 Hz. Cells stimulated with 1000 Hz appear to have a more rounded morphology with many projections. Scale bar is 100 µm.

Schwann cells stimulated with a 1000 Hz signal did not appear to have an overall change in orientation angle but did have a more spread morphology with a higher amount of processes extending from the soma. This phenotype was also observed when cells were exposed to AC stimulation through the media. The next set of polar plots in **Figure 48** show the Schwann cell angle and length measurements for cells exposed to 2, 60, and 1000 Hz with identical stimulation conditions. The plots show that cells did not change orientation in response to these conditions.

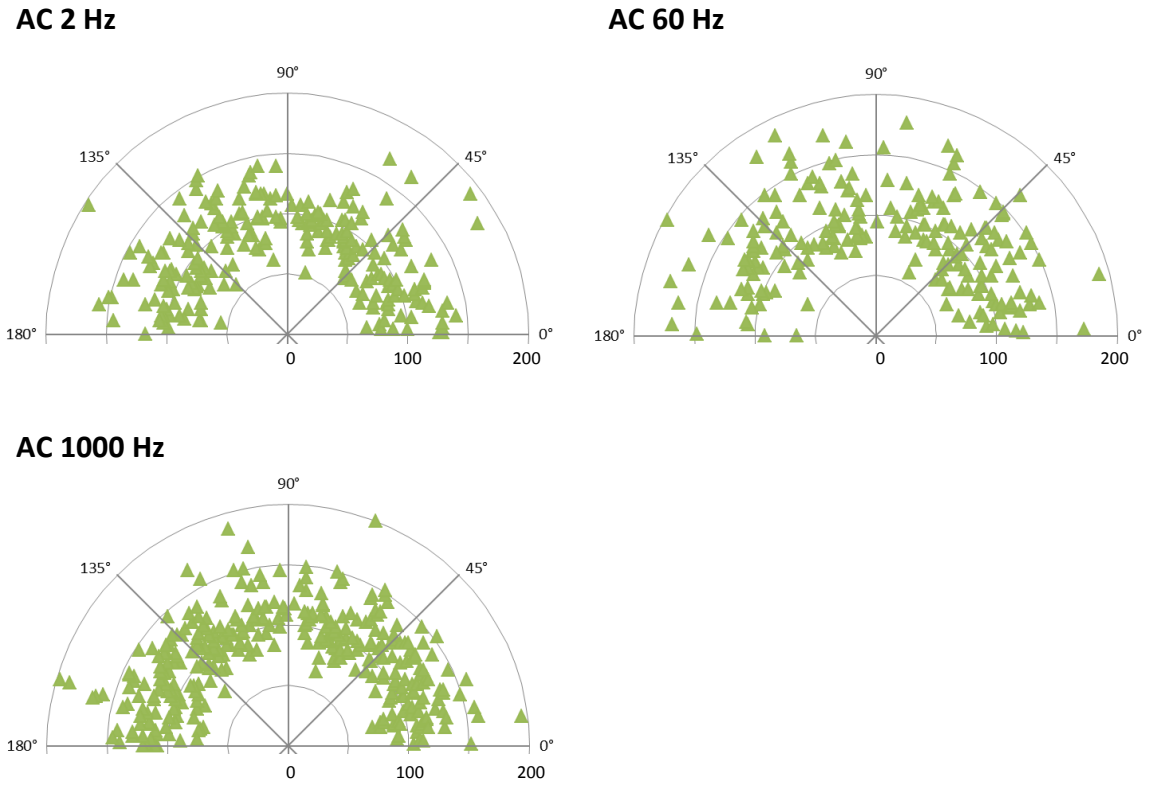

Figure 48. These polar graphs depict the cell length (radius, in µm) and angle of cultures exposed to a constant 15 mV/mm RMS and 3.3 mA current with varying frequencies. The average cell angle of cells exposed to these conditions were not significantly different than control.

The average orientation angle of cell cultures receiving AC stimulation of 2 Hz was -0.01, 60 Hz was 0.02, and 1000 Hz was -0.05. The electrical conditions and cell angle values measured in this experiment have been summarized in **Table 9**.

Table 9. Average electrical and cell measurements for SC experiments stimulated with different AC frequencies

Frequency (Hz)	EF rms (mV/mm)	Resistance (Ω)	Cell angle	Standard deviation	n	p-value
Control	-	-	0.02	0.59	348	
2	15	300	-0.01	0.52	456	0.43
60	15	300	0.02	0.48	433	0.83
1000	15	300	-0.05	0.53	590	0.09

3.4 DISCUSSION

The current study attempts to provide a comprehensive analysis of rat Schwann cell response to EFs applied through media above cell cultures and through the surface of conductive substrates beneath cultures. Earlier work by Erickson and Nuccitelli (1984) examined avian embryonic fibroblast behavior by measuring cell migration, elongation, and alignment in response to changes in EF strength, duration, cross current flow, and AC frequency through the fluid above cell cultures. The data found in their work provided the grounds for the current study in determining which of the electrical parameters have the strongest effect on changing Schwann cell behavior. Furthermore, examining cell behavior on conducting substrates will elucidate the role of electrical devices on living neural tissues.

Experiments with EF stimulation through the MC revealed that rat Schwann cells align perpendicular when exposed to stronger current density or EF. Current density and EF are coupled because the inherent resistance of the media remains the same. Changing

the cross section area or the length of the MC may change the resistance, but the current density and EF will both change together. The original intent of this experiment was to independently change current density while keeping the voltage across the MC unit constant, however, we found this was not possible because resistivity of the media could not be easily changed. Regardless, there were several findings from the MC stimulation experiments.

It was found that Schwann cells can be aligned perpendicular to an applied EF depending upon its strength or the current density related to the EF. By changing the width of the channels, the current density can be changed. When keeping an electrical current constant through the MC while the channel width increases, the current density decreases in proportion to the cross sectional area. Cells exposed to a current density of 106 mA/cm^2 and 245 mV/mm had an average angle alignment of 0.71 relative to the EF. When both values decreased to 36 mA/cm^2 and 90 mV/mm, cell alignment decreased to 0.29. These findings were followed by another experiment where the current density (and thus EF) was kept constant. When the current was ramped from 0.5 to 4 mA, the current density was maintained at approximately 65 mA/cm^2. Under these conditions, Schwann cell angle alignment correlated with the change in current density and not the absolute current strength. This suggests that current density is a more accurate representation of what cells detect in their environment when an ionic current is adjacent to its surface. The EF may also be inferred as playing an important role in cell angle orientation. The EF represents the force exerted on a charged particle within the boundaries of the field. Since charges are found on the cell membrane, membrane receptors, cytosolic constituents,

organelles, and important chemical messengers, force applied to these cellular components may affect cell behavior.

When MCs were stimulated for durations between 2 and 24 hours, there appears to be a limiting time where cell orientation does not increase any further. At 2 hours, cells are still in their alignment process and by 8 hours, the average cell orientation is at its maximum as determined by the current density or EF strength. Further increase in stimulation duration has no effect on changing the average cell orientation.

Stimulating cells with an AC signal did not have an effect on cell orientation. An AC signal constantly switches polarity so there is no net movement of ions within the media. Without a consistent directional growth cue, cells may grow randomly. Again, this suggests that the constant flow of ions or EF may be the direct impetus for cell growth. However, it is interesting to note that the AC signals do affect the cell morphology. Schwann cells, typically being bipolar, have a more rounded, spread shape with many processes extending from the soma when stimulated with AC signals. The reasoning behind this is unknown, but alternating polarity can affect the protein adsorption to the substrate, depolarization and hyperpolarization of the cell membrane, activation of receptors, and oscillation of charged intracellular molecules. Further examination of this phenomenon is needed to explain what is occurring to the cell morphology.

When stimulating Schwann cell cultures through the substrate, electrical values were chosen to be near the values used for EF stimulation through the media and used in previous work by Durgam et al. (2010). Although the two setups are very different in terms of EF and current placement, examining parallel stimulation modalities can provide important implications between the two. Values were selected based on its effect on cell

alignment in the previous experiments, providing starting points for experimenting with EF through the substrate. The middle value chosen (15 mV/mm and 3 mA) demonstrated cell alignment in the EFs through the media, so this was the base value for all experiments for substrate stimulation.

By changing the resistance of the ITO substrate, current and voltage could be changed independently without changing the physical dimensions of the channels as for the MCs. Even with a wide range of values, we did not observe any changes in cell orientation at varying current or voltage strengths. It was observed that cells also have no preferential orientation within 8 hours of stimulation, however at 24 hours of stimulation, cells were aligned parallel to the EF, which is the opposite of what we found in the first set of experiments of EF through media. There is a possibility that this is a result from the sloughing of the Matrigel coating on the surface of the ITO, creating a topology influencing cell alignment. Or perhaps the role of the EF through a substrate plays a different role in directing cellular growth. These results may also imply that EF through the substrate may take longer for the effects to appear, so all of the 6 hour experiments may have been too short to discover any overall effects of the EF. Another interesting observation is that although stimulation with AC frequency did not affect cell orientation, it still affected the morphology. In both stimulating modalities, through the media or substrate, Schwann cells exposed to the alternating signal induced cells to spread and extend processes.

There are several issues that need to be addressed in order to understand what is truly happening in substrate stimulation. First, the COMSOL model shows that the EF penetrates the fluid above it with a slow decay in strength dependent upon the distance of

from the surface. This may not be correct because the electrolytes in the fluid creates a double layer at the charged surface, reducing any effects of the EF. Secondly, the current induced in the media by the current through the ITO may be trivial, such that cells may not experience an ionic current flow. And thirdly, even when the physical dimensions are held constant, the current density may not be calculated correctly because the ionic flow may only be adjacent to the surface.

Regardless of the issues, delivering current through the substrate can produce several phenomena. 1) The charged surface will attract or repel charged species such as ions or proteins in the media (Kotwal and Schmidt 2001), 2) heat produced by current can change protein conformation and cell behavior, 3) the current beneath the cells can induce an ionic current in the adjacent fluid, and 4) the EF along the substrate will also affect the structures adjacent to the ITO glass. Each of these effects can influence cell behavior to change in a positive or negative manner.

Further studies in this area exploring the possibilities of EF stimulation of the substrate is needed to elucidate its effect on cell behavior. It may be possible that the effects do not manifest until a day after stimulation due to environmental restructuring or intracellular metabolic processes. Lack of cell orientation change in substrate stimulation be also be due incorrect stimulation parameters that were modeled from stimulation through the media. The effects that were found when stimulating through the substrate, namely at 24 hour stimulation and using AC stimulation, are encouraging for future studies in using this technology for tissue engineering applications.

Chapter IV:

Extracellular matrix exposed to an electric field aligns Schwann cells

4.1 INTRODUCTION

Electric field (EF) stimulation is an attractive method for enhancing nerve repair as they have been known to be essential in embryogenesis, tissue development, and wound healing (Hotary and Robinson 1994, Nuccitelli 2003). Studies by Hotary (1992) found that disrupting the EF in avian and amphibian embryos can result in limb, tail, and head developmental defects while Nuccitelli (2003) found that amplifying this EF strength can increase the rate of bovine corneal wound healing. Song et al. (2004) demonstrated that intensifying the wound induced EF can increase the number of nerve sprouts on the wound edge but repressing the EF can significantly delay nerve sprout formation.

In animals, cells balance ions by separating charge across tissue layers, creating a difference in electric potential. Damage to this layer allows ions to flow across the tissue's potential gradient, producing an ionic current (Messerli and Graham 2011). The EF that produces the ionic current can direct growth of nerves and improve wound healing, however the mechanisms behind these EF-directed cell response is largely unknown. Investigators have hypothesized EFs place forces on mobile charged species in tissues, changing cell membrane polarization and causing movement of organelles, cell membrane receptors, and intracellular processes. Further investigation of this mechanism will be key to developing a unique method for nerve regeneration.

The majority of current studies have focused on the direct effects EFs have on cell behavior, however few studies have examined the changes electric fields can produce in the extracellular environment. Because EFs affect all charged species within its field, electric stimulation, in addition to directly affecting cell growth and behavior, can possibly produce physical and chemical changes in the extracellular matrix (ECM) environment. Experiments by Cheng et al. (2008) have shown that electrodes submerged in a collagen I gel producing an electrochemical gradient can create local alignment of collagen fibers, a major component of the ECM. However, a major issue to overcome would be the generation of cytotoxic byproducts when electrodes are placed directly in conducting media, producing a hydrolyzing potential within the body. Still, the ability to control ECM fibril alignment by electrical stimulation is an innovative method to create a prolonged regenerative environment for nerve repair.

In this study, rat Schwann cell morphology was observed to model recovery of nerve injury. Schwann cells are glial cells found in the peripheral nervous system (PNS) which form the myelin sheath around nerves and release trophic factors necessary for the survival of the nerve. When nerves are damaged, Schwann cell infiltration precedes axon growth, secreting essential growth factors and laying an ECM pathway for the growing nerve to follow. Schwann cells will often arrange in a linear formation as they proliferate at an injury site, forming Bands of Bungner (Reichert 1994). New nerve sprouts will then grow in close association with these aligned bands. Unsuccessful nerve reinnervation can be attributed to improper formation of bands (Campbell 2008), thus, the ability to align Schwann cells will increase chances of successful target reinnervation.

The current study will describe the use of EF to alter the ECM environment to direct Schwann cell growth. Instead of creating a direct ionic current through fluid, a possible alternative is to apply a current through a conductive material to induce an EF adjacent to its surface. The conductive material will act as a scaffold for cell growth and as a substrate for exposing EF to the ECM. This novel method for EF stimulation will be explored by observing the effects of EF on the ECM and cell morphology.

4.2 MATERIALS AND METHODS

4.2.1 Extracellular matrix hydrogels

Two extracellular matrices (ECM) were used to create hydrogels. Matrigel (8-10 mg/ml growth factor reduced, phenol-red free, LDEV-free, BD Biosciences, Franklin Lakes, NJ) is a basement membrane ECM produced by mouse sarcoma cells containing approximately 60% laminin, 30% collagen IV, and 8% entactin. Rat tail collagen I (8-10 mg/ml BD Biosciences, Franklin Lakes, NJ) is the most abundant type of collagen in the human body and is found in scar tissue. To make hydrogels, aliquots of ECM kept on ice are injected onto substrates. A 40 µl bolus is spread across the surface to create a gel 0.5 x 1.5 cm^2 in area and approximately 50 µm thick. The ECM film was placed in a 100% humid incubator at 37^oC with 5% CO_2 for 15 minutes to allow gelation. Following gelation, cells and/or media was added before EF experimentation. Matrigel was used in all experiments, however for topological imaging, collagen I was also used because it

undergoes extensive fibrillation, creating fibrils 50-100 nm in diameter whereas Matrigel remains amorphous and is difficult to observe topology.

4.2.2 Schwann cell culture

Schwann cells isolated from neonate rat sciatic nerves were purchased from ScienCell (Carlsbad, CA). Cells were cultured on tissue culture plastic in high glucose DMEM medium with 10% fetal bovine serum, 2 μM forskolin (Sigma-Aldrich, St. Louis, MO), and 3 μg/ml bovine pituitary extract (Invitrogen, Carlsbad, CA). Cells reaching 70-80% confluency were detached with 0.25% Trypsin-EDTA for 2 minutes at 37^{o}C, pelleted by centrifuging at 800 rpm for 4 minutes, and resuspended in fresh medium. Only cultures between passages 4-8 were used for experiments. Medium was changed every third day and cells were kept at 37^{o}C with 5% CO_2 in a humid incubator. For EF experiments, approximately 5000 Schwann cells were seeded onto the surface of ECM gels, either during or after EF stimulation. Cultures were maintained in 500 uL of medium for the duration of the experiment before live imaging.

4.2.3 Electrical stimulation of hydrogel

Electrical stimulation of samples was performed on electrically conductive indium tin oxide (ITO)-coated borosilicate microscope glass slides (25 x 33 mm^2, resistance 30-60 Ω, Delta Technologies, Loveland, CO). Polycarbonate wells with inner dimensions of 1.0 x 1.5 cm^2 were secured on to ITO glass using high vacuum grease

(Dow Corning, Midland, MI). The unit was sterilized under UV light for 20 minutes before 40 µl of cold hydrogel was spread on the ITO surface to create a gel approximately 0.5 x 1.5 cm^2. Electrodes were attached to opposite sides of ITO glass such that the applied EF is parallel to the longest edge, shown in **Figure 49**.

Voltage across this two-electrode setup was produced by a multi-potentiostat (1000C Multipotentiostat, CH Instruments, Austin, TX). Samples were stimulated for 2 hours at 10 mV/m in a 100% humid incubator at 37°C with 5% CO_2. Gels that received no electric stimulation served as controls.

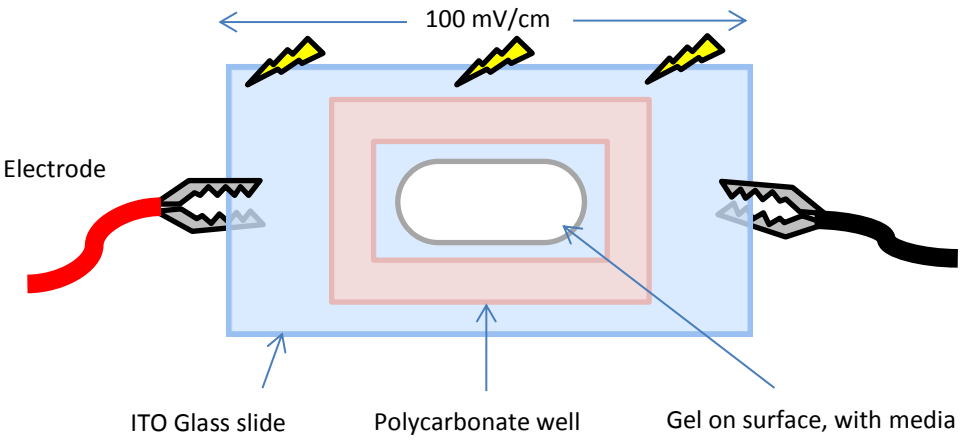

Figure 49. A polycarbonate rectangle is adhered to ITO glass using vacuum grease, creating a cell culture well. A thin layer of gel is spread on the surface before adding media, then electrodes attached to the glass will supply an EF across the gel. Cells may be added afterwards.

4.2.4 Calcium concentration measurement

Immediately following stimulation of gels (without cells) as described earlier, the media was aspirated, polycarbonate wells were detached, and the Matrigel was flash frozen in liquid nitrogen to immobilize all loosely bound molecules. Hydrogels on ITO that received no EF stimulation served as controls. The frozen gels were cut into 5 equal sections and were thawed at 4^{o}C in separate microcentrifuge tubes. Once fluid, 5 µl from each section was mixed into 100 µl of PBS containing 5 mM EDTA and 1 µM calcium green dye (Calcium Green-1, Invitrogen, Carlsbad, CA). The fluorescence emitted from each section was read by a fluorometer with a 485/20 nm excitation and 528/20 nm emission wavelength (FLx800, BioTek, Winooski, VT). Calcium concentration measurements were also conducted 1 and 3 days after stimulation.

4.2.5 ECM stimulation for microscopy

To image ECM gels with an oil immersive objective for confocal microscopy, smaller stimulation chambers were created. Instead of adhering polycarbonate wells to ITO glass, no.2 coverslips were cut and adhered to the ITO creating a trough 15 x 22 mm^2 and 0.2 mm high. ECM was placed in this trough and sealed with a cover glass greased along the edges. Gel stimulation was performed in these chambers and immediately imaged after stimulation.

4.2.6 Imaging and data analysis

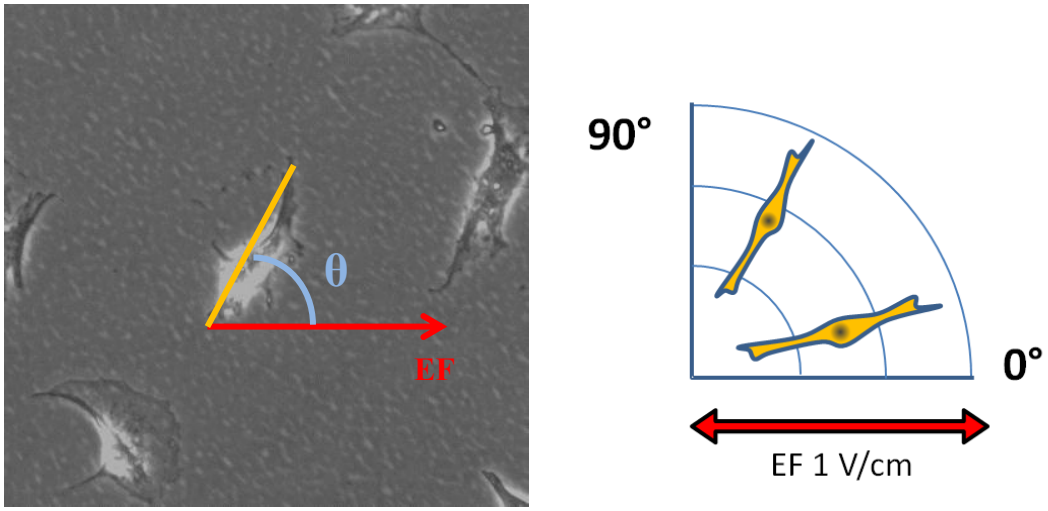

Figure 50. Schwann cell orientation is measured by drawing a line along the longest axis of the cell. The angle between the drawn line and the EF direction, θ, is the cell alignment. Cell angles closer to 0^o are parallel to the EF and angles closer to 90^o are perpendicular to the EF.

Phase contrast images of live Schwann cells was captured with an inverted light microscope (IX-70, Olympus, Center Valley, PA) with an attached CCD camera (Optronics MagnaFire S608000, Goleta, CA). Alignment of cells relative to the EF direction was measured using NIH ImageJ open source software (available at http://rsbweb.nih.gov/ij/). Images of cells were rotated so the EF vector was parallel to 0^o in a polar coordinate system. Cell alignment was measured as the angle between 0^o and a straight line drawn through the longest axis of a cell, shown in **Figure 50**. Curved cells had a single straight measurement to represent the average direction if cell alignment. All measurements lie within 0^o and 180^o (quadrants I and II). Similar to Chapter 3, the cosine of the angle was used to describe the orientation of the cells (pg.51-52). If θ is the cell

angle relative to the EF, then -cos 2θ will give a convenient description of cell alignment where θ closer to +1 is perpendicular to the EF, -1 is parallel to the EF, and 0 has no particular orientation which would be expected for control samples having a random distribution of orientation.

Phase contrast images of collagen samples were imaged with a 40x magnification. Collagen fibril orientation was analyzed with ImageJ with the OrientationJ plugin (Biomedical Engineering Group at Ecole Polytechnique Federale de Lausanne, available here http://bigwww.epfl.ch/demo/orientation/). The program determines the orientation of objects within an image by calculating structure tensors in a local neighborhood. Settings were set to a Gaussian window of 1 pixel, with a minimum coherence of 10% and minimum energy of 1% to analyze the Gaussian distribution of collagen fibril orientation. Data was outputted as an orientation distribution graph and as a redrawn image color-coded based on angle.

Collagen is autofluorescent so confocal reflectance microscopy (CRM) was used to image collagen I fibers without fluorophores. Matrigel was not imaged because it has an amorphous structure unlike the fibers found in collagen I gels. Stimulated collagen I gel samples were quickly washed with PBS, fixed with 4% paraformaldehyde for 15 minutes, washed three times with PBS 5 minutes each, then stored in PBS for imaging. Fixed ECM samples were imaged using an inverted confocal scanning microscope (Leica SP2 AOBS, Leica Microsystems Inc., Buffalo Grove, IL) with a 40x oil immersion objective and a 633 nm He/Ne laser. Although collagen is known to fluoresce with an excitation wavelength near 370 nm, there was no observable difference when excited with a lower energy wavelength. Collagen fibers were analyzed in z-stacked images of 40

sections spanning a depth of 40 μm, at least 10 μm below the glass surface. Collagen fibril angle alignment was calculated as mentioned above.

ECM samples for scanning electron microscopy (SEM) were fixed with 4% paraformaldehyde/ 2% glutaraldehyde for 15 minutes immediately following EF stimulation, aspiration, and a quick PBS wash. Fixative was removed and samples were washed three times with PBS 5 minutes each. Fixed gels were dehydrated by graded ethanol/PBS solutions of 50%, 75%, 85%, 95%, and 100% for 15 minutes each, and a final 100% ethanol solution for 30 minutes. Ethanol was then replaced with a graded hexamethyldisilizane (HMDS)/ethanol solution of 25%, 50%, 75%, and 100% for 15 minutes each, and a final 100% HMDS solution for 30 minutes. Gel samples were air dried overnight in a fume hood, then sputter coated with gold-palladium. SEM images were taken with a Quanta 650 FEG (FEI, Hillsboro, OR) using high vacuum, high voltage of 2-5 kV, spot size of 3.0 nm, working distance approximately 8.5 mm, and magnification between 1000 – 12000x.

One-way ANOVA with Tukey's post-hoc test was used where appropriate to compare calcium concentrations within gels (SPSS v.20, IBM, Armonk, NY). Student's t-test was used to compare cell orientation on stimulated gels with cells on control gels. Statistical significance was determined to be $p<0.05$.

4.3 RESULTS

4.3.1 EF influences calcium distribution across ECM gels

Small strips of Matrigel were spread onto electrically conductive ITO glass and submerged in cell culture medium. A 10 mV/mm EF was applied across the ITO glass for 2 hours to induce ionic flow across the surface. Following stimulation, gels were quickly submerged in liquid nitrogen to inhibit diffusion of mobile molecules. The gel was sectioned into five equal volumes, from cathode to anode (**Figure 51**). Change in ionic distribution near the surface of conducting ITO glass was observed by measuring the calcium green fluorescent intensity correlating with the Ca^{2+} concentration in each section of gel. Experiments were repeated six times and data presented is the average of all experiments.

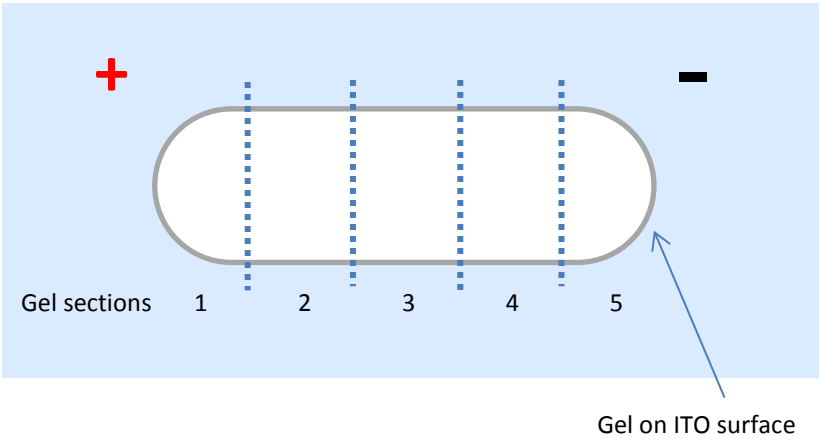

Figure 51. An EF stimulated gel is flash frozen in liquid nitrogen and sectioned into five equal volumes. Each section is analyzed for Ca^{2+} concentration.

The base fluorescence of the calcium green solution was approximately 3000. A standard curve was generated indicating that 500 units of fluorescence equates to a difference of 80 μM of Ca^{2+}. In gels without EF exposure, Ca^{2+} concentrations in each of the five sections were not significantly different, as indicated by the average calcium green fluorescence of 5300-5600 (**Figure 52**). For gels exposed to a substrate EF of 100 mV/cm, Ca^{2+} concentrations in section #5 closest to the negatively charged cathode, had the highest calcium green fluorescence at 5550 and sections #1-4 had gradually lower fluorescence than #5 with readings between 5000-5500. Section 1 and 5 were found to be significantly different with $p<0.02$. Comparing sections between control and stimulated samples showed that there was significant difference between section 1 with $p<0.01$, however, section 4-5 of the control group were not significantly different from the respective sections 4-5 of the stimulated group. Absolute measurements can be found in **Table 10**.

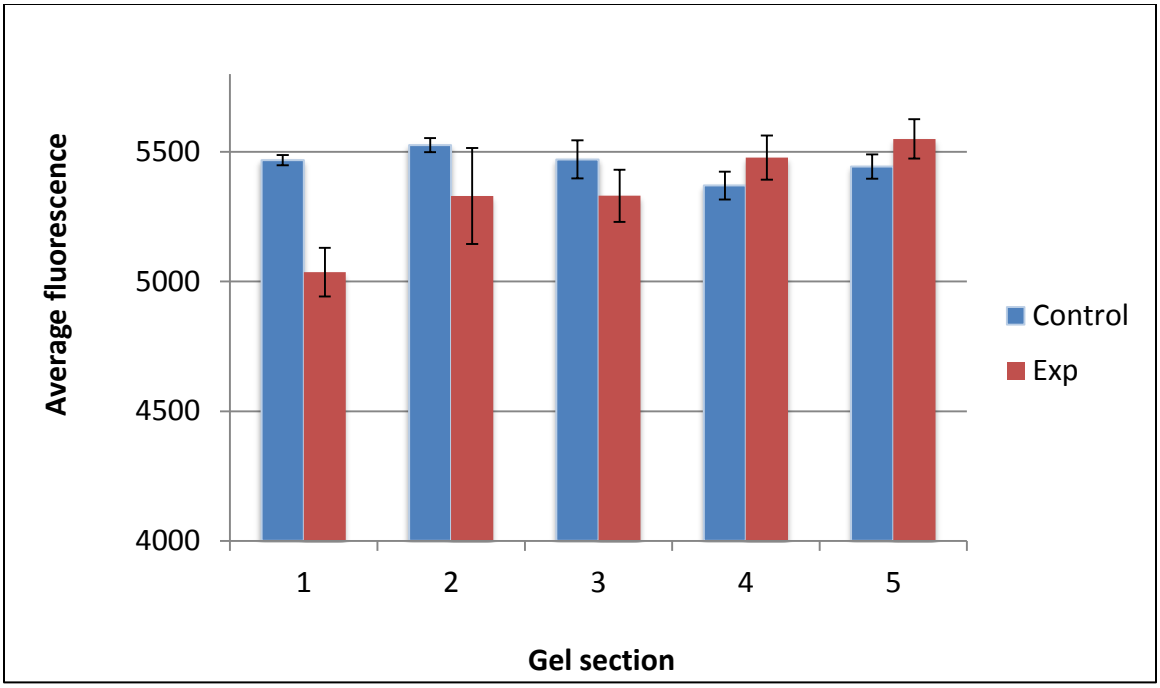

Figure 52. Gels that were not exposed to EF (control – blue bars) had similar concentration of calcium green fluorescence in each of the five sections. Gels exposed to 10 mV/mm (experimental – red bars) had a gradient of calcium fluorescence in the gel sections, increasing from anode to cathode. Error bars represent standard error of the mean.

Table 10. Calcium fluorescence measurements of EF stimulated gels (with standard error)

	Gel Sections (n=6 for each section)				
	1	2	3	4	5
Control	5468 (20)	5526 (27)	5471 (74)	5371 (54)	5444 (47)
EF stim	5036 (94)	5330 (185)	5331 (100)	5478 (85)	5550 (76)

Calcium measurements were also taken 1 and 3 days after stimulation to determine if an ionic gradient is prolonged within the gel. EF stimulation of the gel was performed identically as previous, but the gels were left in the incubator for the allotted time before units were aspirated, frozen, and divided into five sections for calcium green assay. There was no measurable difference in calcium distribution across the gel compared to control samples for either 1 or 3 days after stimulation (data not shown).

4.3.2 ECM gels exposed to EF align Schwann cells

Change in Schwann cell morphology was observed when cultures were introduced to a protein matrix gel previously exposed to an EF. Gels were first spread onto the ITO glass, then stimulated by applying 10 mV/mm across the underlying ITO surface for 2 hours in an incubator. Schwann cells were cultured on the gels either during stimulation or cultured 1, 3, and 7 days after completion of stimulation. Cells cultured on spread gels with no EF served as controls. Two days after cell seeding, live cells were imaged using phase contrast microscopy and cell angles were measured to determine alignment (**Figure 53**). Each condition was repeated at least three times.

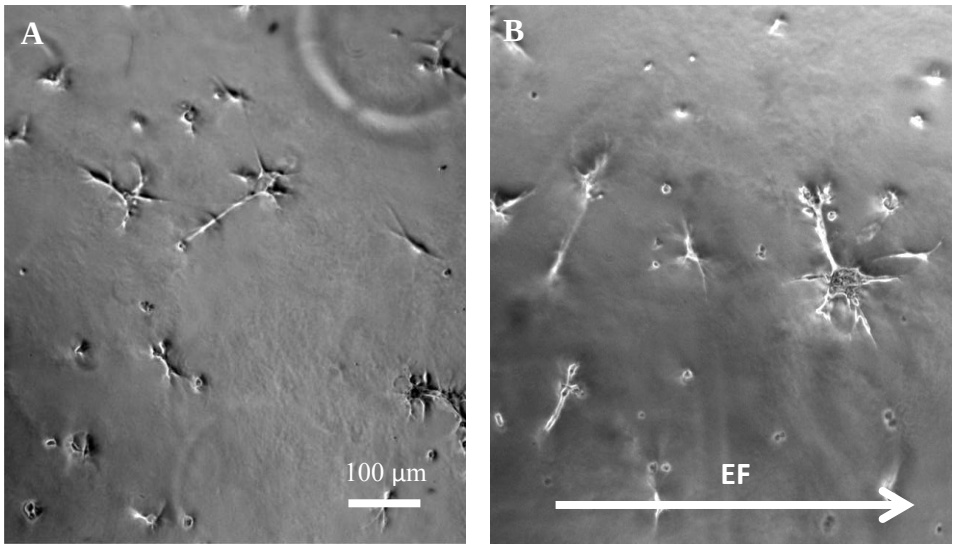

Figure 53. (A) Schwann cells from control groups have random orientation, with an average alignment near -0.03 to the EF. (B) Schwann cells seeded on pre-stimulated Matrigel exhibited cell alignment averaging 0.29.

The average cosine angle of Schwann cells in control samples was -0.03, close to the predicted average of 0 for randomly aligned cells. Schwann cells cultured on gels during EF stimulation had greater perpendicular alignment to the EF with an average angle of 0.29 ($p<10^{-6}$). When seeded 1, 3, or 7 days after gel stimulation, Schwann cells had an average alignment of 0.30, 0.24, and 0.21, respectively (values recorded in **Table 11**. The average angles were each significantly different than control samples ($p<0.01$), but were not statistically different from each other. The data reveals EF stimulation has a lasting effect on the ECM as indicated by Schwann cell alignment found days after stimulation. Although angle alignment of cells seeded on gels 1-7 days after stimulation were not statistically significant from each other, there appears to be a trend where cell cultures on recently stimulated gels show greater perpendicular alignment than cells seeded at a later time.

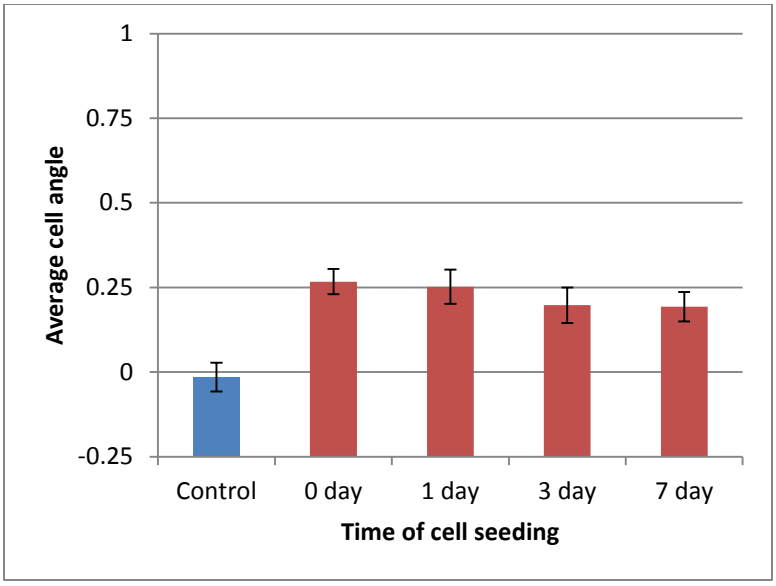

Figure 54. Schwann cells were seeded onto gels during EF stimulation and 1, 3, and 7 days after stimulation (red bars). Average cell angle of cultures on stimulated gels ranged between 0.21-0.30. All samples were significantly different than controls (blue bar), but were not significantly different from each other. However, there appears to be a trend in decreasing Schwann cell orientation when cell seeding is delayed for a longer period after gel stimulation. Error bars represent the standard error of the mean.

Table 11. Electrical parameters and cell measurements for Schwann cells cultured on stimulated Matrigel

Seed time (day)	EF (mV/mm)	EF duration (hours)	Cell angle	Standard deviation	n	p-value
Control	-	-	-0.02	0.60	196	
0	10	2	0.27	0.57	242	10^{-6}
1	10	2	0.25	0.58	129	10^{-4}
3	10	2	0.20	0.56	115	0.002
7	10	2	0.19	0.61	192	0.001

4.3.3 ECM gels exposed to EF before and after fibrillation affect Schwann cells equally

ECM gels containing collagen undergo fibrillation when exposed to higher temperatures, creating a more rigid structure from intertwining collagen fibrils. Because conducting electric current through a material creates heat in addition to inducing surface current, EFs may affect ECM in multiple ways. To observe the effects of EF on collagen fibrillogenesis, substrate electrical stimulation of ECM gels was performed before or after gelation. The onset time of stimulation was initiated while the gel was spread cold (non fibrillated) or initiated after incubating at 37^{o}C for 30 minutes (after fibrillation). Following 24 hours electrical stimulation, Schwann cells were seeded on the gel for 48 hours, then imaged to observe cell morphology. Stimulating the gel before or after fibrillation appears to have no long term effect on cell orientation.

4.3.4 EF stimulated collagen I gels change structure

In a separate study, collagen I was used as a model matrix protein to observe physical structures under independent and controlled settings. Matrigel ECM is composed of 60% laminin and 30% collagen IV, and although collagen I and IV are different, their chemical components are similar. The main difference is collagen I fibrillates under physiological conditions creating large fibril strands that are easily observable under microscopy. Phase contrast, CRM, and SEM microscopy were used to observe structural changes in collagen I gels following 24 hour, 100 mV/cm stimulation on ITO glass. Samples for confocal microscopy were preserved with aldehyde fixatives

and kept in PBS for imaging. Samples for SEM were preserved with aldehyde fixatives, dehydrated with graded ethanol and HMDS replacement, then kept desiccated for imaging.

Phase contrast images of collagen I diluted to 25 μg/ml were analyzed using ImageJ with the OrientationJ plugin. The collagen was sufficiently diluted so collagen fibrils could be detected individually for automated analysis. OrientationJ calculates the distribution of tensor angles of line structures in images. A color distribution of tensor measurements was outputted such that every 15^{o} of angle is represented as a different color, shown in **Figure 55**. Experimental collagen I samples were stimulated with 100 mV/cm in glass chambers for 24 hours (n=5). Control samples (n=4) were placed in identical conditions without electrical stimulation. The graph of average angle distribution indicates greater fibril alignment between 45^{o} and 90^{o}, which is perpendicular to the EF. The integral of the distribution intensities between 45^{o} and 90^{o} shows that EF stimulation increased perpendicular alignment by 7% compared to controls.

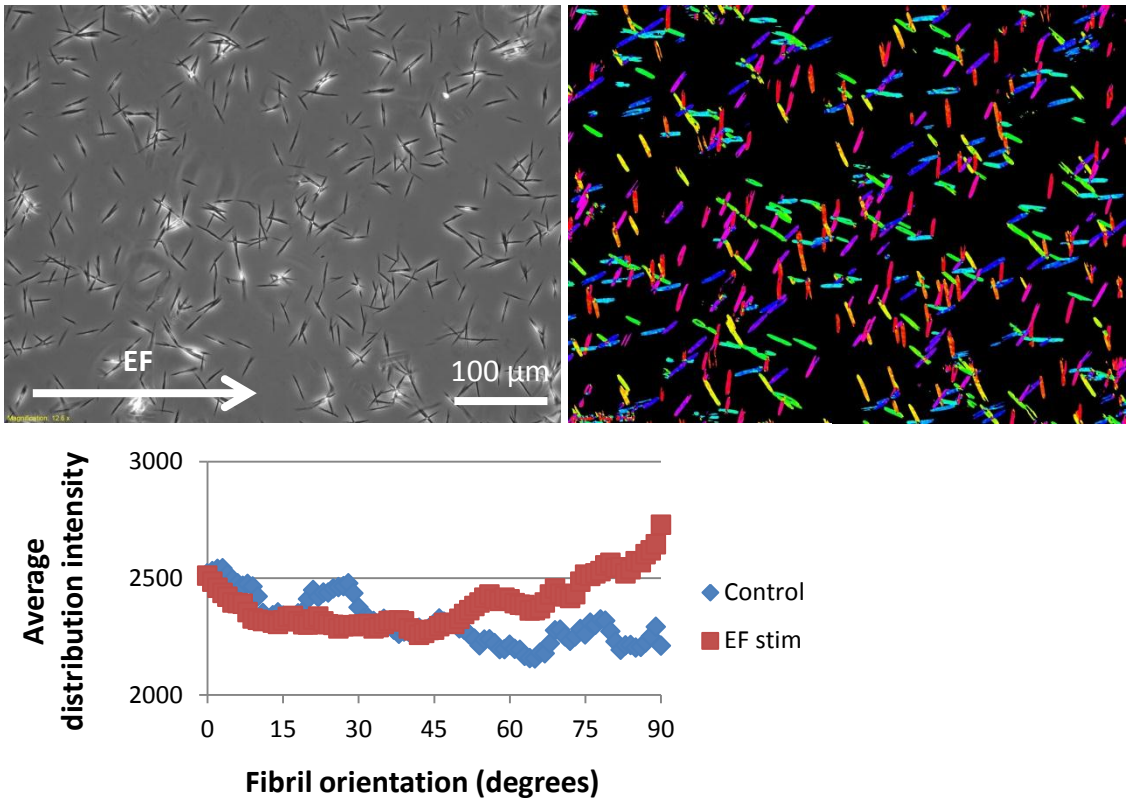

Figure 55. A phase contrast image taken with a 20x objective and corresponding tensor map of diluted collagen are shown in the two pictures above. The distribution of collagen I fibril orientation is graphed below the images, showing greater vertical alignment near 90 degrees. Scale bar is 100 µm.

CRM was achieved by using an HeNe 633 nm laser to autofluoresce the stimulated collagen I fibrils on ITO glass. The collagen I gels were diluted to 250 µg/ml because stock at 10 mg/ml was too dense to visualize and 25 µg/ml was too dilute to view 3D collagen structures. At least 6 controls and 6 stimulated samples were imaged. Confocal images shown in **Figure 56** are maximum projections from 40 slices taken within 40 µm depth, which was at least 10 µm from the coverslip glass. There were two observations in these stimulated dilute collagen I samples: 1) EF stimulation reduces the

homogenous microfibril pattern typically seen in control samples and 2) clusters of large fibril formation are more prevalent under EF sitmulation. However, meaningful quantification of these observations proved difficult to attain because of the random formations of fibrils and gel heterogeneity.

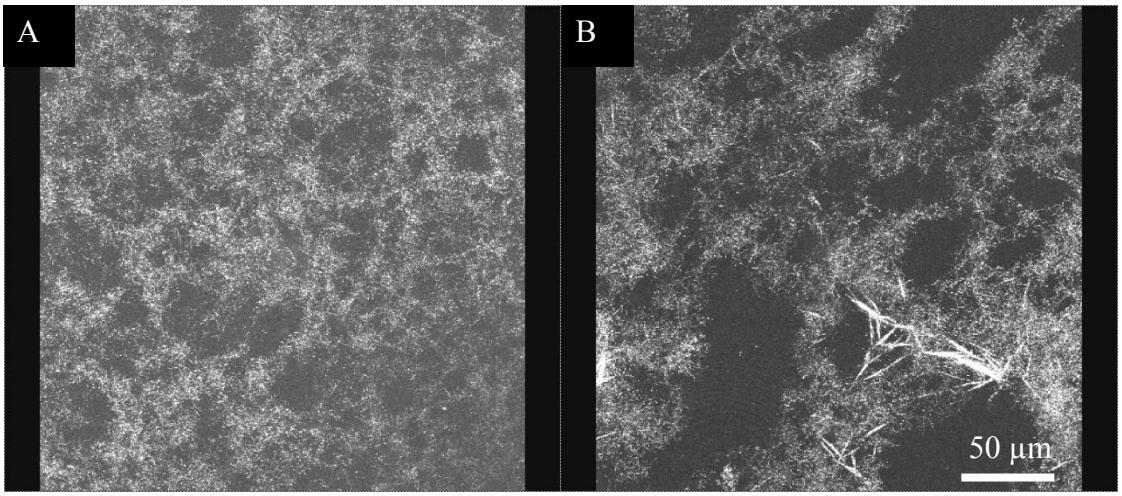

Figure 56. Confocal images of (A) control and (B) EF stimulated dilute collagen I gels show a difference in structural arrangement. Collagen control samples have a relatively uniform pattern for microfibril organization, however, EF stimulated samples appear less homogenous and have more large fibril formations. Scale bar is 50 µm.

SEM of 10 mg/ml collagen samples were imaged after stimulation and HMDS dehydration. Using 10 kV acceleration and 8000x magnification, individual fibrils and fibril bundles can be viewed (**Figure 57**). Fibril bundles are defined as groups of at least five fibril strands that are aligned in the same direction, extend for at least 10 µm, and are packed together, often entwining. It appears that stimulated collagen I gels have more fibril bundles on the surface than collagen I gels without EF exposure.

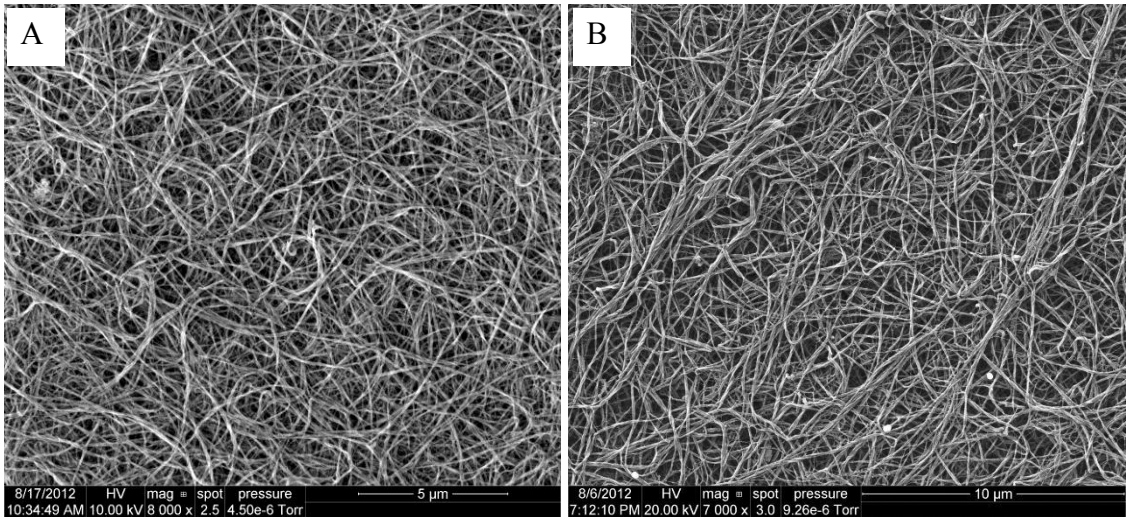

Figure 57. SEM images of (A) control collagen I samples and (B) EF stimulated samples both show fibril arrangement at 7000 – 8000x magnification. Stimulated samples have more fibril bundles, identifiable as grouped fibrils that are aligned and twisted together. Image (B) shows two bundles both aligned around 60-70^{o}.

The field of view was too narrow in images taken at 8000x magnification, so 1000x magnification images were analyzed for counting of fibril bundles. The field of view captured was approximately 150 x 130 μm^2 per image. The control samples were repeated n=4 times with 47 images analyzed and the EF stimulated samples were repeated n=5 times with 66 images analyzed. Prevalence was calculated by summing the fibril bundle count in all images and dividing by the total images for each group. On average, control samples had 0.2 fibril bundles per image and EF stimulated samples had 1.1 fibril bundles per image, graphed in **Figure 58**. The average angle of fibril bundles in EF stimulated collagen samples were found to not be significantly different than the controls ($p>0.35$).

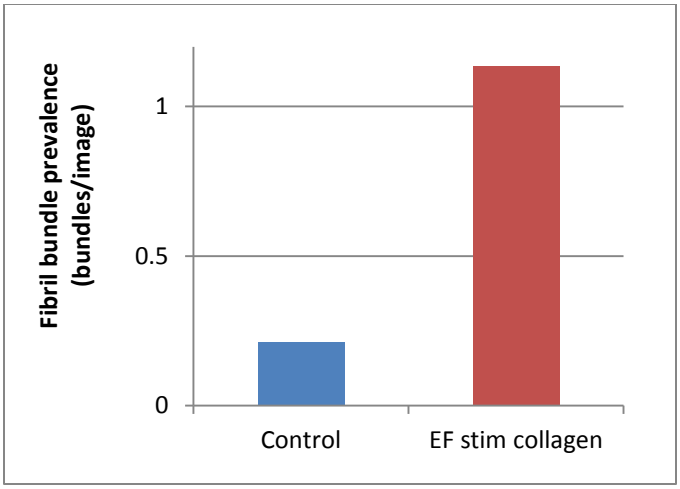

Figure 58. Prevalence of fibril bundle formation on EF stimulated collagen I samples was greater than control samples with an average of 1.1 bundles/image versus 0.2bundles/image for controls. Each image is 150 x 130 μm^2.

4.4 DISCUSSION

Matrigel, an ECM hydrogel consisting of numerous basement membrane proteins and growth factors, and Collagen I hydrogel, a triple helix protein which self assembles into macromolecular fibers found in scar tissue, were selected for these experiments because they are present at the site of injured nerves, forming a support matrix for regrowing nerves and accompanying glial cells. Collagen I was used for visualizing effects of EF because this type of ECM contains visible fibers which are highly organized in mature tissue but are randomly oriented in scar tissue. In the current study, an electrically conductive substrate was used to emit an EF to align matrix proteins, controlling cell growth behavior and possibly improve tissue formation at wound sites.

Although use of EFs and hydrogels in regenerating injured nerves have both been studied, no work has satisfactorily examined the changes that electric stimulation can induce in a hydrogel and in the cellular response to these changes. Traditionally, cells that receive electric stimulation will exhibit alignment perpendicular to the EF lines. In this study, cells seeded onto a pre-stimulated gel exhibited similar alignment with an average cosine angle of 0.29 with respect to EF lines. However, cells seeded onto gels that received no stimulation exhibited random alignment with an average angle of -0.03. The results of this study demonstrate electric stimulation is likely inducing physical changes in the hydrogel that cause the cells to display preferential alignment. Thus, selected chemical and physical characteristics of the extracellular environment post-stimulation were examined.

Examination of the charge distribution in a stimulated hydrogel is a simple way to test for the presence of chemical changes induced by the EF. We expect stimulation may cause positive ions to gather near the negative electrode during electric stimulation, creating a charge gradient in the gel. The concentration of calcium ions in stimulated hydrogel sections was measured using Calcium Green, a dye that emits fluorescence proportional to the concentration of free calcium in solution. As expected, examination of Ca^{2+} distribution in Matrigel post stimulation revealed a statistically greater amount of Ca^{2+} near the cathode end of the gel. Because Ca^{2+} is an important molecule in cell signaling, movement, and growth, neurites may exhibit preferred growth towards an area with a higher Ca^{2+} concentration. Existence of a Ca^{2+} gradient may explain why repeated, independent experiments have shown preferential neural neurite growth towards the cathode (Robinson 1985, Henley and Poo 2004, Ariza et al. 2010). Furthermore,

increased Ca^{2+} presence may benefit Schwann cells because they are calcium dependent during the EF induced increased expression of NGF, nerve growth factor that enhances neurite growth, direction, and survivability (Huang et al. 2010).

While the only ion examined was Ca^{2+}, the results of this experiment are relevant to any mobile charged species. In addition to direct interaction with the cell, EFs can indirectly affect cell behavior through modification of the extracellular environment. It is worthwhile to note the total Ca^{2+} concentration of stimulated gels appears to be lower than that of the control gels. Although the Ca^{2+} concentration of media before and after stimulation was measured, no detectable change could be found (data not shown). It is possible that during EF stimulation of the substrate, a small amount of Ca^{2+} diffuses out of the gel and into the surrounding media while Ca^{2+} gathers towards the cathodal end of the substrate.

To investigate the duration of these EF induced changes, the time was varied between gel stimulation and cell seeding. Although detection of an EF induced ion gradient provides insight into mechanisms of EF guided nerve growth, this chemical change is likely only relevant as long as the gel is receiving stimulation. Without continuous stimulation, this temporary chemical gradient wears off quickly, causing loss of beneficial nerve guidance. Schwann cells exposed to an EF while cultured on gels aligned at 54^{o} and Schwann cells seeded onto gels 1, 3 and 7 days after the completion of electric stimulation had average cell alignment at 54^{o}, 52^{o}, and 51^{o}, respectively. Although these values were not significantly different from each other, there appears to be decreasing alignment the longer cell seeding is delayed. The effects on the gel may have a relaxation period as indicated by the trend in decreasing alignment over time. As

EF induced effects in the gel are long lasting, we hypothesize that electric stimulation is likely altering the physical structure of the hydrogel.

In later experiments, collagen I was chosen as a substitute for Matrigel for two reasons: (1) collagen I contains easily identifiable fibrils when brought to physiological temperature for gelation, whereas Matrigel is difficult to image because it remains amorphous when gelled and (2) collagen I is similar in chemical makeup to non-fibrillar collagen IV, which is a major component of Matrigel. If EFs applied across conductive ITO glass exert a force on proteins adjacent to the surface, it was hypothesized that EF effects on Matrigel would be similar to effects on collagen I. Cell experiments on EF stimulated collagen showed exactly this. Cell alignment on collagen was not significantly different than cells aligned on Matrigel under the same conditions. Fibrillated collagen was then used for any experiments requiring imaging of the gel structure.

There have been no comprehensive studies that have examined physical or chemical changes in an electrically stimulated milieu, however, several groups have shown that strong electromagnetic fields can induce permanent alignment of fibers in a collagen solution (Dubey et al. 1999, Guo and Kaufman 2007, Huang et al. 2010). In our study, we observed EF stimulated matrix protein also had a long term effect on cell alignment. Because collagen is a major component of Matrigel, electrical stimulation of Matrigel across a conductive surface may possibly align collagen, as exhibited by the aligned cells cultured on the gel. To observe changes in physical structure, stimulated collagen I fibrils were imaged using phase contrast, confocal reflectance, and scanning electron microscopy.

Phase contrast microscopy of dilute collagen I samples show that individual fibrils have greater alignment perpendicular to the EF when stimulated. Confocal images show that structural changes in the gel occur after stimulation, breaking the homogenous fibril organization and inducing more large fibril formation. The EF may have a direct effect on fibrillation, or the heating from applying a current through the ITO substrate may be changing the fibrillation of the gel. Because gel structures were difficult to analyze in bulk, the results found from these experiments remain unclear. And finally, SEM images show that collagen fibril bundles were nearly six times more likely to form on the surface of collagen I gels under EF stimulation than on control samples. Fibril architecture dictates the topology of the gels and is a key factor in cell adhesion. These findings may be indicative of the structural changes that occur in Matrigel during EF stimulation, leading to prolonged effects on cellular orientation.

ECM hydrogel is a series of cross-linked, water soluble polymers containing many charged residues. These gels are prevalently chosen as tissue scaffolds because their physiochemical properties can be tightly controlled and they present cell adhesive cues. ECM gel can also be injected as a liquid to accommodate different injuries and then hardened to form a semi-solid that has similar mechanical properties to soft tissues in the body. The time dependency of EF induced effects is an important factor in proper reinnervation of the target by the new nerve. To gauge the viability of solely using a pre-stimulated hydrogel in our nerve guidance device, we must examine the permanent aspects of EF induced changes in the gel. Should the guidance effects disappear, reinnervation of the target will be less than optimal.

Researchers are currently unsure of the exact mechanism by which EF can enhance nerve growth. However, this study has provided evidence that EFs direct cell growth and alignment through interaction with the extracellular environment. EFs are able to change the architecture of the extracellular matrix, possibly influencing cell growth and orientation. Further understanding the exact nature of how EFs interact with the extracellular environment will provide much needed insight into the role of EFs in nerve regeneration.

Chapter V:

Electric field stimulation through a biodegradable polypyrrole substrate enhances neural cell growth

5.1 INTRODUCTION

Although chemical and physical cues have been used to promote neural regeneration, cellular response to electrical cues has not been thoroughly investigated. Galvanotaxis and galvanotropism (directing cellular growth and migration using an electric field) are promising modalities for manipulating cell behavior because of their essential roles in tissue development and wound healing (Altizer et al. 2001, McCaig et al. 2002, Nuccitelli 2003, McCaig et al. 2005, Levin 2009). These endogenous electric fields (EF) are created from the separation and movement of charged biochemicals. By emulating these EFs in vivo and in vitro, researchers are able to control cell migration, elongation, and polarization (Al-Majed et al. 2000, Henley and Poo 2004, Yao et al. 2008, Zhao 2009, Ariza et al. 2010). Understanding these interactions will give researchers a useful method for controlling cell growth, whether for repairing damaged nerves (Brushart et al. 2002) or inhibiting cancer growth (Kirson et al. 2007, Schoenbach et al. 2007).

Most studies in this field typically apply a voltage gradient through the media so that an ionic current flows above the cells (Song et al. 2007). The goal for this project was to use a conductive substrate to recreate the endogenous electrical cues that have been known to promote neurite growth. Another possible method for delivering electrical

stimulation cues is to drive an electrical current through the substrate. A current applied across an electrically conductive material in an electrolyte solution will induce movement of charged species in the area adjacent to the surface affecting any molecules and structures near the device (Kotwal and Schmidt 2001, Durgam et al. 2010). This ionic current creates a chemical gradient in the solution which may lead to asymmetrical protein adsorption, intracellular biochemical reorganization, and membrane potential disruption, all of which influences cell behavior.

The current standard for nerve repair is use of autologous nerve grafts, where the damage nerve is replaced with a healthy nerve harvested from the same individual. Although effective, multiple surgeries, long operation, increased complications, loss of function at the donor site, and chance of no improved outcome are serious consequences to this technique. To avoid these drawbacks, nerve conduits synthesized mostly from silicone, extracellular matrix, or degradeable polymers have been used as an alternative. These conduits have shown efficacy because they physically direct regrowing axons towards the distal stump and prevent infiltration of scar formation, but typically lack additional growth cues. By creating a conduit made of electrically conductive materials, addition of EF growth cues can be incorporated into the device for improved regeneration.

Over the past several decades, many experiments have been conducted to assess the role of various biomaterials for use in neural regeneration (Schmidt and Leach 2003, Seal et al. 2001). A fundamental aspect of the project is selecting a substrate material that can produce an electric field when implanted inside the body. Polypyrrole (PPy) has been

chosen because of its historic usage as a semiconductor coating in the technology industry and its known history as a biocompatible polymer (Wang 2003).

The production, modification, and structural arrangement of PPy can be controlled by chemical precipitation or electrical deposition of the polymer onto a surface. These methods of polymerization allow the construct to take the form of the surface template, allowing researchers the option to design the material's final shape. Without modification, PPy is a relatively insulative semiconductor, only able to conduct electricity along the intra-chain polymeric backbone (**Figure 59**). However, in a process called doping, negative or positive charge-carriers are introduced to the polymerization process and can mediate electron mobilization between polymer chains (MacDiarmid 1997, Norden 2000), as shown in **Figure 60**. When applying a voltage across the doped PPy material, an electric current can become 1000 times greater than undoped PPy (conductivity reaches approximately 100 S/cm). While also improving its conductivity, various dopant molecules can be incorporated into the material to manipulate mechanical strength and control cellular interaction. Having the ability to control polymer electrical conductivity and biocompatibility makes PPy an attractive material to use.

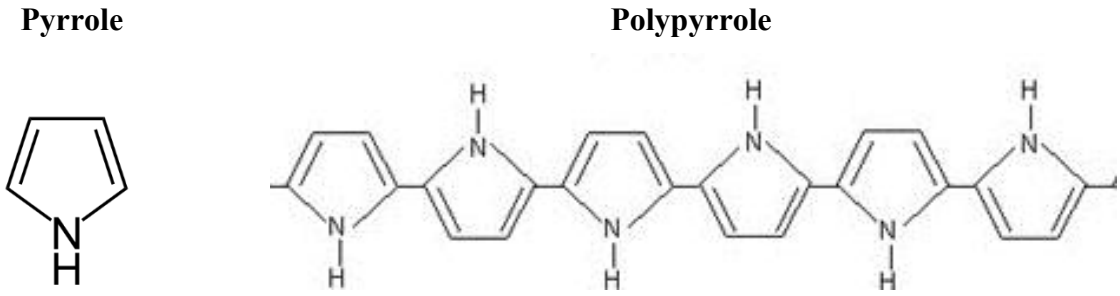

Figure 59. The backbone of the polypyrrole unit can conduct electrical charge.

Tosylate groups **Polystyrene sulfonate**

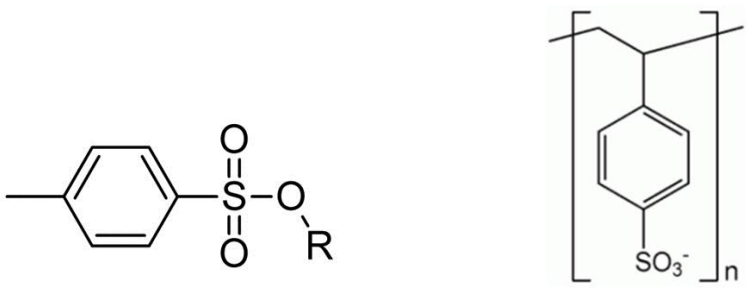

Figure 60. Anionic molecules can be added to the pyrrole polymerization as dopants. Small tosylate groups or longer chain polystyrene sulfonate molecules act as charge carriers between polypyrrole chains, increasing bulk conductivity up to 1000x.

Because there are many parameters associated with delivering electrical signals (including voltage strength, current strength, AC/DC (alternating current/ direct current), and duration, as illustrated in Chapter III), the EF experiments involved in this project will use stimulation values that were successful in enhancing cell growth found in studies by Durgam et al. (2010). Cell viability and adhesion on electrically conductive PPy films will be assessed first, then cell response to electrically stimulated PPy substrates will be measured.

5.2 MATERIALS AND METHODS

The biocompatible, biodegradable, electrically conductive PPy materials are manufactured by TDA, Inc in two forms – as conductive films and nerve conduits. The films were used for early studies of cell interactions and material properties while the conduits represented the final form of the device for exposing cells to EF. In order for the

device to be an effective conduit for nerve regeneration, mechanical properties of the PPy material were assessed qualitatively by its structural rigidity and its ability to be sutured. The unit must be biocompatible to allow proper cell growth and prevent immunological response when inside the body. The material must remain conductive within the amount of time needed to conduct electricity.

5.2.1 Polymer substrate synthesis

Fully polymerized PPy is biocompatible but typically does not break down within the body. In order to make it biodegradable, block copolymers were synthesized with polypyrrole (PPy) and poly(ε-caprolactone) (PCL) using a two-step process described in previous experiments (Luebben et al. 2007, Durgam et al. 2009). Briefly, PCL oligomers were terminated with PPy end groups, then co-polymerized with pyrrole using chemical oxidation (**Figure 61**). Upon exposure to water, PCL degrades through hydrolysis, leaving PPy macromolecules available for macrophage clearance. PPy-PCL copolymer films and conduits used for this study were synthesized by TDA, Inc. Films were cut into strips approximately 5 x 25 mm^2 and conduits were 1.1 mm in diameter and 12 mm in length. The average thickness of the material is 30 μm and average resistance measuring between the ends of a film or conduit was 4 kΩ·cm.

Polypyrrole-poly(ε-caprolactone) (PPy-PCL)

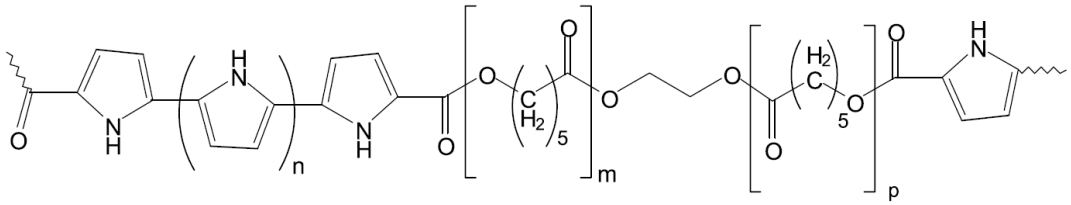

Figure 61. PPy-PCL is synthesized with block polymers of PCL between block ends of PPy. Hydrolysis of the PCL units allows the material to be degraded within the body. (Durgam et al. 2009)

5.2.2 Evaluation of PPy-PCL functional integrity

A nerve conduit must have mechanical strength to keep the lumen open and survive the rigors of implantation, yet still be pliable for suturing and manipulation at the surgical site. The simplest method to determine these properties is to have a surgeon qualitatively assess the nerve conduit's ability to perform under surgery. A graduate and a post-doctoral student with extensive training in rat surgeries were chosen to assess the handling and suturing of 4 PPy-PCL conduits each. Conduits were submerged in PBS for at least 10 minutes, then operators sutured the ends using a 5-0 and 10-0 gauge suturing needle. Their responses were recorded.

An electrically conductive conduit implanted in the body needs to remain conductive for the amount of time required for EF therapy. Under wet conditions, PPy-PCL may degrade and reduce the material's conductivity. Film strips of PPy-PCL were submerged in phosphate buffered saline (PBS) with the ends attached to electrodes above the liquid surface, depicted in **Figure 62**. The length of PPy-PCL in 10 ml of PBS were

approximately 1.5 cm. A potentiostat (1000C Multipotentiostat, CH Instruments, Austin, TX) was adjusted to supply 1-100 μA across the submerged strips. Resistance was measured before submerging the film and after 20 minutes of stimulation. A current-time graph was recorded to determine change in material conductivity.

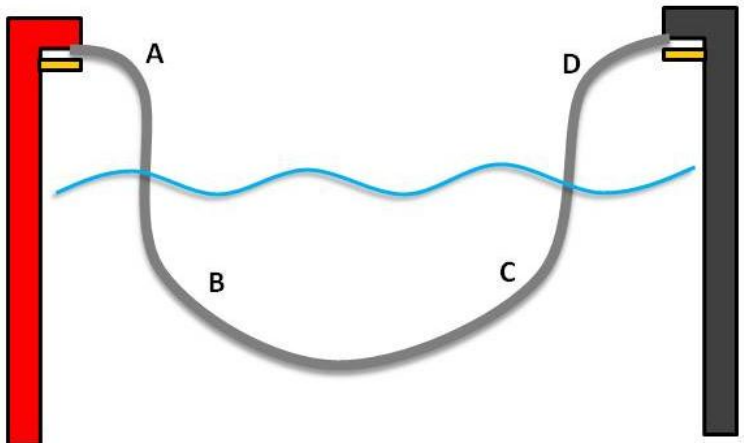

Figure 62. A thin film of PPy-PCL was submerged such that only the middle portion was in PBS while the edges connected to electrodes remained dry. By stimulating the material in this manner, conductivity can be measured over time. A-D are various sections of the material where resistance was measured across.

5.2.3 Cell culture

Two cell types were chosen to represent the axon regeneration of the PNS system. PC12 cells were used for experiments assessing the experimental conditions and dorsal root ganglia (DRG) were used to observe axon growth across the electrically stimulated PPy-PCL substrates.

The rat pheochromocytoma PC12 cell line (purchased from ATCC, Manassas, VA) are neuroendocrine cells which differentiate into a neuronal phenotype upon exposure to nerve growth factor (NGF 2.5s, Promega, Madison, WI). Although not a true neuron, neurite projections from these cells simulate neurite growth from neural cells. PC12 cells do not adhere well to tissue culture plastic, so cells were grown on 100 mm tissue culture plastic dishes coated with 0.35 $\mu g/cm^2$ of rat tail collagen I (BD Biosciences, Franklin Lakes, NJ). Cultures were maintained in RPMI 1640 media with 10% heat-inactivated horse serum, 5% fetal bovine serum, and exposed to 50 ng/ml NGF for at least 3 days before experimentation. Medium was changed every third day and kept at 37^oC with 5% CO_2 in a humid incubator. Cells were detached with 0.25% Trypsin-EDTA for 2 minutes at 37^oC, pelleted by centrifuging at 800 rpm for 4 minutes, resuspended in fresh medium, and triturated with a 23 gauge needle to break cell clumps prior to seeding 8,000 cells/cm^2 on collagen-coated PPy-PCL substrates. During experiments, 1% penicillin/ streptomycin/ amphotericin B (PSA) was added to the media. All cultures were kept in an incubator at 37^oC with 5% CO_2 and 100% humidity.

DRGs are spheres located near the spine that contain the cell bodies of sensory neurons. The DRG neurons project their axons throughout the body to receive stimuli, acting as the afferent fibers of the PNS. Thus, observing DRG axon growth in vitro is directly related to axon regeneration of damaged nerves. DRGs were harvested from postnatal Sprague Dawley rats 2-4 days after birth in accordance to approved protocol (IACUC AUP-2009-00110, Austin, TX). Briefly, the spinal column was dissected from the body and cut ventrally to remove the spinal cord and expose the DRGs. Approximately 26 DRGs were removed from a single spine by gentle plucking with a

microforcep under a 5-10x binocular dissecting microscope. The whole DRGs were quickly washed in ice cold phosphate buffered saline (PBS) with 50 μg/ml gentamycin. The explants were then placed in fresh cold PBS and trimmed free of axons. The DRG spheres were halved before embedding in Matrigel (BD Biosciences, Franklin Lakes, NJ), an ECM containing approximately 60% laminin, 30% collagen IV, and 8% entactin. Two DRGs were embedded in a 40 μl strip (spread 0.5 x 1.2 cm^2) of Matrigel on PPy-PCL films, approximately 6 mm apart to avoid any interactions, and surrounded by at least 1.5 mm radius of Matrigel. Cultures were maintained in RPMI 1640 media supplemented with 10% FBS, 1% PSA, and 50 ng/ml NGF to promote axon outgrowth, and kept in an incubator at 37°C with 5% CO_2 and 100% humidity.

5.2.4 Choosing a hydrogel for in vitro studies

The proposed device will be a conductive PPy cylinder filled with a hydrogel, providing nutritive and mechanical support for axon growth through the lumen. Five hydrogel formulations known for their ability to promote nerve regeneration will be compared for cell viability and neurite extension within a conduit (Deister and Schmidt 2006, Deister et al. 2007). Rat tail collagen I and Matrigel were gelled in their pure forms, collagen buffered with HEPES, DMEM, and collagen-hyaluronic acid gels were created following Deister et al.'s protocol (2007). PC12 cells were encapsulated in the hydrogels by mixing 5 x 10^6 cells/ml into gel at room temperature. Each hydrogel/cell mixture was injected into five sterile 2.5cm silicone tubes with an inner diameter of 1 mm (**Figure 63**). The hydrogels were then placed in the incubator at 37°C for 15 minutes to

permit gel solidification. The units were then submerged in RPMI 1640 media supplemented with 10% horse serum, 5% fetal bovine serum, and 50 ng/ml NGF, and allowed to grow for 2 days in an incubator. Tubes were removed after 2 days for live phase contrast imaging and fluorescent imaging of live/dead cells with calcein AM and ethidium homodimer-1 fluorescent dyes (Live/Dead Viability Kit, Invitrogen, Carlsbad, CA)..

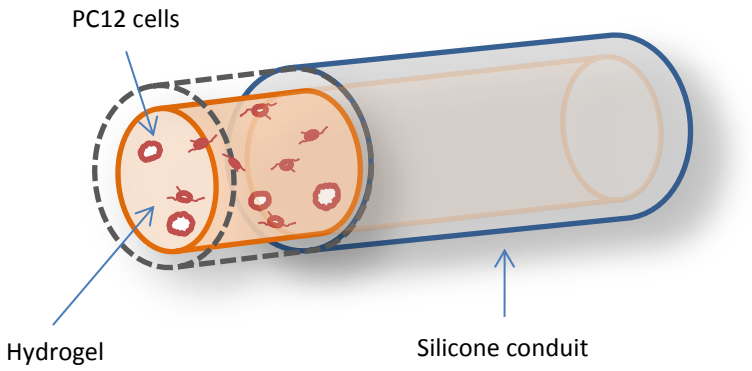

Figure 63. The drawing depicts PC12 cells encapsulated in a hydrogel that has been injected into a sterile silicone conduit. The entire unit is submerged in media for 2 days, then imaged to determine viability of growing tissue.

5.2.5 Electrical stimulation of PPy 2D film strips

Strips of PPy were cut into rectangles measuring 0.5 x 2.5 cm^2. The strips were adhered to microscope glass slides using high vacuum silicone grease (Dow Corning, Midland, MI) and secured with a polycarbonate well with inner dimensions measuring 1.0 x 1.5 cm^2 (**Figure 64**). Edges of the PPy extending beyond the well perimeter were

adhered to the glass with copper tape. The entire unit was UV-sterilized for 20 min before experimentation. A two-electrode setup with a multi-potentiostat supplied the electrical stimulation to the material. The working electrode was connected to one edge while the opposite edge was connected to the counter/reference electrode. Cells were added to the well (PC12 at 8,000 cells/cm^2 or 2 halved DRGs) in 500 µl of media and incubated for 24 hours to adhere before exposure to electrical stimulation. A constant potential of 100 mV/cm was applied across the PPy strip yielding a total potential of 200-250 mV for a duration of 2 hours. For experiments involving alternating currents (AC), the voltage signal applied was a sine wave with a peak-to-peak value of +200 mV to -200 mV at a frequency of 60 Hz. Samples were then fixed with 4% paraformaldehyde 24 hours after stimulation for PC12 cells and 72 hours for DRGs.

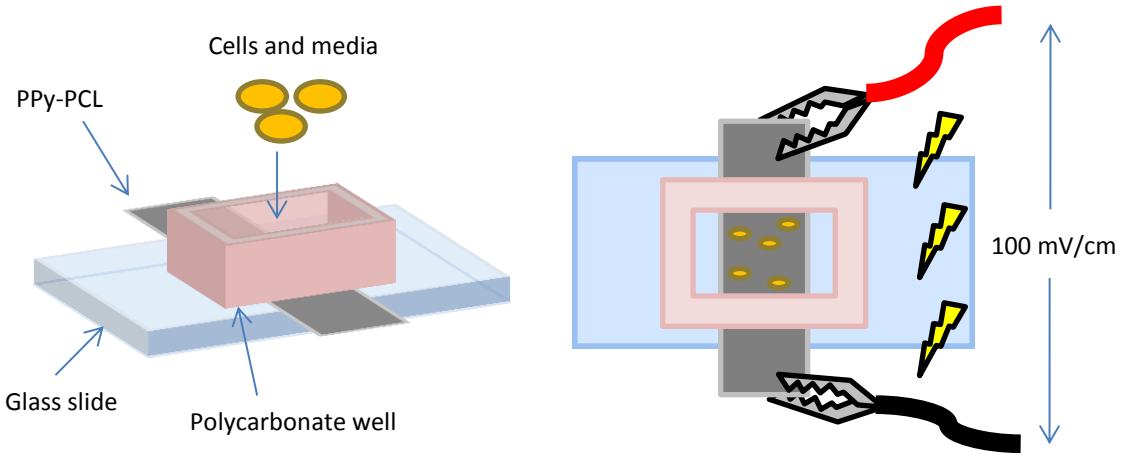

Figure 64. To stimulate a PPy-PCL film, a polycarbonate well is placed above a strip of film and adhered to a microscope glass slide with vacuum grease. Cells are cultured in the well and receive EF stimulation from electrodes attached to the edge of the PPy-PCL.

5.2.6 Electrical stimulation of PPy 3D conduits

Two DRG explants were inserted into the lumen of each PPy-PCL conduit. First, 6 µl of hydrogel (chosen beforehand as described earlier) will be injected into the conduit and a DRG will be placed in contact with the gel. Second, another 8 µl of gel is injected into the lumen from the same side to displace the initial ganglion and gel, then a second DRG is place in the lumen. And finally, the end is capped with 6 µl of gel to keep the second DRG inside the lumen (**Figure 65**).

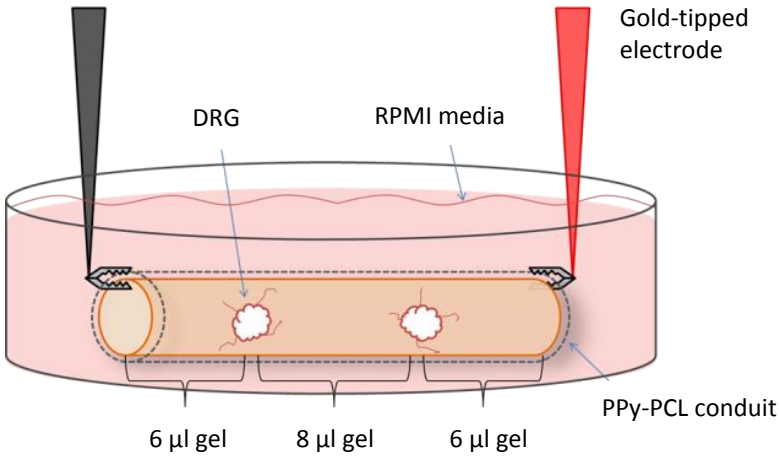

Figure 65. Two DRGs are implanted into the PPy-PCL conduit in a symmetrical fashion, far enough from the edges and from each other to prevent cell interactions. The ends of the conduit are attached to gold tipped electrodes, submerged in 10 ml of media.

Once the unit is assembled, the conduits are placed in an incubator for 15 minutes to allow gelation of the hydrogel. Gold tipped electrodes were attached to the ends of the conduit and submerged in 10 ml of RPMI media supplemented with 10% FBS, 1% PSA,

and 50 ng/ml NGF. Gold was used to reduce reduction-oxidation byproducts during electrical stimulation. Stimulation parameters were identical to those of 2D substrates described earlier with an increased 72 hours for axon growth after stimulation. Samples were then fixed with 4% paraformaldehyde for 2 hours before embedding in 4% agar and cutting axially with a vibratome (Vibratome 1000 Plus, Intracel LTD, Hertfordshire, UK). Half cylinders were then processed using immunohistochemistry.

5.2.7 Cell adhesion and viability on PPy-PCL

Although polymerized PPy materials are generally considered to be non-toxic, pyrrole monomer and oligomers present in the starting materials are toxic (Fonner et al. 2008). Residues of these chemicals may be embedded within the bulk of the final product and can elicit various degrees of cytotoxicity. To address this issue, multiple washes and electrical stimulation of the material has been shown to reduce cytotoxicity (Fonner et al. 2008, Durgam et al. 2009). An electrical current through the PPy causes the material to slightly expand due to polymer chain repulsion and moving charge pushes charged, loosely associated molecules out of the bulk, also known as de-doping. This electrical stimulation of the material to reduce cytotoxic residues before introducing cells is termed pre-stimulation. This is required to purify the material before cells are introduced to the substrate.

Several samples of the current material were pre-stimulated before experimentation to address concerns of toxicity. For these samples, film strips were electrically stimulated using the protocol described above with a 100 mV/cm DC current

without cells. After pre-stimulation, the wells were aspirated, washed with PBS, then washed with water and allowed to air dry. The 2D stimulation protocol is followed once more with a 100 mV/cm DC current with cells. Twenty four hours after the stimulation, cells are stained with calcein AM and ethidium homodimer-1 live/dead fluorescent kit. To determine the number of cells adhered to the surface of the material, images of fluorescent cells taken with an Olympus microscope were processed with ImageJ (NIH) to measure the cell area coverage on the material.

For measuring cell viability on PPy-PCL, cells grown on normal and pre-stimulated films for 24 hours were assessed using a luminescent ATP detection assay (CellTiter Glo Luminescent ATP Assay, Promega, Madison, WI). Adenosine-5'-triphosphate (ATP) is produced in live cells as a chemical energy source to sustain metabolic activity, so measuring the presence of this biochemical in experimental cultures indicate cell viability. The media in stimulated cell cultures was aspirated and replaced with 100 µl of new media and 100 µl of detection reagent for 30 minutes at 37^{o}C. Once the components have reacted with ATP from the cells, the supernatant from each well was transferred to a 96-well plate and analyzed with an FLx800 luminescent microplate reader (BioTek Instruments, Inc., Winooski, VT). Wells with known cell numbers were calibrated against luminescence intensity for each assay to create a linear fit standard curve.

5.2.8 Cell imaging and data analysis

Following stimulation of DRGs on 2D film strips and 3D conduits, samples were allowed 72 hours to extend axons before fixation. Samples were washed with warm PBS, fixed with 4% paraformaldehyde for 2 hours, washed three times with PBS 15 minutes each, permeabilized with 0.25% Triton-X 100 for 30 minutes, washed three times with PBS 15 minutes each, then incubated in primary antibody β-III tubulin (Abcam, Cambridge, MA) diluted 1:1000 in blocking solution containing 3% goat serum in PBS and kept at 4^{o}C overnight. The samples were washed three times with PBS 15 minutes each then counter-stained with a secondary antibody conjugated with Alexafluor 488 at 4^{o}C overnight. Samples were washed three times with PBS 15 minutes each then stored in PBS before imaging.

Cell images were obtained with an inverted phase contrast/ fluorescent microscope (Olympus IX-70, Olympus Corporation, Tokyo, Japan) with an attached color CCD camera (MagnaFire S60800, Optronics, Goleta, CA). Before measurements, images of the samples were rotated so the PPy-PCL strip was oriented horizontally, where the counter electrode is at 0^{o} (reference for 0 V) and the working electrode is at 180^{o} in polar coordinates (+ 200 mV). Axon length, angle, and density were measured with NIH ImageJ open source software (available at http://rsbweb.nih.gov/ij/). Processes that fluoresced brightly (indicating greater thickness) and were 1x longer than the soma diameter were measured. Axon length was measured by drawing a straight line from the soma to the tip of the axon. For axons that branched or curved, a single measurement was made to represent the average length and direction. The angle was measured to determine if an EF influences neurite alignment. Assuming the EF is aligned on the x-axis, angle θ

is measured between the axon and the positive x-axis direction (towards the cathode). Because angles are symmetrical about the x- and y-axes, axons extending into quadrants II and III of a coordinate system are mirrored onto quadrants I and IV. All values in quadrant IV are then mirrored onto quadrant I so that any axons extending parallel to the EF are represented with angles closer to 0^o and axons extending perpendicular to the EF have angles closer to 90^o (as shown in **Figure 66**). DRGs with an average axon angle of 45^o indicate a homogenous radial distribution of axons.

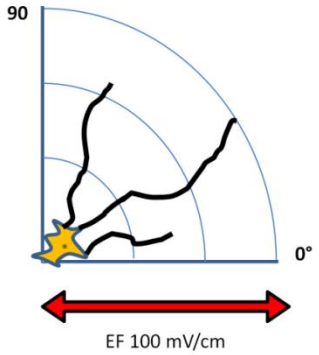

Figure 66. Axons angle measurements close to 0^o indicate axon growth parallel to the EF while angle measurements closer to 90^o indicate axon growth perpendicular to the EF.

All data reported are mean values with standard error. Statistical significance was calculated using an unpaired, unequal variance, two-tailed Student T-test to compare the experimental values with the non-stimulated control from each group. Significance was defined as data with a p-value of 0.05 or less.

5.3 RESULTS

5.3.1 Evaluation of PPy-PCL mechanical and conductive integrity

Mechanical suitability of the PPy-PCL conduit was assessed by two experienced lab members of the Schmidt Lab at the University of Texas at Austin. Jon Nickels (a 5th year graduate student who has performed at least 5 sutures) and Zin Khaing (a post-doctoral student with several years' experience with suturing) performed mock sutures of wet conduits in a dry environment using a 5-0 gauge and 10-0 gauge suturing needle and thread. The conduits were easily pierced by the needle without tearing the material. Both operators believed the conduit performed well when stitched with thread – the material had ample strength to support threading. They felt that the current PPy-PCL material is mechanically suitable for use as a nerve conduit.

To evaluate conductive integrity of the material, a strip of PPy-PCL was submerged in PBS and ends kept dry to attach electrodes. Current was conducted across these strips at 1, 10, and 100 μA while submerged. After 20 minutes of stimulation, resistance of the material generally increased in relation to the amount of current conducted as shown in **Table 12**. At 100 uA current, loss of conductivity quickly happened within the first minute of stimulation, whereas 1 μA had no change in conductivity and 10 μA current had a gradual decay in conductivity as shown in an I-t current-time graph in **Figure 67**.

Table 12. Initial and final resistance of stimulated PPy-PCL in PBS

Current (µA)	Initial resistance (kΩ)	Resistance after 20 min (kΩ)
1	10	10
10	10	19
100	10	2000

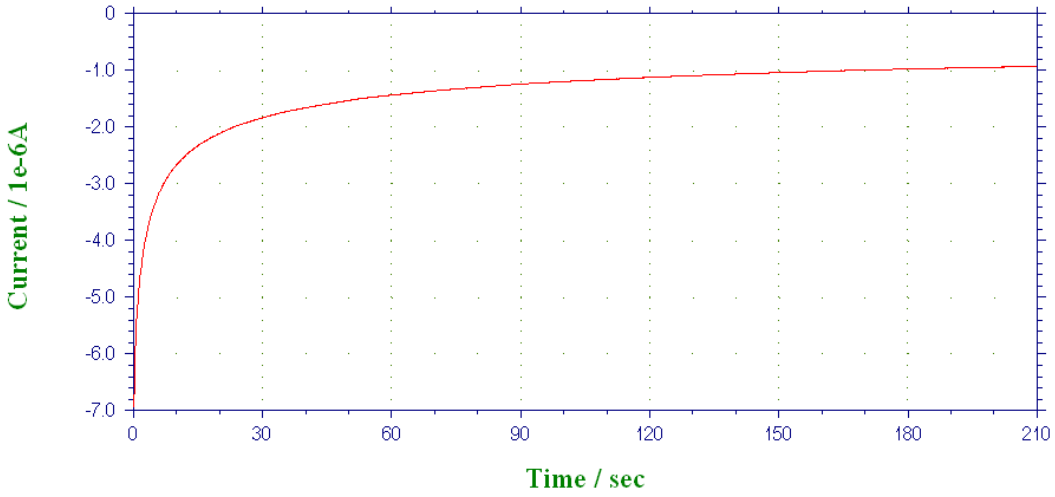

Figure 67. This three minute I-t current-time curve shows the initial change in current over time across a strip of PPy-PCL when a potential is held constant. Current typically ramps within the first several seconds and plateaus in a logarithmic fashion, slowly decreasing over time. This decay in current is due to decay in material conductivity.

At the chosen stimulation of 100 mV/cm, the average current through the PPy-PCL film strip is between 1- 10 µA, so we did not expect the conductivity to decrease too much. We found that that after 2 hours of stimulation, the strips loses conductivity by an order of magnitude. So substrates with initial resistance of 10 kΩ typically become 100

kΩ following the stimulation protocol of 100 mV/cm for 2 hours (data not shown). In reference to **Figure 62**, we found that the greatest change in conductivity occurred between A-B, where the anode comes in contact with the liquid.

5.3.2 Choosing a hydrogel for in vitro studies

Neurite extension of differentiated PC12 cells was imaged with phase contrast microscope to determine cell viability of cultures embedded in hydrogel within a conduit. Five types of hydrogels were used to determine cell viability when suspended in 3D. When growing PC12 cells in a silicone conduit, the cells appeared healthier in Matrigel versus pure collagen I, collagen buffered with HEPES, collagen buffered with 10x DMEM, or collagen/hyaluronic acid hydrogel (**Figure 68**). Phase contrast images through transparent silicone tubes demonstrate that live cells are present in all five hydrogels, however, more neurites extended from cultures in Matrigel. Artifacts seen in the images are due to the thickness of the gel and the silicone tube.

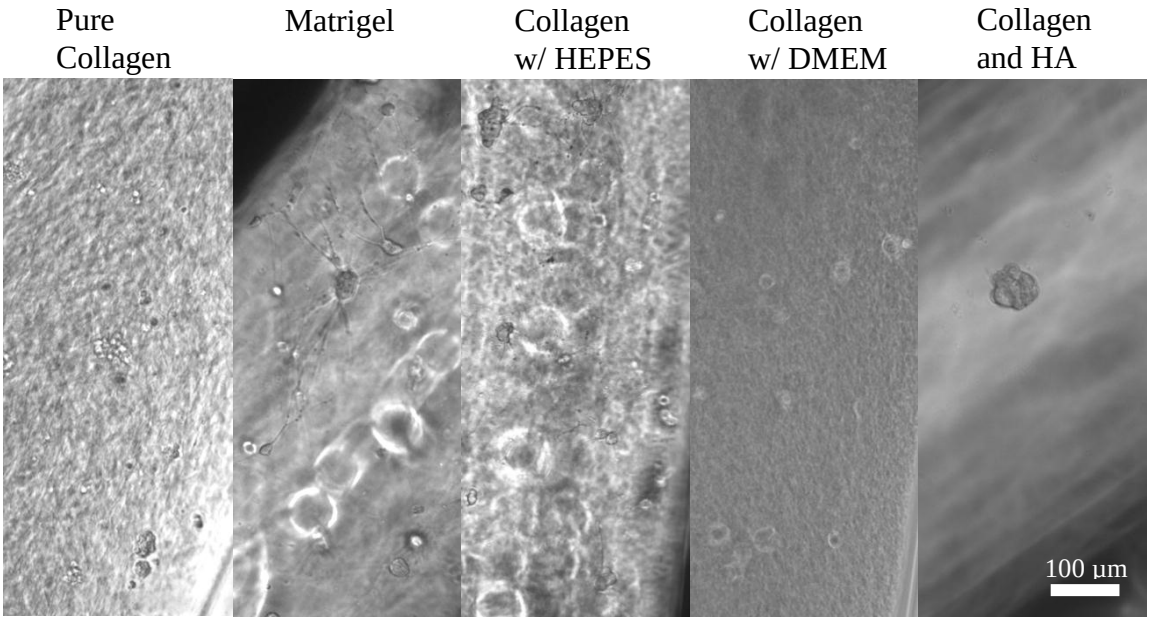

Figure 68. Phase contrast images at 100x of PC12 cells in hydrogel within a silicone conduits indicate that cultures can survive enclosed in the gel for 2 days. Cells appear to extend more neurites when grown in Matrigel compared to the other gels.

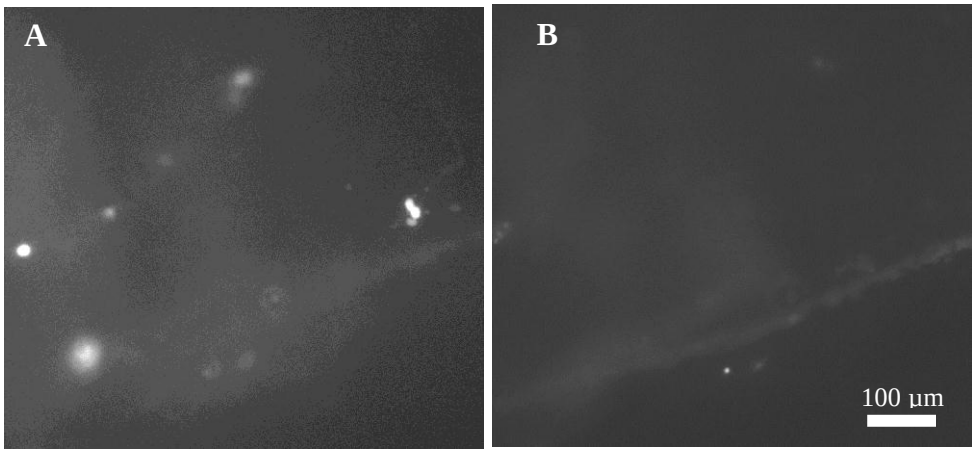

Figure 69. PC12 cells were stained with a live/dead cell assay kit and imaged with fluorescence microscopy at 100x. (A) Live cells in hydrogel within a conduit and (B) dead cells within the same field of view show minimal cell death after 2 days embedded in the unit. Scale bar is 100 µm.

Live/dead stains show cell morphology as well as cytotoxicity of the hydrogel/conduit system. Most cells appear to be alive when viewed under fluorescence, however the cell uptake of the dyes was poor because of transport issue through the hydrogel within a conduit (**Figure 69**). Quick assessment of the ratio of live:dead cells are equivalent to normal cell culture on tissue culture plastic (data not shown). This indicates that the gel can support live cells and Matrigel, in particular, appears to have stronger promotion of neurite extension. The following studies will use Matrigel as the hydrogel substrate.

5.3.3 PC12 cytotoxicity and cell adhesion on PPy-PCL substrates with DC EF

PC12 cell viability and adhesion was evaluated when grown on PPy-PCL substrates without ECM coating. Cells were placed into a well that was sealed on top of the PPy-PCL strip and were given one day to adhere to the strip. The cells were then stained with a live/dead fluorescent kit to determine the cytotoxicity of the PPy-PCL material. The ratio of live:dead PC12 cells when cultured on pre-stimulated and control PPy-PCL films did not change, the ratio was similar to cells grown on tissue culture plastic (data not shown) (**Figure 70**).

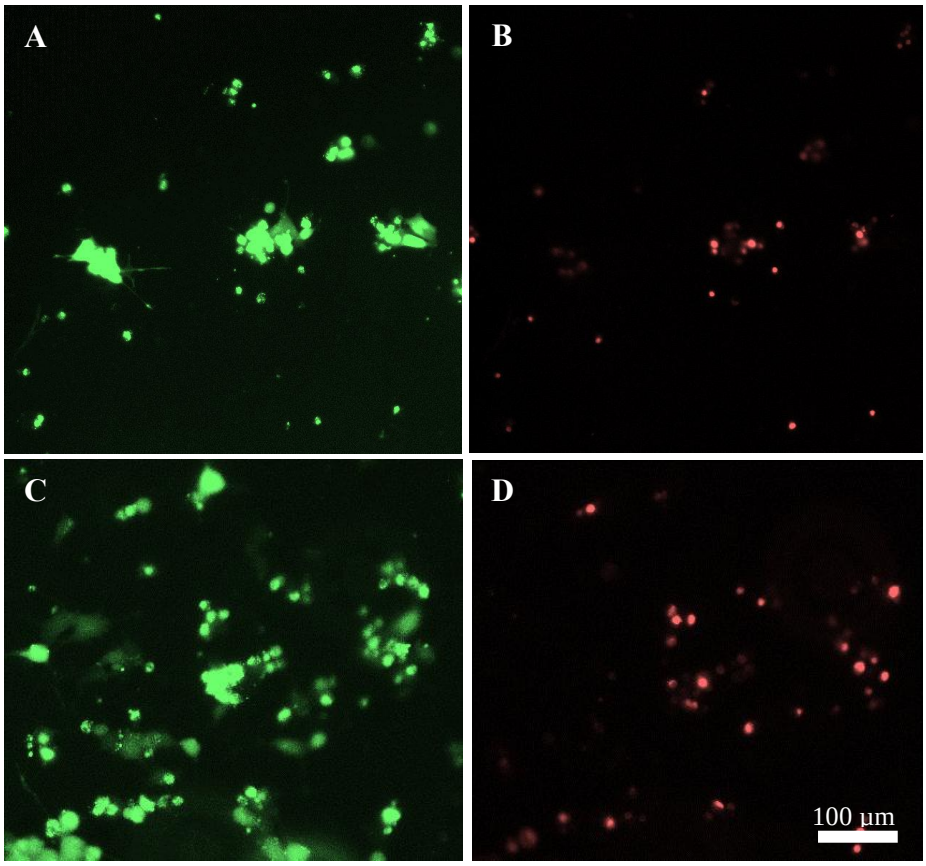

Figure 70. PC12 cell viability on PPy-PCL substrates was measured with live/dead staining (green = live, red = dead). (A,B) PC12 cells grown on the pre-stimulated PPy without any electrical stimulation and (C,D) PC12 cells grown on non-pre-stimulated PPy show that the ratio of live:dead cells remain similar. Scale bar is 100 µm.

To measure cell adherence, ImageJ software was used to threshold the fluorescent images of PC12 cells stained with calcein to reveal the surface area covered by cell spreading. The total number of cells adhered to the substrate was calculated by taking the average surface area covered by an individual cell and dividing the total amount of cell coverage within a single image. One representative image was taken per PPy-PCL strip. PC12 cells were cultured on the two substrates: pre-stimulated PPy-PCL (PS) and non-

pre-stimulated PPy-PCL (NonPS). Cell adhesivity was compared on both substrates when exposed to DC EF stimulation (stim) and no EF stimulation (control). The average number of PC12 cells adhering to NonPS without EF (control, n=4) was 600 cells/mm^2 and with EF (stim, n=12) was 680 cells/mm^2. The average number of PC12 cells adhering to PS without EF (control, n=4) was 230 cells/mm^2 and with EF (stim, n=12) was 180 cells/mm^2, as shown in **Figure 71**.

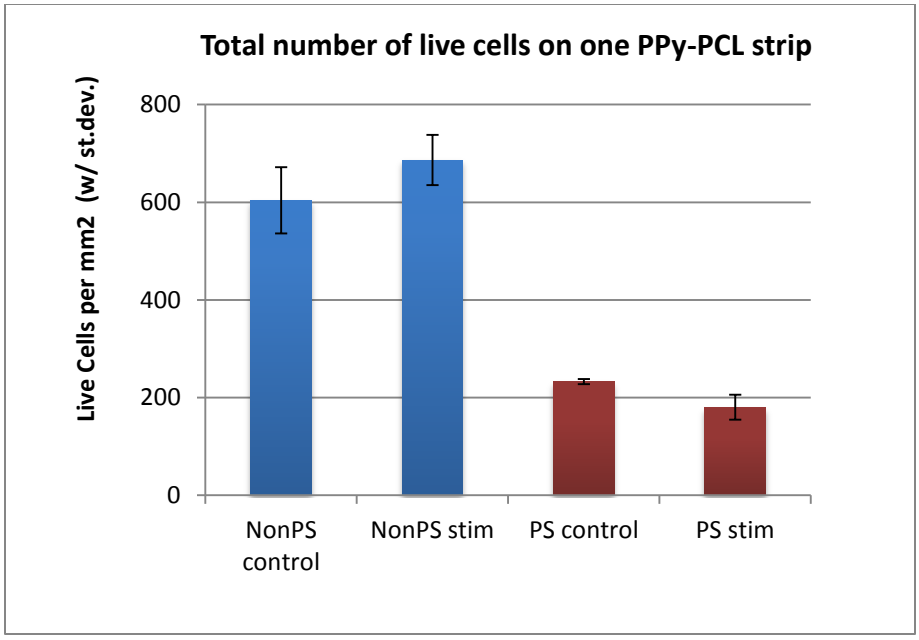

Figure 71. The total amount of live cells on pre-stimulated (PS) and non-pre-stimulated (NonPS) substrates are the same before and after stimulation. However, the number of cells adhering to the surface of NonPS is three times greater than on PS films.

The number of live cells before and after EF stimulation was not significantly different on either of the substrates. Although PS films had less cell adherence, the ratio of live:dead cells was the same for NonPS. This finding indicates that cytotoxicity is not

changed when material of this size is stimulated with 200 mV DC total for 2 hours before or after cell culture.

5.3.4 DRG axon extension on PPy-PCL with DC EF

DRGs were embedded in a 40 µl thin layer of Matrigel on top of a PPy-PCL strip. The freshly extracted DRG was allowed to acclimate for one day in vitro, the PPy-PCL was EF stimulated, then the DRGs were given another three days to extend axons before the samples were fixed, stained for beta III tubulin, and imaged at 20x. Because there were many processes extending from a single DRG body, only thick axons that were visibly discernible were measured for analysis. These axons were also the longest processes extending from the ganglion, as shown in **Figure 72**.

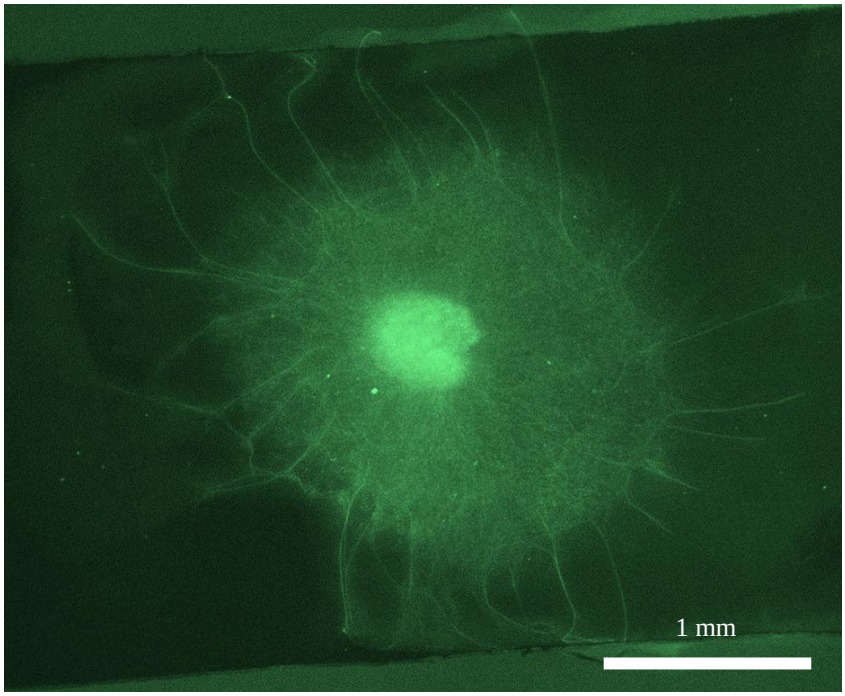

Figure 72. This fluorescence microscopy image at 20x is of a DRG embedded in Matrigel on top of a PPy-PCL strip (this particular strip is smaller at only 3 mm tall). The DRG was given 1 day to grow in the gel, then electrically stimulated for 2 hours at 200mV DC, and allowed to grow for another 3 days before fixing and staining. The black background is the PPy-PCL strip, the faint white blur that is present everywhere but at the edges and the bottom left corner is background fluorescence from the gel. The DRG body is the bright white object in the center. The gray cloud surrounding the DRG is composed of axons and migrating Schwann cells. The longer processes extending beyond the cloud surrounding the ganglion are the thicker axons that were measured. The cloud surrounding the ganglion contains Schwann cells and smaller neurites. Scale bar is 1 mm.

Long axons were measured for length and the axon terminals were plotted on an x-y graph where the origin represents the soma body. From looking at **Figure 73**, there was no obvious difference in increased length or alignment. The only trend witnessed by this method was that there was greater prevalence of short axons found in control samples, represented as more data points near the origin. There were 24 DRGs with

approximately 340 axons counted for each of the control group and experimental groups. DRGs grown on both NonPS and PS PPy-PCL stimulated with a 200 mV DC signal for 2 hours extended axons with an average length of 927 µm and 890 µm, respectively. The control group of DRGs grown on PPy-PCL without stimulation had an average axon length of 821 µm. Cell exposure to substrates stimulated with a DC EF increased DRG axon growth by 13% ($p<0.01$, Student's t-test of stimulated sample versus control), summarized in **Table 13**.

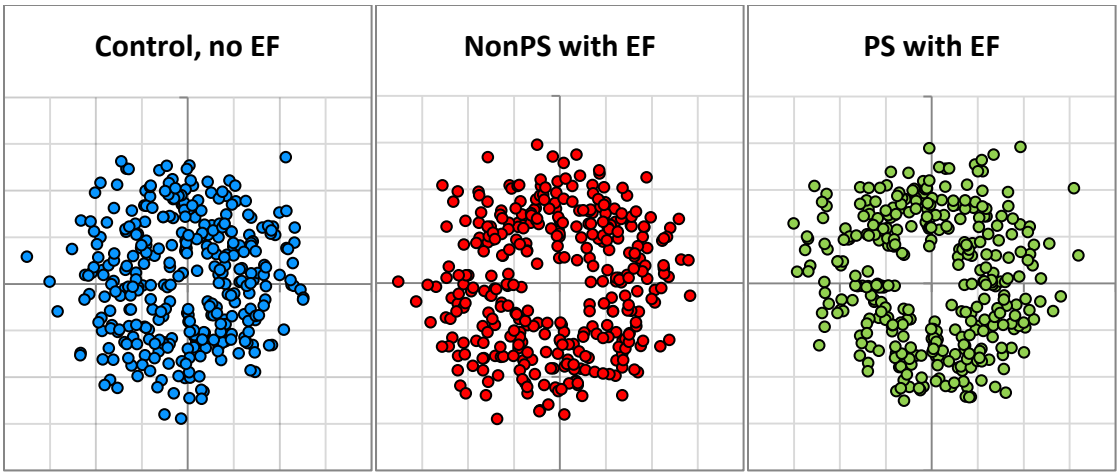

Figure 73. DRG axon terminals were plotted in a Cartesian x-y coordinate grid where the origin represents the edge of the ganglion body. Plots of DRG axons grown on NonPS with no EF stimulation (Control), axons on NonPS with EF stimulation, and axons on PS with EF stimulation were plotted on 4 mm x 4 mm graphs, each grid mark representing 0.5 mm. Radial distribution of axons appear homogenous for DRGs with and without EF. With EF stimulation, axons tend to have a greater minimum length compared to controls, as observed from the vacant center of stimulated samples.

Table 13. Summary of average DRG axon length when stimulated with DC EF

	Average axon length (μm)	Standard Deviation	Standard Error	Student's t-test	n
Control	821	302	17		334
NonPS with EF	927	278	15	$p << 0.001$	358
PS with EF	890	278	15	$p < 0.003$	358

The data shown in **Figure 73** masks the observation that DRGs tended to extend axons towards the closest electrode. Because there were two DRGs for each PPy sample, one lies closer to the cathode and the other towards the anode. The DRGs were placed 5mm apart so their growth was not influenced by the other's presence and each DRG was equidistant from edges of the Matrigel surrounding it, depicted in **Figure 74**.

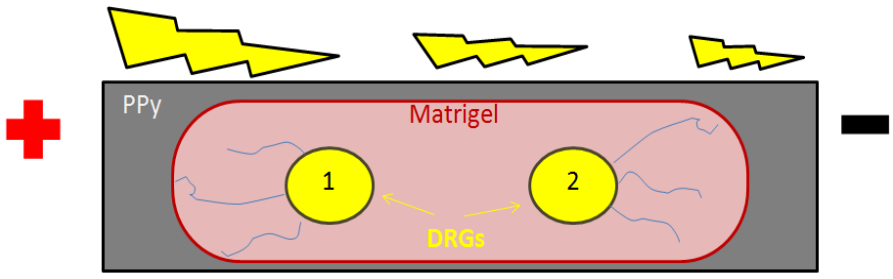

Figure 74. A schematic of the stimulation experiment shows positioning of two DRGs embedded in a single strip of Matrigel on top of a strip of PPy-PCL. DRG 1 is located near the anode and DRG 2 is located near the cathode. Gel surrounds all sides of the DRGs, however, there is a greater amount in the center between the two bodies. The drawing emphasizes how axons extend greater towards the nearest electrode when EF stimulated.

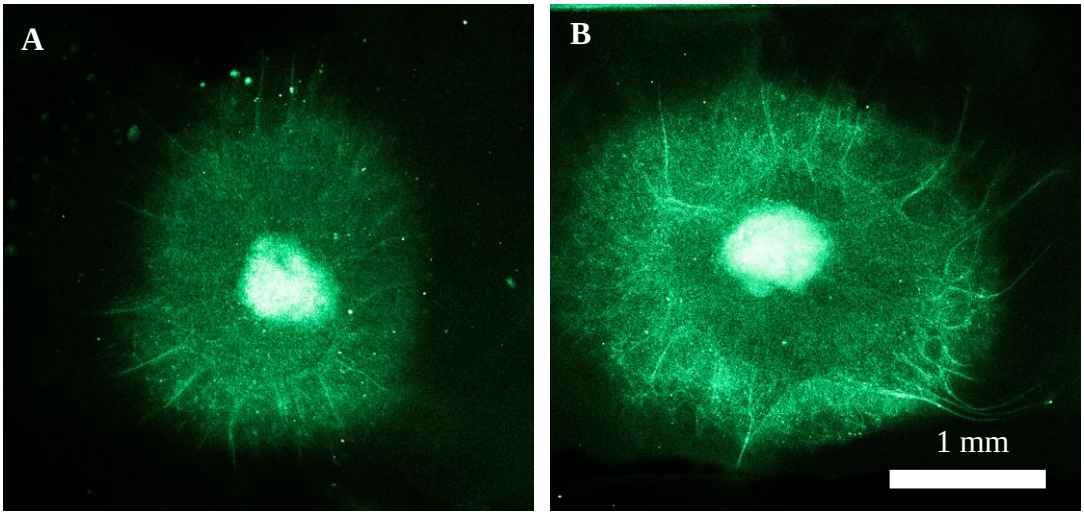

Figure 75. Fluorescent images of DRGs grown on PPy-PCL (A) without EF stimulation and (B) with stimulation show how EF exposure can increase axon length. Notice how axons from (B) extend more towards the right.

Under normal growing conditions without an EF, it would be expected that axons grow outwards equally in all directions, however it was observed that DRGs near a voltage source extended axons further towards the source. The data from NonPS PPy-PCL was separated so that DRGs closer to the anode (labeled as DRG 1) and DRGs closer to the cathode (labeled as DRG 2) were grouped independently. By calculating the x- and y- components of all axon measurements, the average axon terminal displacement was found for the two DRG positions. On average, DRGs in position 1 extended axons more towards the left anode by 160 μm and DRGs in position 2 extended axons more towards the right cathode by 115 μm (**Figure 76**). The average axon displacement in the perpendicular direction was not significantly different than controls. DRGs stimulated on PS substrates followed the same trend, but was not significantly different versus controls (data not shown) so further experiments were performed on NonPS PPy-PCL.

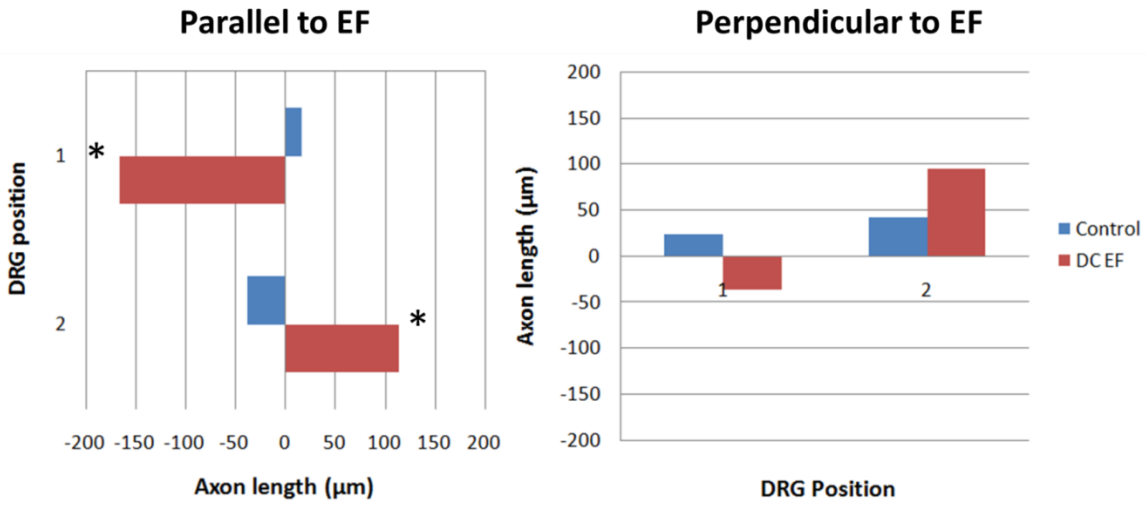

Figure 76. By separating the x- and y- components of DRG axon measurements (axon growth parallel and perpendicular to EF), it was observed that neurons near an electrode extend longer axons towards that electrode. Average axon lengths extending in the direction towards the nearest electrode was more significant (* = $p<0.05$) than control samples and average axon length in the orthogonal direction was not significantly different.

5.3.5 DRG axon extension on PPy-PCL with AC EF

Using the same experimental setup as the previous section, DRG cultures adhered to NonPS PPy-PCL film substrates were stimulated with an AC EF. An AC EF applies the same 100 mV/cm voltage across the substrate, but reverses the polarity 60 times a second (60 Hz). There is no net directional current because the voltages constantly switch polarity so directional cues may be lost, but the electrical stimulation still has the ability to disrupt membrane potential, activate membrane receptors, and change cell physiology.

When stimulating the PPy-PCL with +/- 200 mV 60 Hz AC for 2 hours, the resistance of the 0.5 x 2.0 cm^2 film strips increases such that the current at the end of the experiment are approximately 0.05 – 0.1 μA, which is comparable to currents generated during the DC experiments. DRGs embedded in Matrigel grown on AC stimulated film increased axon growth, similar to DRGs grown on DC stimulated films. The average axon length of the 24 DRGs for each group was 792 μm for controls and 996 μm for stimulated. Cell exposure to substrates stimulated with a AC EF increased DRG axon growth by 21% ($p<<0.01$), as summarized in **Table 14**.

Table 14. Summary of average DRG axon length when stimulated with AC EF

	Average axon length (μm)	Standard Deviation	Standard Error	Student's t-test	n
Control	792	335	26		172
AC EF	996	343	21	$p<<0.001$	281

5.3.6 DRG axon extension in 3D PPy-PCL conduits with AC EF

Two DRGs were placed in Matrigel inside the lumen of PPy-PCL conduit and allowed to acclimate for 24 hours. Gold electrodes were attached to the ends of the conduit and fully submerged while stimulating at +/- 200 mV 60 Hz AC for 2 hours. The cells were grown for another 72 hours before fixing, sectioning, and staining for beta III

tubulin. Fluorescent images show that DRGs encased in the conduits have decreased axon length and density, with or without EF stimulation (**Figure 77**).

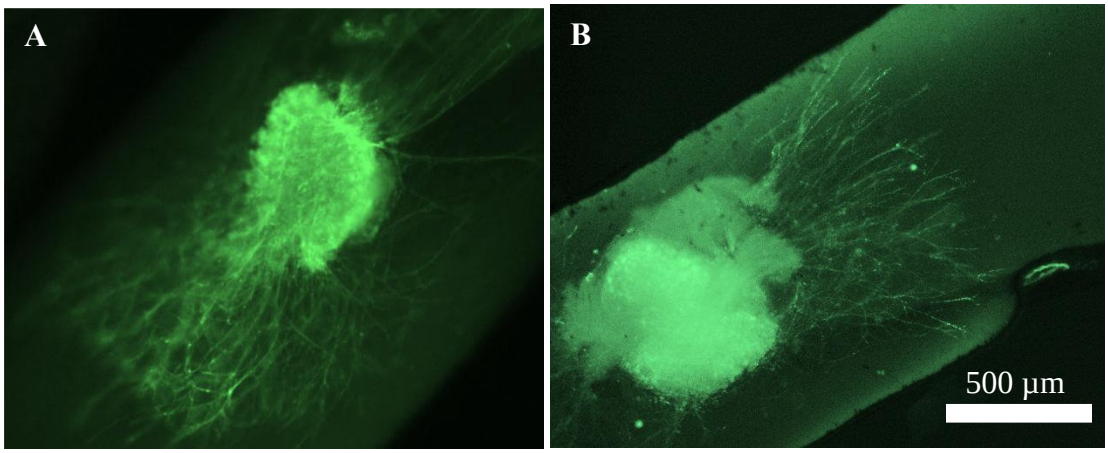

Figure 77. Fluorescent images of beta III tubulin labeled DRGs show that axon growth in stunted when embedded in Matrigel inside a conduit. EF stimulation resulted in decreased axon length and axon density. (A) DRG in a conduit with no electrical stimulation and (B) a DRG in a conduit with electrical stimulation of 100 mV/cm AC for 2 hours. Scale bar is 500 µm.

The axon lengths were measured from the samples inside the conduit with images taken at 60x. There were originally 30 conduits for the control group and another 30 for the AC stimulation group, however, most of the DRGs did not survive or extend many axons. The average number of axons counted for either group is approximately 60. We found that DRGs from both groups extended axons approximately 550 µm long, and were not significantly different from each other. The data is summarized in **Table 15**.

Table 15. Summary of average DRG axon length when stimulated with AC EF inside a PPy-PCL conduit

	Average axon length (μm)	Standard Deviation	Standard Error	Student's t-test	n
Control	541	241	31		65
AC EF in 3D	561	186	27	$p < 0.6$	55

The DRGS from both the control and experimental groups extended shorter axons, indicating that there may be issues with the experimental setup. One issue that was addressed was use of AC stimulation to reduce corrosion of the submerged electrode tips. However, we still were able to detect physical changes on the surface of the electrode. The DRGs were also encased inside a semi-permeable PPy-PCL film, which may inhibit adequate flow and transfer of nutrients/waste inside the lumen.

5.4 DISCUSSION

Autologous nerve grafts continue to be the most effective treatment for peripheral nerve damage because it can present multiple growth cues for axons to regrow across the injury. This paper introduces an alternative nerve conduit with the ability to provide electrical growth cues to healing tissue. To be an effective conduit for nerve regeneration,

the PPy-PCL material was assessed for its structural rigidity and biocompatibility with neural cells. To be an effective modality for delivering electrical growth cues, the material was assessed for integrity of electrical conductivity and its ability to promote neural growth during stimulation.

Mechanical strength is an important factor for nerve conduits because the implants need to withstand suturing and the implanted structures need to remain patent for cells and axons to migrate through the lumen. A good method to test this ability is to simply have surgical operators manipulate the material. Two surgically adept students from the Schmidt lab performed mock sutures with a 5-0 and 10-0 gauge needle and thread. When the conduit was wet, they felt the material was pliable enough without being too brittle or fragile, and thought it would handle well during operation.

Once inside the body, the implant will need to retain its ability to conduct electricity for the duration of the therapy. It was found that 1-10 μA of current increased material resistance from 10 kΩ to 10-19 kΩ within two hours of stimulation. However, using higher 100 μA currents reduced the material's conductivity by three orders of magnitude after two minutes. There are two possibilities that play a likely role in reducing PPy-PCL conductivity. The PPy units are conductive when sufficiently near each other and improve in conductivity when dopants are introduced to the network (Ateh et al. 2006). The dopants are not covalently bound to anything so remain loosely associated with the PPy-PCL chains. When a voltage is applied across the material, migration of electrons cause the bulk to expand through charge repulsion. The expansion of the pores and repulsive forces drive the charged dopants out of the system. Lower amounts of dopant will reduce the electrical conductivity of the material. Another

possibility the PPy-PCL material would lose conductivity is through reduction-oxidation reactions. Creating a voltage across the polymer causes one side to act as an anode and the other a cathode. In an electrochemical cell, oxidation occurs at the anodic side as electrons are stripped away from the system. Oxidation of PPy inhibits further electron transfer, so conductivity will decrease. At high currents, there is more electromotive force moving electrons which can accelerate the release of dopants and oxidation of PPy. Applying a current in the 1–10 μA range will allow longer stimulation times with minimal degradation of PPy-PCL conduction.

A hydrogel will be injected into the lumen of the conduit for increased structural support, scaffolding for cell migration, and cell exposure to ECM cues. Five hydrogels were chosen including variations of collagen I and added buffers, Matrigel, and collagen with hyaluronic acid. These ECM hydrogels have been used extensively in the literature for 3D cell cultures and have shown to be excellent scaffolds. The current project briefly compares the hydrogels in terms of ease of production and permitting neurite growth. It was found that all five gels provided a healthy growing environment within a conduit, however, after two days more neurite extension was found in Matrigel samples. This may be due to the presence of growth factors and numerous proteins found in the matrix. One issue with using this matrix is that it is produced from tumor cells and contains many biochemical components that have not been identified. In the future, an FDA approved hydrogel will be chosen for eventual translation of this device for human use. This ECM increases neurite extension, can be easily purchased, and requires no preparation before use. Even with the drawbacks, using Matrigel was still justifiable for use as an ECM model to support cell growth inside an electrically conductive conduit.

Previous studies by Durgam et al. (2009) demonstrate that the PPy-PCL material is biocompatible and can be rendered non-toxic by pre-stimulation. In the current study, pre-stimulation did not increase cell viability because the ratio of live:dead cells on PS and NonPS films were identical. This change in improved cytocompatibility is not understood, however, it may be due to creating and processing conduits versus coated glass slides from the previous study. Additionally, **Figure 71** indicates that pre-stimulation appeared to inhibit cell adhesion. On average, with or without EF stimulation, NonPS substrates had approximately 640 cells/mm^2 whereas PS substrates had 205 cells/mm^2, nearly three times as many cells adhering and spreading on the surface. One possibility is that removal of dopants from the material by electrical stimulation creates a surface less conducive to cell adhesion. More PCL may be exposed from the removal of dopants, although known to be biocompatible it is typically not cell adhesive (Tang et al. 2004). By adding ECM to the device, cell adhesion to the surface is circumvented because the surface will be coated with recognizable proteins. The material may lose cell adhesivity during stimulation, but the PPy-PCL film material is not cytotoxic and adhesion is improved by presence of ECM proteins, so the system remains a viable concept as a nerve conduit.

DRGs were chosen to place on EF stimulated substrates because injury to peripheral nerves will likely involve damage of the DRG axons and glia. When electrically stimulating DRGs on flat strips of PPy-PCL films coated with Matrigel for 2 hours, it was found that DC EF of 100 mV/cm increased average axon length by 13% and AC EF of 100 mV/cm increased axon length by 21% after 3 days.

For DC stimulation, overall axon length increased however this extra elongation was not witnessed in axons growing in the direction perpendicular to the EF, nor was it witnessed with axons growing parallel to the EF towards the center of the gel. DRGs under this condition appeared to extend axons towards the nearest electrode, averaging 160 μm closer to the anode and 115 μm closer to the cathode. A DC EF has been known to induce unilateral growth/migration (McKasson et al. 2008, Messerli and Graham 2011), perpendicular alignment (Ariza et al. 2010), or growth with no polarized alignment (Wood and Willits 2009, Koppes et al. 2011), but there have been no reports of cell growth towards both electrodes. There is suspicion that gel towards the edge was thinner and promoted nutrient/waste transfer more quickly compared to the center areas, however this does not explain why axons did not extend in the perpendicular direction where the gel was also thin. Because the electric field creates an ionic current through the material, gel, and media, the current may influence transport and structural organization in the gel, leading to greater axon growth near the sources of the current. It may be worthwhile to examine heat exchange and gel mechanical properties near the electrode since these parameters can affect or be affected by gel architecture, and thus cell interaction with the ECM gel. Further investigation of this phenomenon is needed to elucidate the role of EF on ECM gels and its effect on cell growth.

Under AC stimulation, overall DRG axon length was greater than when stimulated with DC EF. There was no consistent alignment of axons observed. The 21% increase in axon length appeared to have uniform radial distribution. It should be noted that with AC EF, long axons were projected radially in all directions whereas DC EF caused DRG axons to extend longer in one direction and shorter in the opposite direction.

The axon lengths found in AC EF samples would thus have a higher average than DC EF samples. Therefore, the absolute lengths of the longest axons from both experiments may not be significantly different. These sets of experiment indicate that DC and AC voltages applied across a conductive PPy-PCL film substrate improve axonal growth of DRGs embedded in Matrigel on the film.

Only AC EF was used for 3D stimulation of DRGs embedded in Matrigel within the lumen of the PPy-PCL conduits. In preliminary experiments (data not shown), use of DC currents resulted in corrosion of submerged electrodes, introducing possible cytotoxicity issue. Alternating the voltage from positive to negative effectively oxidizes and reduces the electrodes in an equal manner. Corrosion of the tip may be circumvented by balancing red-ox reactions which is a common industrial solution. Additionally, the tips of the electrode were made of inert gold to further limit creation of possible toxic metal compounds from reactions. After stimulating the PPy-PCL conduits submerged in media and processed identically to the 2D films, the unit was cut axially using a vibratome, and each half was stained with beta III tubulin to view DRG growth within the lumen. The axon length of EF stimulated DRGs was not significantly different from DRGs receiving no stimulation. Axon length and axon density for both conditions was dramatically less than DRGs grown on 2D substrates. Reduction in cell growth may be due to several reasons. Firstly, the 1.5 cm long, 1 mm diameter conduits had greater difficulty in washing the lumen compared to washing the surfaces of 2D films before cell seeding. This may have an impact on residual chemicals that would inhibit cell viability. And secondly, transport of nutrients/wastes through the lumen of the conduit is inhibited by the low permeability of the material, the Matrigel hydrogel, diameter of the conduit

ends, and occlusion of the lumen by the DRG body (typically ranging between 0.3 - 0.8 mm). Although PC12 cell viability and growth was permissive in earlier studies under similar growing conditions, DRG bodies contain a higher concentration of cells and were cultured in the conduit for a longer time. These conditions incur greater metabolic load and would need better transport to maintain healthy cells.

No conclusions about DRG axon growth could be drawn from AC EF stimulation of the PPy-PCL conduits. Overall cell growth in 3D conduits was stunted under experimental and control conditions with an approximate average axon length of 550 μm compared to 800 μm on 2D film experiments. Future studies will address the transport issue inside a small-diameter conduit, possibly by creating a material with better permeability. But an immediate solution to the current problem would be to place the DRG body outside of the conduit and measure the axons entering the lumen. Not only will the DRG have greater respiration, this modality better represents clinical EF stimulation at the injury site, where damaged axons are exposed to therapeutic repair and not the DRG body itself.

Novel PPy-PCL co-block polymer films have been synthesized to be electrically conductive and degradable under aqueous environments for tissue engineering applications. Thin PPy-PCL substrates were shown to be non-toxic and can conduct microampere electrical currents for prolonged use under physiological conditions. EF stimulation of 2D substrates using DC and AC signals increased axon length of DRGs grown in Matrigel on top of the films. When using DC signals, DRGs tended to extend longer axons towards the edge closest to a voltage source, whereas AC signals did not have an influence on axon direction. These observations of DC experiments may be due

to constant ion flow and possible EF-induced structural changes to ECM at the edges of the gel. DRGs embedded in Matrigel within the lumen of PPy-PCL conduits had stunted growth. With or without stimulation, the number of DRGs extending axons, density of axons, and length of axons were all less than DRGs grown on flat substrates. The reduced transport within an enclosed space with high cell density may have caused the decrease in neural growth. For future studies, the schematics will be re-examined to prevent congestion of cell respiration. Having the DRG body outside the conduit and stimulating only the axons and glia migrating into the lumen may be a good solution and be more clinically relevant. PPy-PCL was found to be an effective means for electrically stimulating cells for nerve regenerative applications, however, more consideration of the stimulation arrangement will be needed to examine the material's efficacy to enhance nerve growth as a conduit. In summary, a biodegradable electrically conductive substrate is an effective means to deliver EF growth cues to enhance axon growth of neural cells cultured on the surface.

Chapter VI:

Summary

Directed neurite growth is essential to successfully re-establish severed connections beyond a nerve injury. After a peripheral nerve is damaged, a cascade of events involving debris clearance and Wallerian degeneration may eventually lead to conditions conducive to axon regeneration. One possible growth cue is generated from the electric gradient caused by the natural separation of charged biochemicals surrounding the wound site. The potential differences across tissue layers have been measured during embryogenesis and wound healing, but the conditions and parameters associated with the presentation of the endogenous EF remain largely unknown.

During embryogenesis and nerve regeneration, measured potential gradients ranging from 1 – 1600 mV/mm have been postulated to provide electrical cues for developing neural tissue (McCaig et al. 2005). Simulating these conditions by applying an EF across in vitro and in vivo cultures has demonstrated favorable cell response including enhanced neurite length, cell alignment, directed motility, and faster growth rates (Al-Majed et al. 2000, Geremia et al. 2007, Yao et al. 2008). Most published studies apply current through the media above cells, but the work presented in this study investigated if the same electrical parameters can be used on conducting substrates beneath the adhered cell layer. The advantages of stimulating cells adjacent to a conductive substrate include localized stimulation, reduced red-ox reactions, control of topology, and in the case of nerve conduits, isolation of the regenerating site from scar tissue.

In Chapter III, we are able to show that Schwann cell orientation can be aligned by controlling the EF strength and current density flowing through the media above cell cultures. Because the inherent resistivity of media could not be changed without creating an inhospitable cell environment, the effects of EF and current density could not be examined independently. By changing the voltage applied across cell cultures and the cross sectional area of the conductive media, the current density and current strength were able to be changed independently. We discovered that change in Schwann cell orientation correlates with change in current density, not absolute current strength. This makes sense when approaching the situation from the standpoint of a cell attached to a surface. Cells receive information from their environment by detecting chemicals that are within their vicinity. With a higher current density flowing above a surface, there are more charged species available to interact with in the volume surrounding the cell. Conversely, because current density is coupled with EF, there is a possibility that cell orientation is a result of the EF strength. A stronger EF above a cell culture places a stronger electromotive force on charged species in and around the cells. This may equally lead to cell alignment in response to the heterogeneous distribution of charge in the cell's milieu. When exposing these cells to a constant EF and varying the duration of exposure, we found there to be a limiting factor to the amount of cell alignment. The average cell orientation dependent upon the EF strength (or current density) reaches a maximum alignment by 8 hours of stimulation. And when stimulating cultures with 2-1000 Hz AC frequencies commonly used in related studies, Schwann cells did reorient in response to the EF. However, it was observed that Schwann cell bodies were more round, flat, large, and had more protuberances from the lamellipodia than controls or DC stimulated cells.

Stimulation through the substrate proved less fruitful. The stimulation parameters chosen were ineffective at changing cell orientation, however, long term stimulation (of at least 24 hours) induced cells to align parallel to the EF. This was not found homogeneously in the SC, so it may be the result of local changes in the Matrigel coated surface of the ITO. This implies that EFs may be used to alter the extracellular environment to control cell behavior. Again, when stimulating with an AC signal, Schwann cell morphology was observed to have wider bodies with many processes. This reaction to electrical signals has been undocumented, so further investigation into this phenomenon is warranted.

In Chapter IV, the focus of the study shifted from observing cell response during EF stimulation to observing changes in the cellular environment. Cells are in constant communication with its surrounding, receiving cues that may change its adhesion, migration, metabolic activity, differentiation, and protein expression. It was hypothesized if EFs were affecting cell orientation by rearranging the charged species surrounding the cell, then these effects may reveal itself as the reorganization of the extracellular milieu. Furthermore, conductive ITO was used to expose EFs to cell cultures to determine if substrate stimulation is an effective means for controlling cell behavior.

Initial studies of Schwann cells seeded onto Matrigel ECM stimulated on ITO glass demonstrated that cell orientation can be influenced by an underlying EF. To determine the ionic distribution within the cell's environment, a gel stimulated under identical conditions without cells was analyzed with calcium green to determine ion distribution throughout the gel. It was discovered that there was a higher concentration of calcium near the cathode, suggesting that the EF does have an effect on charged

components within the cellular environment not just within the cell. Taking this observation one step further, gels were stimulated under identical conditions and cells were seeded days after stimulation ended. Schwann cells that were seeded onto stimulated gels were still aligning perpendicular to the initial EF, indicating that the EF has a semi-permanent effect on the ECM. This would be beneficial for clinical purposes requiring long term implants that can be improved by electrical stimulation or ECM organization, such as conductive nerve conduits.

Collagen I was then used as a model ECM protein for visual analysis due to several reasons. Collagen I fibrillates at physiological conditions, producing fibrils and structures that are readily visualized. Matrigel is mainly composed of laminin and collagen IV, which are both difficult to image and determine structural changes. Collagen I and IV have different tertiary structures do to slight changes in their moieties, however their chemical composition are fundamentally the same. By replacing Matrigel with collagen I, we would be able to observe ECM structural changes under EF stimulation.

Diluted collagen was stimulated under the same conditions as the Matrigel samples, then imaged with phase contrast and confocal microscopy. Tensor analysis of collagen fibril images indicate that there are more perpendicularly aligned fibrils when samples were under EF stimulation. Confocal microscopy showed that microfibrils tend to dominate the bulk of the gels, however, collagen exposed to EF had greater heterogeneity in structure and increased formation of larger fibrils. It should be noted that these changes in architecture may also be influenced by joule heating, the heat emitted by a resistive element when current flows through it. Although the temperature of media

above stimulated ITO have been measured to have negligible change, the local heating at the ITO surface may affect the gel.

SEM of collagen gels showed fibrils on the surface of the gel had a different architecture. More fibril bundles were formed with aligned and twisted fibrils compared to control samples which appear to have a more homogeneous distribution of fibril orientation. The three imaging techniques to analyze collagen I were all able to detect differences in ECM architecture. The data suggests that EF stimulation can change protein structures found in the extracellular environment.

In Chapter V, a biodegradable, conductive polymer was developed by collaborators to assess its ability to be an effective nerve conduit. In order to supply an EF in vivo for an extended period of time, PPy was chosen because its conductivity and biocompatibility can be controlled through simple manufacturing procedures. Furthermore, the material can present both topological and electrical cues to the regrowing nerve. Because the popular use of autologous nerve grafts harbors many drawbacks, synthetic nerve grafts are attractive alternatives. Creating a nerve conduit with PPy will incorporate therapeutic EF stimulation with similar attributes that make autografts favorable, such as guide axons, prevent infiltration of inhibitory cells, and channel distal chemical cues towards the proximal end.

The initial experiments for this project began with assessing the cytotoxicity of the material and its cell-adhesive properties. In previous studies from members of our lab (Durgam et al. 2009), the material needed to be rendered cytocompatible through pre-stimulation, meaning the material was exposed to an EF for 2 hours and washed of toxic species before cell seeding. It was found that the current iteration of the PPy-PCL

material did not need to pre-stimulated. In fact, greater cell adhesion was found when the cells were seeded on material without any pre-stimulation. Even with this positive change, an ECM gel was needed to improve cell adhesion and viability on the polymer device. Matrigel was chosen as a model ECM gel because it is historically known to promote axon growth for in vitro models. As this was the early phase of developing the device, we wanted to increase the viability of our cells. In the future, Matrigel will be changed to a defined ECM gel that is FDA approved for human implantation.

DRGs are balls of efferent sensory neurons and Schwann cells located along the spine of vertebrates. DRGs extend their axons to the periphery, so injury to limbs resulting in damaged nerves often involves axons from these cells. Thus, these primary extracts from neonatal rats were a good model for measuring nerve regeneration in our system. On first stimulation of DRGs embedded in Matrigel on PPy-PCL, it was found that DC EF of 100 mV/cm increased axon extension up to 13% compared to controls. Upon further examination, we noticed that DRGs near an electrode would tend to extend longer axons in that direction. We are unsure why this indiscriminate extension occurs to both the anode and cathode sides, but it may be due to increased transport at the edges of the gels near the electrodes or increased joule heating at the edges. AC EF was also selected as a possible stimulating signal because DC fields produced between electrodes in the body would create red-ox reactions at the electrodes. By constantly switching anode and cathode functions at the electrode, cytotoxic byproducts from red-ox reactions are minimized. When stimulating DRGs using AC EF, there was greater axon extension in all directions, up to 21% increase compared to controls. Unlike DC EF, there was no discernible preference of axon extension in any direction. And lastly, when stimulating

whole DRGs within the PPy-PCL conduits using AC signals, we found that cell viability dramatically decreased. This is most likely due to low transport through the embedded Matrigel and the high cell concentration within the ganglion. In the future, the DRG will be left outside the conduit and axon extension into the conduit will be measured. This better represents and injured nerve model and will obviate problems with nutritional transport. The results shown from this work demonstrate that conductive PPy-PCL is a promising material for bioelectrical interfaces and conductive nerve conduits.

The three projects described in this dissertation span multiple aspects of neural stimulation with EFs. The first project characterizes the cell response to numerous EF parameters and methodologies of stimulation. The second project is exploratory, where we are searching for the underlying mechanisms of how an EF may affect cell behavior. And in the third project, our group is collaborating with industrial partners to develop a device that will translate this technology to real world clinical use. Understanding EFs and their role on biology is still in its infancy. The work published here aims to improve the community's knowledge in this field and to utilize these discoveries to advance biomedical engineering.

References

Ahlborn P, Schachner M, and Irintchev A. 2007. One hour electrical stimulation accelerates functional recovery after femoral nerve repair. Exp Neurol 208:137-144.

Al-Majed AA, Neumann CM, Brushart TM and Gordon T. 2000. Brief electrical stimulation promotes the speed and accuracy of motor axonal regeneration. J Neurosci 20(7): 2602-2608.

Al-Majed AA, Brushart TM, and Gordon T. 2000. Electrical stimulation accelerates and increases expression of BDNF and trkB mRNA in regenerating rat femoral motoneurons. Eur J Neurosci 12:4381-4390.

Alexander JK, Fuss B and Colello RJ. 2006. Electric field-induced astrocyte alignment directs neurite outgrowth. Neuron Glia Biol 2(2): 93-103.

Altizer AM, Moriarty LJ, Bell SM, Schreiner CM, Scott WJ, and Borgens RB. 2001. Endogenous electric current is associated with normal development of the vertebrate limb. Dev Dynam 221:391-401.

Ariza CA, Fleury AT, Tormos CJ, Petruk V, Chawla S, Oh J, Sakaguchi DS, and Mallapragada SK. 2010. The influence of electric fields on hippocampal neural progenitor cells. Stem Cell Rev 6(4):585-600.

Armstrong SJ, Wiberg M, Terenghi G and Kingham PJ. 2007. ECM molecules mediate both Schwann cell proliferation and activation to enhance neurite outgrowth. Tissue Eng 13(12): 2863-2870.

Ateh DD, Navsaria HA, and Vadgama P. 2006. Polypyrrole-based conducting polymers and interactions with biological tissues. J R Soc Interface 3:741-752.

Aydin MA, Comlekci S, Ozguner M, Cesur G, Nasir S, and Aydin ZD. 2006. The influence of continuous exposure to 50 Hz electric field on nerve regeneration in a rat peroneal nerve crush injury model. Bioelectromagnetics 27:401-413.

Bahr M and Bonhoeffer F. 1994. Perspectives on axonal regeneration in the mammalian CNS. Trends Neurosci 17:473-479.

Borgens RB, Shi R, Mohr TJ, and Jaeger CB. 1994. Mammalian cortical astrocytes align themselves in a physiological voltage gradient. Exp Neurol 128:41-49.

Borgens RB. 1999. Electrically mediated regeneration and guidance of adult mammalian spinal axons into polymeric channels. Neurosci 91(1):251-264.

Bruder JM, Lee AP, and Hoffman-Kim D. 2007. Biomimetic materials replicating Schwann cell topography enhance neuronal adhesion and neurite alignment in vitro. J Biomater Sci Polymer Edn 18(8):967-982.

Brushart TM, Hoffman PN, Royall RM, Murinson BB, Witzel C and Gordon T. 2002. Electrical stimulation promotes motoneuron regeneration without increasing its speed or conditioning the neuron. J Neurosci 22(15): 6631-6638.

Calabrese EJ. 2008. Enhancing and regulating neurite outgrowth. Crit Rev Toxicol 38: 391-418.

Campbell WW. 2008. Evaluation and management of peripheral nerve injury. Clin Neurophysiol 119:1951-1965.

Canty AJ and Murphy M. 2008. Molecular mechanisms of axon guidance in the developing corticospinal tract. Progr Neurobiol 85: 214-235.

Cheng X, Gurkan UA, Dehen CJ, Tate MP, Hillhouse HW, Simpson GJ, and Akkus O. 2008. An electrochemical fabrication process for the assembly of anisotropically oriented collagen bundles. Biomaterials 29:3278-3288.

Curinga G and Smith GM. 2007. Molecular/genetic manipulation of extrinsic axon guidance factors for CNS repair and regeneration. Exp Neurol 209: 333-342.

Deans JK, Powell AD, and Jefferys GR. 2007. Sensitivity of coherent oscillations in rat hippocampus to AC electric fields. J Physiol 583(2):555-565.

Deister C and Schmidt CE. 2006. Optimizing neurotrophic factor combinations for neurite outgrowth. J Neural Eng 3:172-179.

Deister C, Aljabari S, and Schmidt CE. 2007. Effects of collagen I, fibronectin, laminin and hyaluronic acid concentration in multi-component gels on neurite extension. J Biomat Sci Polym Ed 18(8):983-997.

Dubey N, Letourneau PC, and Tranquillo RT. 1999. Guided neurite elongation and Schwann cell invasion into magnetically aligned collagen in simulated peripheral nerve regeneration. Exp Neurol 158:338-350.

Dubson M. PhET Interactive Simulations: Charges and Fields. University of Colorado. Version 2.04.00, build June 5, 2011. http://phet.colorado.edu/ (accessed September 2012)

Duchet J, Legras R and Demoustier-Champagne S. 1998. Chemical synthesis of polypyrrole: structure-properties relationship. Synthetic Met 98: 13-122.

Durgam H, Sapp S, Deister C, Khaing Z, Chang E, Luebben S, and Schmidt CE. 2009. Novel degradable co-polymers of polypyrrole support cell proliferation and enhance neurite out-growth with electrical stimulation. J Biomater Sci Polym Ed 21(10):1265-1282.

Fawcett JW and Keynes RJ. 1990. Peripheral nerve regeneration. Annu Rev Neurosci 13:43-60.

Fletcher DA and Mullins RD. 2010. Cell mechanics and cytoskeleton. Nature 463:485-492.

Fonner JM, Forciniti L, Nguyen H, Byrne J, Kou YF, Syeda-Nawaz J and Schmidt CE. 2008. Biocompatibility implications of polypyrrole synthesis techniques. Biomed Mater 3(3):034124.

Geremia NM, Gordon T, Brushart TM, Al-Majed AA and VergeVMK. 2007. Electrical stimulation promotes sensory neuron regeneration and growth-associated gene expression. Exp Neurol 205(2): 347-359.

Gomez N and Schmidt CE. 2007. Nerve growth factor-immobilized polypyrrole: Bioactive electrically conducting polymer for enhanced neurite extension. J Biomed Mater Res 81A: 135-149.

Guo C and Kaufman LJ. 2007. Flow and magnetic field induced collagen alignment. Biomaterials 28:1105-1114.

Hadlock T, Sundback C, Hunter D, Cheney M and Vacanti JP. 2000. A polymer foam conduit seeded with Schwann cells promotes guided peripheral nerve regeneration. Tissue Eng 6(2): 119-127.

Henley J and Poo M. 2004. Guiding neuronal growth cones using Ca2+ signals. Trends Cell Biol 14(6):320-330.

Hotary KB and Robinson KR. 1992. Evidence of a role for endogenous electrical fields in chick embryo development. Development 114:985-996.

Hotary KB and Robinson KR. 1994. Endogenous electrical currents and voltage gradients in Xenopus embryos and the consequences of their disruption. Dev Biol 166:789–800.

Hronik-Tupaj M and Kaplan DL. 2012. A review of the responses of two- and three-dimensional engineered tissues to electric fields. Tissue Eng Pt B 18(3):167-180.

Huang J, Ye Z, Hu X, Lu L, and Luo Z. 2010. Electrical stimulation induces calcium-dependent release of NGF from cultured Schwann cells. Glia 58:622-631.

Hudson TW, Evans GR, and Schmidt CE. 2000. Engineering strategies for peripheral nerve repair. Orthop Clin North Am 31(3):485-498.

Hudson TW, Liu SY, and Schmidt CE. 2004. Engineering an improved acellular nerve graft via optimized chemical processing. Tissue Eng 10(9/10):1346-1358.

Hudson TW, Zawko S, Deister C, Lundy S, Hu CY, Lee K and Schmidt CE. 2004. Optimized acellular nerve graft is immunologically tolerated and supports regeneration. Tissue Eng 10(11/12): 1641-1651.

Kandel ER, Schwartz JH and Jessell TM. 2000. Principles of Neural Science 4th ed. New York: McGraw-Hill.

Kirson ED, Dbaly V, Tovarys F, Vymazal J, Soustiel JF, Itzhaki A, Mordechovich D, Steinberg-Shapira S, Gurvich Z, Schneiderman R, Wasserman Y, Salzberg M, Ryffel B, Goldsher D, Dekel E and Palti Y. 2007. Alternating electric fields arrest cell proliferation in animal tumor models and human brain tumors. PNAS 104(24): 10152-10157.

Koppes AN, Seggio AM, and Thompson DM. 2011. Neurite outgrowth is significantly increased by the simultaneous presentation of Schwann cells and moderate exogenous electric fields. J Neural Eng 8:1-13.

Kotwal A and Schmidt CE. 2001. Electrical stimulation alters protein adsorption and nerve cell interactions with electrically conducting biomaterials. Biomaterials 22: 1055-1064.

Kuffler DP. 1996. Chemotropic factors direct regenerating axons. News Physiol Sci 11: 219-222.

Levin M. 2009. Bioelectric mechanisms in regeneration: unique aspects and future perspectives. Semin Cell Dev Biol 20:543-556.

Lewin GR and Barde YA. 1996. Physiology of the neurotrophins. Annu Rev Neuroscience 19: 289-317.

Li N and Folch A. 2005. Integration of topographical and biochemical cues by axons during growth on microfabricated 3-D substrates. Exp Cell Res 311:307-316.

Lodish H, et al. 2007. Molecular cell biology, 6th Ed. New York, NY: W.H.Freeman Publisher.

Lu MC, Ho CY, Hsu SF, Lee HC, Lin JH, Yao CH, and Chen YS. 2008.Effects of electrical stimulation at different frequencies on regeneration of transected peripheral nerve. Neurorehab Neural Re 22(4):367-373.

Luebben S, Elliott B and Wilson C. 2007. US Patent No. 7,279,534.

Lundborg G. 2000. A 25-year perspective of peripheral nerve surgery: evolving neuroscientific concepts and clinical significance. J Hand Surg 25:391-414.

MacDiarmid AG. Polyaniline and polypyrrole: where are we headed? 1997. Synthetic Met 84: 27-34.

Mahoney MJ, Chen RR, Tan J and Saltzman WM. 2005. The influence of microchannels on neurite growth and architecture. Biomaterials 26: 771-778.

Mattila PK and Lappalainen P. 2008. Filopodia: molecular architecture and cellular functions. Nat Rev Mol Cell Bio 9:446-454.

McCaig CD. 1990. Nerve brancing is induced and oriented by a small applied electric field. J Cell Sci 95:605-615.

McCaig CD and Rajnicek AM. 1991. Electrical fields, nerve growth and nerve regeneration. Exp Physiol 76:473-494.

McCaig CD, Rajnicek AM, Song B and Zhao M. 2002. Has electrical growth cone guidance found its potential? Trends Neurosci 25 (27): 354-359.

McCaig CD, Rajnicek AM, Song B and Zhao M. 2005. Controlling cell behavior electrically: current views and future potential. Physiol Rev 85: 943-978.

McKasson MJ, Huang L, and Robinson KR. 2008. Chick embryonic Schwann cells migrate anodally in small electrical fields. Exp Neurol 211:585-587.

Metcalf MEM and Borgens RB. 1994. Weak applied voltages interfere with amphibian morphogenesis and pattern. J Exp Zool 268: 322-338.

Messerli MA and Graham DM. 2011. Extracellular electrical fields direct wound healing and regeneration. Biol Bull 221:79-92.

Miller C, Jeftinija S, and Mallapragada S. 2002. Synergistic effects of physical and chemical guidance cues on neurite alignment and outgrowth on biodegradable polymer substrates. Tissue Eng 8(3):367-378.

NCHS. 1995. National Center for Health Statistics. http://www.cdc.gov/nchs/ (accessed July 2008)

Norden B. The Nobel Prize in Chemistry, 2000: Conductive polymers. Kungl. Vetenskapsakademien: The Royal Swedish Academy of Sciences. 2000.

Nuccitelli R. 2003. Endogenous electric fields in embryos during development, regeneration and wound healing. Radiat Prot Dosim 106(4):375-383.

NSCISC. January 2008. National Spinal Cord Injury Statistical Center. http://www.spinalcord.uab.edu/ (accessed July 2008).

Patel NB and Poo MM. 1984. Perturbation of the direction of neurite growth by pulsed and focal electric fields. J Neurosci 4(12):2939-2947.

Pfister LA, Alther E, Papaloizos M, Merkle HP and Gander B. 2008. Controlled nerve growth factor release from multi-ply alginate/chitosan-based nerve conduits. Eur J Pharm Biopharm 69: 563-572.

Pfister BJ, Gordon T, Loverde JR, Kochar AS, Mackinnon SE, and Cullen DK. 2011. Biomedical engineering strategies for peripheral nerve repair: surgical applications, state of the art, and future challenges. Crit Rev Biomed Eng 39(2):81-124.

Rajnicek AM, Foubister LE and McCaig CD. 2006a. Temporally and spatially coordinated roles for Rho, Rac, Cdc42 and their effectors in growth cone guidance by a physiological electric field. J Cell Sci 119: 1723-1735.

Rajnicek AM, Foubister LE and McCaig CD. 2006b. Growth cone steering by a physiological electric field requires dynamic microtubules, microfilaments and Rac-mediated filopodial asymmetry. J Cell Sci 119: 1736-1745.

Ravichandran R, Sundarrajan S, Venugopal JR, Mukherjee S, and Ramakrishna S. 2010. Applications of conducting polymers and their issues in biomedical engineering. J R Soc Interface 7:S559-579.

Reichert F. 1994. Peripheral nerve injury induces Schwann cells to express two macrophage phenotypes: phagocytosis and the galactose-specific lectin MAC-2. J NeuroSci 14:3231-3245

Reid B, Song B, McCaig CD, and Zhao M. 2005. Wound healing in rat cornea: the role of electric currents.FASEB J 19:379-386.

Richardson JA, Rementer CW, Bruder JM, and Hoffman-Kim D. 2011. Guidance of dorsal root ganglion neurites and Schwann cells by isolated Schwann cell topography on poly(dimethyl siloxane) conduits and films. J Neural Eng 8:1-12.

Robinson KR. 1985. The Responses of Cells to Electrical Fields: A Review. J Cell Bio 101:2023-2027.

Rutkowski GE, Miller CA, Jeftinija S and Mallapragada SK. 2004. Synergistic effects of micropatterned biodegradable conduits and Schwann cells on sciatic nerve regeneration. J Neural Eng 1: 151-157.

Schmidt CE and Leach JB. 2003. Neural tissue engineering: strategies for repair and regeneration. Annu Rev Biomed Eng 5: 293-347.

Schmidt CE, Shastri VR, Vacanti JP and Langer R. 1997. Stimulation of neurite outgrowth using an electrically conducting polymer. Proc Natl Acad Sci USA 94: 8948-8953.

Schoenbach KH, Hargrave B, Joshi RP, Kolb JF, Nuccitelli R, Osgood C, Pakhomov A, Stacey M, Swanson RJ, White JA, Shu X, Jue Z, Beebe SJ, Blackmore PF and Buescher ES. 2007. Bioelectric effects of intense nanosecond pulses. IEEE Trans Dielectrics and Electrical Insulation 14(5): 1088-1109.

Seal BL, Otero TC and Panitch A. 2001. Review: Polymeric biomaterials for tissue and organ regeneration. Mater Sci Eng R Rep 34: 147-230.

Seil JT and Webster TJ. 2010. Electrically active nanomaterials as improved neural tissue regeneration scaffolds. WIREs Nanomed Nanobiotechnol 2(6):635-647.

Sheikh AQ, Taghian T, Hemingway B, Cho H, Kogan AB, and Narmoneva DA. 2012. Regulation of endothelial MAPK/ERK signaling and capillary morphogenesis by low-amplitude electric field. J R Soc Interface, publish online.

Shi R and Borgens RB. 1995. Three dimensional gradients of voltage during development of the nervous system as invisible coordinates for the establishment of embryonic pattern. Dev Dyn 202:101–114.

Song B, Zhao M, Forrester J, and McCaig C. 2004. Nerve regeneration and wound healing are stimulated and directed by an endogenous electrical field in vivo. J Cell Sci 117:4681-4690.

Song B, Gu Y, Pu J, Reid B, Zhao Z, and Zhao M. 2007. Application of direct current electric fields to cells and tissues in vitro and modulation of wound electric field in vivo. Nat Protoc 2(6):1479-1489.

Sontag W and Kalka D. 2006. No effect of pulsed electromagnetic fields on PC12 and HL-60 cells. Radiat Environ Biophys 45:63-71.

Tang ZG, Black RA, Curran JM, Hung JA, Rhodes NP, and Williams DF. 2004. Surface properties and biocompatibility of solvent-cast poly[ε-caprolactone] films. Biomaterials 25:4741-4748.

Walker JL, Kryscio R, Smith J, Pilla A, and Sisken BF. 2007. Electromagnetic field treatment of nerve crush injury in a rat model: effect of signal configuration on functional recovery. Bioelectromagnetics 28:256-263.

Wang X, Gu X, Yuan C, Chen S, Zhang P, Zhang T, Yao J, Chen F and Chen G. 2003. Evaluation of biocompatibility of polypyrrole in vitro and in vivo. J Biomed Mater Res 68A(3):411-422.

Winter JO and Schmidt CE. 2002. Biomimetic Strategies and Applications in the Nervous System. In A.K. Dillow, A.M. Lowman, Ed., Biomimetic Materials and Design, Marcel-Dekker, p. 375-415.

Wood MD and Willits RK. 2009. Applied electric field enhances DRG neurite growth: influence of stimulation media, surface coating and growth supplements. J Neural Eng 6:1-8.

Yao L, Shanley L, McCaig C and Zhao M. 2008. Small applied electric fields guide migration of hippocampal neurons. J Cell Physiol 216: 527-535.

Yao L, McCaig CD, and Zhao M. 2009. Electric signals polarize neuronal organelles, direct neuron migration, and orient cell division. Hippocampus 19:855-868.

Yu LM, Leipzig ND and Shoichet MS. 2008. Promoting neuron adhesion and growth. Mater Today 11(5): 36-43.

Yu TT and Shoichet MS. 2005. Guided cell adhesion and outgrowth in peptide-modified channels for neural tissue engineering. Biomaterials 26: 1507-1514.

Zhao M, Agius-Fernandez A, Forrester JV, and McCaig CD. 1996. Orientation and directed migration of cultured corneal epithelial cells in small electric fields are serum dependent. J Cell Sci 109:1405-1414.

Zhao M, Pu J, Forrester JV and McCaig CD. 2003. Membrane lipids, EGF receptors and intracellular signals co-localize and are polarized in epithelial cells moving directionally in a physiological electric field. Faseb J 17: 397-406.

Zhao M. 2009. Electrical fields in wound healing – an overriding signal that directs cell migration. Semin Cell Dev Biol 20:674-682.

Zhang Y, Ding J, and Duan W. 2006. A study of the effects of flux density and frequency of pulsed electromagnetic field on neurite outgrowth in PC12 cells. J Biol Phys 32:1-9.

Zhang Z, Rouabhia M, Wang Z, Roberge C, Shi G, Roche P, Li J and Dao LH. 2007. Electrically conductive biodegradable polymer composite for nerve regeneration:

electricity-stimulated neurite outgrowth and axon regeneration. Artif Organs 31(1): 13-22.

Vita

Hieu Nguyen was born in San Jose, CA in September of 1980 as the third and final child. He attended the University of California, Berkeley for his undergraduate studies where he earned a Bachelors of Science in Bioengineering on May 2002. He had his first research experience working with Dr. Song Li on cardiovascular and orthopedic tissue engineering applications during his tenure at Berkeley. Between 2003 – 2006, he was a Research Assistant at Skeletal Kinetics, LLC., a startup orthopedic biomaterials company. After successfully commercializing three iterations of products with guidance from Brent Constantz, Dave Delaney, and Duran Yetkinler, he returned to academia to follow his true love – tissue engineering, mobility and visual restoration. He studied for his Masters of Science in Biomedical Engineering between 2006 – 2008 under the supervision of Christine Schmidt and committee member Wolfgang Frey. He continued researching with Christine Schmidt with an NDSEG Fellowship to complete his Doctor of Philosophy in Biomedical Engineering at the end of 2012, with immense support from committee members Richard Aldrich, Aaron Baker, Henry Rylander, and Laura Suggs. After finishing his education, Hieu will continue to research in functional restorative technologies.

Permanent email: hueyhieu@gmail.com

This dissertation was typed by the author.